

## ABSTRACT

**Title of Document:**           **EXPANDING OUR UNDERSTANDING OF THE REGULATORY MACROPHAGE**

Bryan David Fleming, Doctor of Philosophy, 2014

**Directed By:**                   Dr. David M. Mosser, Professor  
Department of Cell Biology & Molecular Genetics

Macrophages readily change their phenotype in response to exogenous stimuli. In this work, macrophages were stimulated under a variety of experimental conditions, and phenotypic alterations were correlated with changes in gene expression. We identified three transcriptionally related populations of macrophages with immunoregulatory activity. They were generated by stimulating cells with lipopolysaccharide (LPS), a toll like receptor (TLR) ligand, in the presence of three different “reprogramming” signals; high density immune complexes (IC), prostaglandin E<sub>2</sub> (PGE<sub>2</sub>), or adenosine (Ado). All three of these cell populations produced high levels of transcripts for IL-10, as well as growth and angiogenic factors. They also secreted reduced levels of inflammatory cytokines IL-1 $\beta$ , IL-6, and IL-12. These three activated macrophages could partially rescue mice from lethal endotoxemia, and therefore we consider each to have immunoregulatory activity. This immunoregulatory activity occurred equally well in macrophages from *stat6*-deficient mice. The lack of STAT6 did not affect macrophages’ ability to reciprocally change cytokine production or to rescue mice from lethal endotoxemia. Furthermore, macrophages treated with IL-4 do not exhibit the immunoregulatory phenotype and

associated transcriptional alterations. This work demonstrates that there are multiple ways to generate macrophages with immunoregulatory activity. These Regulatory macrophages (R-M $\phi$ ) are transcriptionally and functionally related, and quite distinct from macrophages treated with IL-4.

# **EXPANDING OUR UNDERSTANDING OF THE REGULATORY MACROPHAGE**

By

**Bryan David Fleming**

Dissertation submitted to the Faculty of the Graduate School of the  
University of Maryland, College Park, in partial fulfillment  
of the requirements for the degree of  
Doctor of Philosophy  
2014

**Advisory Committee:**

Professor David M. Mosser, Chair  
Associate Professor Najib El-Sayed  
Associate Professor Wenxia Song  
Associate Professor Louisa Wu  
Professor Philip DeShong, Dean's Representative

© Copyright by  
Bryan David Fleming  
2014

## **Acknowledgements**

I have to start by thanking my parents for all of the support they have provided over the years. I would not have made it this far in my science career without your love and dedication. I would like to thank my brother and sister for cheering me up when I had a hard work week and for providing me with many happy memories.

I would like to thank the fellow members of the Mosser lab with whom I have had the pleasure of working with over the years. I would like to thank Rahul and Bess for the many good memories grading immunology exams and laughing at wrong answers. I would like to thank Andy Stewart for the advice and guidance he has bestowed upon me over the last few years. I would like to thank the Kevins (Knapstein and Roelofs) for being my partners in crime and my drinking buddies. I owe special thanks to Shanjin Cao who took me under his wing during my early graduate career. I also owe special thanks to Prabha Chandrasekaran for being a good friend and for helping me finish my graduate studies. I would also like to thank the members of my committee and my many professors that have given me advice and imparted their knowledge on me during my time at the University of Maryland.

Finally, I owe the most thanks to Dr. Mosser. You have guided my development from an undergraduate, into a lab tech, and finally into a PhD student. It feels like only yesterday that I was answering questions in your class about the polio vaccines. I am glad that you took a chance on the kid that got the lowest B in your class. Thanks for everything.

# Table of Contents

<b>Acknowledgements</b>	<b>ii</b>
<b>Table of Contents</b>	<b>iii</b>
<b>List of Tables</b>	<b>v</b>
<b>List of Figures</b>	<b>vi</b>
<b>List of Illustrations</b>	<b>viii</b>
<b>List of Abbreviations</b>	<b>ix</b>
<b>Acknowledgement of Assistance</b>	<b>xiv</b>
<b>Chapter 1: Introduction</b> .....	<b>1</b>
<i>The Innate Immune System</i> .....	1
<i>Cells of the Myeloid Lineage</i> .....	3
Granulocytes.....	3
Mononuclear Phagocytes.....	5
<i>Classification Systems of Macrophages</i> .....	10
Classical Activation (M1).....	10
Alternative Activation (M2a).....	11
M1/M2 Classification.....	13
Regulatory Activation (M2b).....	16
Color Wheel.....	19
<b>Chapter 2: Tools for Studying Regulatory Macrophages</b> .....	<b>21</b>
<i>Studying at the DNA Level</i> .....	21
Background.....	21
Experimental Applications.....	22
<i>Studying at the RNA Level</i> .....	22
Background.....	22
Experimental Applications.....	24
<i>Studying at the Protein Level</i> .....	24
Background.....	24
Experimental Applications.....	26
<i>Research Objectives</i> .....	26
<b>Chapter 3: Comparative Analysis of Activated Macrophage Populations</b> .....	<b>28</b>
<i>Introduction</i> .....	28
<i>Methods and Materials</i> .....	30
Mice.....	30
Murine Macrophage Generation.....	30
Human Macrophage Culture.....	31
Cell Culture and Stimulation.....	31
ELISA.....	32
Membrane Protein Array.....	33
Bioplex Assay.....	34
RNA Isolation and cDNA Synthesis.....	34
Conventional PCR.....	35
qRT-PCR.....	38

RNA-seq Data Generation and Processing.....	38
Data Quality Assessment and Differential Expression Analysis.....	39
Ingenuity Pathway Analysis.....	39
Macrophage Metabolism.....	40
Flow Cytometry.....	40
Lethal Endotoxin Challenge.....	40
Statistics.....	41
<i>Results</i> .....	41
Cytokine and Chemokine Profiles of Immunoregulatory Macrophages .....	41
RNA-seq Analysis of Murine Macrophages.....	48
Differentially Expressed Genes.....	52
Activated ‘Disease and Functions’ Identified by IPA Analysis.....	66
Metabolism in Regulatory Activation is Similar to that of LPS Treated Cells...	71
Identification of Candidate Biomarkers.....	74
Detecting Candidate Biomarkers on the Protein Level.....	80
Regulatory Activation Offers Protection from Lethal Endotoxin Challenge.....	85
Cytokine Expression Profile of Human Macrophages.....	85
<i>Discussion</i> .....	87
<b>Chapter 4: Conclusions.....</b>	<b>96</b>
<b>Chapter 5: Future Directions.....</b>	<b>98</b>
<i>Continued Studies at the DNA Level</i> .....	98
<i>Continued Studies at the RNA Level</i> .....	98
<i>Continued Studies at the Protein Level</i> .....	100
<b>Bibliography.....</b>	<b>102</b>

## List of Tables

Table 1: Primer Pairs Sequences.....	36
Table 2: Top 100 Upregulated Genes In LPS Treated Macrophages.....	53
Table 3: Top 100 Upregulated Genes In LPS+Immune Complex Treated Macrophages .....	56
Table 4: Top 100 Upregulated Genes In LPS+Adenosine Treated Macrophages.....	59
Table 5: Top 100 Upregulated Genes In IL-4 Treated Macrophages.....	62
Table 6: Top 25 Genes Uniquely Induced Following IL-4 Stimulation.....	65
Table 7: Genes Induced Following Regulatory Activation.....	67
Table 8: Shared Predicted Genes Induced Following Regulatory Activation.....	68
Table 9: Metabolic Pathways Identified by IPA Analysis (Z-score).....	72



## List of Figures

Figure 1: Cytokine secretion by Regulatory macrophages.....	42
Figure 2: Regulatory macrophage induction is independent of the STAT6 signaling pathway.....	44
Figure 3: Alternative Activated macrophage markers are dependent on the STAT6 signaling pathway.....	45
Figure 4: Regulatory activation results in alterations of cytokine/chemokine profiles.....	46
Figure 5: Relative induction of cytokines/chemokines in activated macrophages.....	47
Figure 6: Comparison of global RNA expression profiles of differentially activated macrophages .....	49
Figure 7: Four way Venn diagrams of genes differentially expressed following activation.....	51
Figure 8: Top activated and repressed ‘Diseases and Functions’ associated with regulatory activation in macrophages.....	69
Figure 9: Top 15 activated ‘Diseases and Functions’ associated with M1 and Alternatively Activated macrophages.....	70
Figure 10: Glucose and lactate production in Regulatory macrophages.....	73
Figure 11: Induction profile of control genes in activated macrophages.....	75
Figure 12: Induction profile of regulatory genes in activated macrophages.....	76

Figure 13: Induction profile of regulatory genes in activated macrophages is independent of STAT6 signaling.....	77
Figure 14: Induction profile of immune complex induced genes in activated macrophages .....	78
Figure 15: Induction profile of IL-4 induced genes in activated macrophages .....	79
Figure 16: Induction of immune complex induced genes is independent of STAT6 signaling in activated macrophages.....	81
Figure 17: Validation of regulatory gene candidates in activated macrophages .....	82
Figure 18: Failed validation of regulatory gene candidates in activated macrophages .....	83
Figure 19: CCR1 expression is associated with regulatory activation of macrophages .....	84
Figure 20: Regulatory macrophages provide protection from lethal endotoxemia.....	86
Figure 21: Cytokine profile of human macrophages under regulatory stimulation conditions.....	88

## **List of Illustrations**

Illustration 1: Overview of Toll Like Receptor 4 Signaling.....	12
Illustration 2: Overview of Interleukin-4 Receptor Signaling.....	14
Illustration 3: Overview of Receptor Signaling in Regulatory Activation .....	18
Illustration 4: Color Wheel.....	20

## List of Abbreviations

AA-M $\phi$	Alternatively Activated macrophages
Ado	Adenosine
AP	Alkaline phosphatase
APCs	Antigen presenting cells
Arg-1	Arginase-1
BCG	Bacillus Calmette-Guerin
BMDM	Bone marrow derived macrophages
BMM	Bone marrow media
bp	Base pair
CA-M $\phi$	Classically Activated macrophages
cAMP	Cyclic adenosine monophosphate
CCL	C-C chemokine ligand
CCR	C-C chemokine receptor
CD	Cluster of differentiation
cDNA	Complementary deoxyribonucleic acid
CHIP	Chromatin immunoprecipitation
CREB	Cyclic AMP response element binding protein
C <sub>T</sub>	Comparative threshold cycle
CXCL	C-X-C chemokine ligand
CXCR	C-X-C chemokine receptor

DCs	Dendritic cells
DMEM	Dulbecco's modified Eagle's medium
DNA	Deoxyribonucleic acid
dNTPs	Deoxynucleotide triphosphates
DTT	Dithiothreitol
ELISA	Enzyme-Linked Immunosorbent Assay
ERK	Extracellular signal-regulated kinases
FcR	Fc (fragment crystallizable region) receptor
FACS	Fluorescence activated cell sorting
FBS	Fetal bovine serum
GADPH	Glyceraldehyde-3-phosphate dehydrogenase
G-CSF	Granulocyte colony stimulating factor
GM-CSF	Granulocyte macrophage colony stimulating factor
H	Histone protein subunit
HBSS	Hank's balanced salt solution
hr	Hours
HRP	Horse radish peroxidase
IC	Immune complex
IFN	Interferon
Ig	Immunoglobulin
IKK	I $\kappa$ B kinase
IL	Interleukin

iNOS	Inducible nitric oxide synthase
IPA	Ingenuity pathway analysis
IRAK	Interleukin-1 receptor associated kinase
IRF	Interferon regulatory factor
JAK	Janus kinase
kg	Kilogram
KO	Knock out
LCCM	L929 cell conditioned media
LPS	Lipopolysaccharide
M $\phi$	Macrophages
M1-M $\phi$	M1 macrophages
M2-M $\phi$	M2 macrophages
MAC	Membrane attack complex
MAP	Mitogen activated protein
MAPK	Mitogen activated protein kinase
M-CSF	Macrophage colony stimulating factor
mDC	Myeloid dendritic cells
MEK	MAP/ERK kinase kinase
MFI	Mean florescence intensity
mg	Milligram
MHC	Major histocompatibility complex
ml	Milliliter
mM	Millimolar

mRNA	Messenger ribonucleic acid
MyD88	Myeloid differentiation primary response gene 88
nM	Nanomolar
NADH	Nicotinamide adenine dinucleotide
NADPH	Nicotinamide adenine dinucleotide phosphate
NF- $\kappa$ B	Nuclear factor- $\kappa$ B
ng	Nanogram
OVA	Ovalbumin
PAMPs	Pathogen associated molecular patterns
pNPP	Para-nitrophenylphosphate
PBS	Phosphate buffered saline
PCA	Principle component analysis
PCR	Polymerase chain reaction
pDC	Plasmacytoid dendritic cells
PE	Phycoerythrin
PGE <sub>2</sub>	Prostaglandin E <sub>2</sub>
PLC	Phospholipase C
qRT-PCR	Quantitative real time polymerase chain reaction
R-M $\phi$	Regulatory macrophages
RM $\phi$ -Ado	Regulatory macrophages induced with adenosine
RM $\phi$ -IC	Regulatory macrophages induced with immune complexes
RM $\phi$ -PGE <sub>2</sub>	Regulatory macrophages induced with PGE <sub>2</sub>

RNA	Ribonucleic acid
RNase	Ribonuclease
RNA-seq	RNA-sequencing
RT	Reverse transcriptase
SEM	Standard error of the mean
STAT	Signal transducers and activators of transcription
Syk	Spleen tyrosine kinase
TGF- $\beta$	Transforming growth factor- $\beta$
Th	T helper cells
Th1	T helper 1 type response
Th2	T helper 2 type response
TLR	Toll like receptor
TMB	Tetramethylene benzidine
TNF- $\alpha$	Tumor necrosis factor- $\alpha$
TRAF	TNF receptor associated factor
TRIF	TIR domain containing adapter inducing interferon $\beta$
$\mu\text{g}$	Microgram
$\mu\text{l}$	Microliter
$\mu\text{M}$	Micromolar
WT	Wild type
WTSS	Whole transcriptome shotgun sequencing



## **Acknowledgements of Assistance**

I would like to thank Rahul Suresh for his help in isolating and stimulating the macrophages used in the RNA-seq experiment. The generation and analysis of the transcriptomic results would not have been possible without our collaboration with Dr. Najib El-Sayed and Laura Dillon. The PCA analysis, heat map analysis and Venn diagrams were all generated through the hard work of Laura Dillon.

I would like to thank Bess Dalby for her assistance with the IPA analysis and the metabolism experiments. It was her preliminary studies that brought our attention to metabolic difference in activated macrophages.

The membrane array, bioplex and flow cytometry experiments were performed with the aid of Prabha Chandrasekaran. It was here technical abilities that that made this experiments possible. Additionally, the flow cytometry experiment received additional help from Arup Sarkar.

I would like to thank those that guided me in making revisions to my dissertation. I would like to start by thanking my committee for their many suggestions and comments. I would like to thank Prabha Chandrasekaran who corrected the rough drafts and suggested points of improvement. Finally, I would like to thank Dr. David Mosser for helping to conceive the experiments that made this dissertation possible.

# Chapter 1: Introduction

## *1.1 The Innate Immune System*

The innate immune system is an evolutionarily old defense strategy, often referred to as an organism's first line of defense against pathogens. This system has evolved over millennia and can be broken down into three major categories. The first and most primitive way of deterring pathogens was the formation of physical barriers. The development of stratified epithelial layers that contain keratin provided protection against abrasions and makes it difficult for pathogens to enter the body. Additionally, the secretion of mucin helped to protect vulnerable internal membranes. The formation of a thick mucus layer made it difficult for pathogens to make contact with the epithelium. These barriers provided protection against the entry of pathogens, but could not protect the host if a pathogen made it into the body.

The development of non-specific, antimicrobial molecules added a new form of protection. This second method included the release of complement proteins into the blood, gastric acid into the stomach, and lysozyme into tears. These secretions made the body a hostile environment for many pathogens. Complement proteins form an important arm of the innate immune response and provide several important antimicrobial functions including opsonization, agglutination and lysis<sup>1,2</sup>. Complement mediated responses facilitate immune cell recruitment and promote inflammatory responses.

There are three different pathways of complement activation. The first two ways to initiate complement activation is through the classical and lectin pathways<sup>1,2</sup>. The classical pathway is initiated by the C1 complex, comprised of C1q, C1r and C1s proteins, upon its association with antigen bound IgG or IgM antibodies. The lectin pathway relies on mannose-binding lectin which has the ability to directly bind to mannose residues on bacteria<sup>1,2</sup>. Regardless of how this pathway is initiated, the next step is the activation of complement proteins C2 and C4, which combine to activate C3. The third pathway of complement activation is referred to as the alternative pathway. This pathway relies on the constant low level hydrolysis of C3 proteins and the association of factor B. These two proteins function to convert a second molecule of C3 into its active form. The classical pathway, alternative pathway and the lectin pathway all converge at this point to facilitate the activation of C5 and the membrane attack complex. This membrane attack complex or MAC, inserts itself into the membrane of gram negative bacteria forming a pore and ultimately lysing the bacteria. The protective role of complement is well-described in bacterial infections causing sepsis<sup>3,4</sup>. Deficiencies in complement components can be attributed to a wide range of disease manifestations. Failure to initiate complement can lead to recurring bacterial infections, in particular, infections by bacteria in the genus *Neisseria*<sup>4</sup>. Additionally, changes in the level of complement proteins/factors have been associated with a wide range of human diseases including Alzheimer's disease and systemic lupus erythematosus<sup>5,6</sup>.

The cellular component forms the most important arm of the innate immune system. This consists of granulocytes like neutrophils, basophils, eosinophils, and mast cells.

Additionally, it is also comprised of mononuclear phagocytes, which includes monocytes, macrophages and dendritic cells. Each of these cells are different in their structure and function, with each being specialized towards the various pathogens they combat. These cells have germline encoded receptors that allow them to recognize molecular patterns primarily associated with pathogens<sup>7</sup>. They all release cytokines that attract and activate immune cells to the sites of infections. Even though it is rare, defects in receptor signaling pathways can severely affect the function of innate immune cells<sup>7</sup>. These individuals often have recurring infections by pyogenic bacteria including members of Staphylococcus, Streptococcus and Pseudomonas families<sup>8</sup>. The combination of these three components resulted in the formation of the innate immune system.

## **1.2 Cells of the Myeloid Lineage**

### **1.2.1 Granulocytes**

Granulocytes are comprised of neutrophils, eosinophils, basophils and mast cells. The circulating amounts are highly variable from person to person and are known to change drastically in cases of infection. Neutrophils make up the largest percentage and can range from 60-70% of the total circulating white blood cells<sup>9</sup>. Neutrophils have short lifespans and can only survive for a few hours to a few days<sup>10</sup>. These cells exhibit a high level of motility, and can rapidly leave the blood to enter sites of infections<sup>9,11</sup>. This cellular migration is mediated by chemical, cytokine and chemokine gradients that form during early immune responses. The production of C5a during complement activation and the

release of IL-8 and other chemokines by activated neutrophils helps to recruit immune cells into infected tissues<sup>11</sup>.

Neutrophils, like many of our immune cells, have a diverse array of surface receptors for the detection of pathogens. They have complement receptors that help to identify bacteria marked by activated complement. They have Fc receptors that aid in the internalization of antibodies binding to bacteria<sup>12</sup>. Most importantly, they have a wide array of toll like receptors (TLRs) that recognize pathogen associated molecular patterns (PAMPs)<sup>12</sup>. PAMPs include lipopolysaccharides and lipoteichoic acids that make up bacterial membranes, as well as bacterial DNA. Neutrophils internalize bacteria and kill them through exposure to reactive oxygen species that are generated by NADPH oxidase<sup>9</sup>. They also release granules that contain myeloperoxidases, hydrolytic enzymes and lactoferrins<sup>9</sup>. These granules function to kill bacteria through the production of oxygen radicals and the digestion of structural proteins. Additionally, evidence has shown that neutrophils release extracellular traps that are composed of DNA and proteases that are capable of trapping and killing bacteria<sup>13</sup>. In addition to these anti-microbial responses, they also release inflammatory cytokines such as IL-1 $\beta$ , IL-6, and TNF- $\alpha$ <sup>9</sup>. These inflammatory cytokines are responsible for changes in the vascular epithelium permeability and the generation of fevers<sup>14</sup>.

The eosinophil represents a much smaller portion of circulating white blood cells than the neutrophils, with around 3-6% considered average<sup>15</sup>. They are longer-lived than neutrophils with a lifespan of about two weeks<sup>15</sup>. While neutrophils specialize in eliminating bacteria, eosinophils have been associated with parasite infections as well as

some anti-viral and allergic responses<sup>16,17</sup>. They are most often associated with helminthic infections and have been shown to be important in their clearance<sup>18</sup>. They are attracted to the site of infection through various chemokines including CCL11 (eotaxin-1) and CCL24 (eotaxin-2)<sup>17</sup>. Eosinophils have been associated with anti-viral responses because of their production of eosinophil-derived neurotoxins and cationic proteins which exhibit RNase activities<sup>17,19</sup>. They have been associated with the release of pro-inflammatory cytokines, IL-5, IL-12 and TNF- $\alpha$ <sup>16,17</sup>.

The basophil represents the lowest percentage of the circulating immune cells with less than 1% being considered normal<sup>20</sup>. Basophils have lifespans similar to neutrophils and have been reported to live only a few days<sup>20</sup>. They express high levels of Fc $\epsilon$ RI, which when cross linked, causes the release of large amounts of leukotrienes and histamine which help to promote allergic responses<sup>21</sup>. Basophils and mast cells were often thought of as being related cell populations. The main visible difference was that basophils were found in the blood while mast cells were associated with tissue<sup>20</sup>. New evidence has revealed that basophils release IL-4 and IL-13 after the cross linking of their Fc $\epsilon$ RI, while these cytokines have not been associated with mast cell degranulation<sup>22</sup>.

### **1.2.2 Mononuclear Phagocytes**

Mononuclear phagocytes are comprised of monocytes, dendritic cells and macrophages. These three cell populations all have similar characteristics, but one of their most important characteristics is their ability to function as antigen presenting cells (APCs). These APCs are important in initiating a specific arm of the immune response known as

adaptive immunity. When a mononuclear phagocyte internalizes a pathogen, antigenic fragments are processed and displayed on the membrane in the context of major histocompatibility complex class II (MHC class II) and co-stimulatory molecules CD80 and CD86. In addition, they secrete cytokines that attract the cells of the adaptive immune system, T cells and B cells.

Monocytes in blood make up to 10% of the circulating leukocytes<sup>23</sup>. Monocytes were long-thought to be an intermediate between bone marrow precursors and macrophages. However, recent studies have identified specific effector functions associated with these cells<sup>23</sup>. Monocytes can be divided into two primary subsets based on phenotype and function<sup>24,25</sup>. The CD14<sup>++</sup>CD16<sup>-</sup> classical human monocytes or intermediate CD14<sup>++</sup>CD16<sup>+</sup> monocytes correspond to mouse GR1<sup>+</sup>/Ly6C<sup>high</sup> inflammatory monocytes which have a phenotype of CCR2<sup>+</sup>Cx3CR1<sup>low</sup>. The non-classical CD14<sup>dim</sup>CD16<sup>+</sup> human monocytes correspond to the GR1<sup>-</sup>/Ly6C<sup>low</sup> mouse monocytes that are CCR2<sup>-</sup> and express high amounts of Cx3CR1. GR1<sup>+</sup>/Ly6C<sup>high</sup> monocytes and their human CD14<sup>++</sup>CD16<sup>-</sup> or CD14<sup>++</sup>CD16<sup>+</sup> counterparts are rapidly recruited to sites of infection/injury and have the potential to differentiate into either inflammatory macrophages or monocyte-derived DC<sup>24,25</sup>. They efficiently produce inflammatory mediators such as TNF- $\alpha$ , nitric oxide, and reactive oxygen species. These inflammatory monocytes play a critical role in protection against several pathogens as demonstrated with the mice models of infection for *Listeria*, *Mycobacterium*, and herpes simplex virus<sup>26-28</sup>. Human CD14<sup>dim</sup>CD16<sup>+</sup> non-classical monocytes and their mouse Ly6C<sup>low</sup> equivalents patrol blood vessels and mediate early responses against tissue damage<sup>24</sup>. These cells have

also been shown to promote wound healing and angiogenesis in models of atherosclerosis and cardiac infarction<sup>29-31</sup>.

Dendritic cells (DCs) induce and regulate adaptive immunity against pathogens, and tolerance against self-antigens and commensal microorganisms. Dendritic cells reside in the periphery during their immature state, where they recognize and capture antigens. Upon appropriate stimulation, DCs migrate to lymphoid organs where they present the processed antigens to T cells in the context of MHC class I or II<sup>32</sup>. DCs can either be tolerogenic, which happens when they encounter a self-antigen or a tolerogenic signal such as  $\beta$ -catenin or E-cadherin<sup>33</sup>. They can also be inflammatory in the presence of microbial products or pro-inflammatory cytokines. Inflammation leads to the maturation of DCs associated with an enhanced ability to initiate T cell responses through surface upregulation of MHC and co-stimulatory molecules. DCs can be classified into two subsets (a) plasmacytoid DCs (pDCs) and (b) conventional/myeloid DCs (mDCs)<sup>25,34</sup>. The pDCs play a crucial role against viral infection by producing vast amounts of type I interferon in response to the ligation of TLR7 and TLR9 or intracellular sensor triggering<sup>35</sup>. Human mDCs can be divided into two main subsets based on the surface markers BDCA-1/CD1c or BDCA-3/CD141. BDCA-1<sup>+</sup> mDCs produce high levels of IL-12 upon stimulation, a cytokine essential to inducing Th1 response and cross-priming of CD8<sup>+</sup> T cells<sup>36</sup>. There is only limited data available on the functions and specializations of these DC subsets.

The macrophage can be found in almost every tissue of the body and plays an important role in maintaining tissue homeostasis. Kupffer cells, osteoclasts, and microglial cells are just a few of the specialized macrophages found in the liver, bones, and brain,



respectively. All of these cells have taken on unique functions that give them all specific phenotypes; Splenic red-pulp macrophages are required to take up senescent red blood cells and specifically utilize the transcription factor SPI-C to transcribe the genes necessary for iron uptake<sup>37</sup>. Osteoclasts maintain ionic balance, alveolar macrophages in the lungs initiate anti-microbial responses, cardiac macrophages provide necessary signals for angiogenesis and neonatal heart regeneration, and microglial macrophages in the brain mediate several functions such as the repair of neural tissue and synaptic stripping<sup>38</sup>. These are just a few examples of how macrophages play important roles in the maintenance of tissue homeostasis.

An important role of macrophages is to initiate an immune response to pathogens and foreign antigens. These cells express a wide array of surface receptors that recognize pathogen associated molecular patterns (PAMPs). Some of these pattern recognition receptors are toll-like receptors, C-type lectin receptors, NOD like receptors and RIG-I like receptors<sup>39,40</sup>. These receptors are specialized for the motifs they recognize. For example, there are 13 TLRs in total, each recognizing a particular motif; TLR2 senses peptidoglycan from gram positive bacteria, TLR4 recognizes LPS from gram negative bacteria, TLR9 detects CpG rich DNA and so on. Signaling through TLRs initiates two different pathways (a) MyD88 dependent pathway and (b) TRIF dependent pathway<sup>41,42</sup>. When respective ligands bind to TLR (except TLR3), MyD88 signaling is initiated, ultimately leading to the activation of NF- $\kappa$ B and MAP kinases. Translocation of NF- $\kappa$ B into the nucleus and binding to specific sites on the DNA initiates transcription of inflammatory genes such as IL-6, TNF- $\alpha$ , pro-IL-1 $\beta$ , and IL-12p40. Binding of double stranded RNA to TLR3 and

sometimes, LPS to TLR4 initiates the activation of TRIF which in turn activates interferon regulated factor 3 (IRF3) or NF- $\kappa$ B. IRF3 activates type I interferon production and signaling. Unlike signaling through other TLRs, TLR3 signaling occurs mostly in DCs and not in macrophages. Thus sensing of pathogens in macrophages through these pattern recognition receptors initiate inflammatory responses that in turn lead to the amplification of the adaptive immune response. Another important receptor on the macrophage surface is the Fc receptors that recognize the Fc portion of the antibodies. This receptor helps macrophage to identify antibody-coated antigens and to phagocytize them. Soluble antigens when bound with antibodies form immune complexes (IC) that trigger complement activation. This leads to opsonization and the subsequent phagocytosis by macrophages.

Throughout the years, discoveries have helped us to rethink the role of macrophages in the body. It is now understood that macrophages have several roles far beyond phagocytosis and that macrophages exist in several phenotypic forms. Accumulating knowledge suggests that different macrophage activation states are associated with the non-stereotypical functions of macrophages, including immune regulation, maintenance of tissue homeostasis, and wound healing. Understanding the correlations of phenotypic functions is important for classifying the macrophages and for redefining the various populations of macrophages with known functions.

### 1.3 Classification Systems of Macrophages

#### **1.3.1 Classical Activation (M1)**

The Classically Activated macrophage was the first phenotypic alternation of macrophages to be described, and it has been the most extensively studied. The term macrophage activation was introduced by Mackaness in the 1960s in an infection context to describe the antigen-dependent, but non-specific, microbicidal activity of macrophages toward *BCG* (*Bacillus Calmette-Guerin*) and *Listeria* upon secondary exposure to the pathogens<sup>43</sup>. The term, Classically Activated macrophages, is now generally reserved to cells primed with IFN- $\gamma$  and stimulated with bacterial products, such as LPS, or the cytokine TNF- $\alpha$  which is produced in response to bacterial products. The term M1-macrophages has developed to describe macrophages that exhibit generalized inflammatory responses regardless of the stimuli used for generating them. The three most common and prototypical inflammatory stimuli were TNF- $\alpha$ , TLR ligands (with or without IFN- $\gamma$ ) and GM-CSF<sup>44,45</sup>. Other stimuli include inflammatory cytokines such as IL-1 $\beta$  and IL-6. Regardless of the stimuli, these M1 macrophages generate large amounts of inflammatory cytokines including IL-1, IL-6, TNF- $\alpha$ , IL-12 and IL-23<sup>45-47</sup> and chemokines like CCL2, CCL3, CCL4, CCL5, CXCL9, CXCL10, and CXCL11<sup>45</sup>. In addition, these cells produce reactive oxygen and nitrogen intermediates that are capable of killing internalized pathogens<sup>45,48</sup>. These macrophages also express high levels of co-stimulatory molecules CD80/CD86 and MHC class II which facilitate their interaction with T cells, resulting in lymphocyte proliferation<sup>44</sup> and their polarization into T-helper cells<sup>44</sup>.

There are multiple signaling pathways that are responsible for the generation of Classically Activated macrophages. The presence of IFN- $\gamma$  causes an increase in STAT1 and IRF1 signaling<sup>45,49</sup>. TLR ligation leads to MyD88 signaling pathways which activate various MAP and I $\kappa$ B kinases with the end result being AP-1 and NF- $\kappa$ B translocation into the nucleus<sup>44,45</sup> (Illustration 1). The pro-inflammatory responses generated by these signaling pathways are important in macrophage mediated clearance of intracellular pathogens like *Leishmania*<sup>40</sup> and bacteria like *Listeria*<sup>45,50</sup>. Despite their protective role against infections, overt signaling from these macrophages can result in immunopathologies resulting in unnecessary destruction of cells and tissues.

### **1.3.2 Alternative Activation (M2a)**

The discovery that IL-4 and IL-13 caused murine macrophages to increase mannose receptor expression and to reduce their production of pro-inflammatory cytokine, led Stein and colleagues to propose an alternative activation phenotype<sup>51</sup>. This activation state was different from IFN- $\gamma$  activation but far from deactivation<sup>51,52</sup>. This activation state was termed Alternatively Activated or M2a macrophages<sup>40,53</sup>. These macrophages failed to induce inflammatory cytokines but displayed increased expression of Ym1, Fizz1, Arg-1 and mannose receptors<sup>45,54</sup>. These proteins have been associated with tissue remodeling and in parasitic infections<sup>53</sup>. The chemokines CCL17, CCL22, and CCL24 have also been reported as markers for M2 activation in macrophages<sup>46</sup>. These cells fail to upregulate co-stimulatory molecules CD80 and CD86 and show low expression of MHC class II<sup>44</sup>. The fact that they arise from IL-4 and not IFN- $\gamma$  suggests that these cells are mostly associated

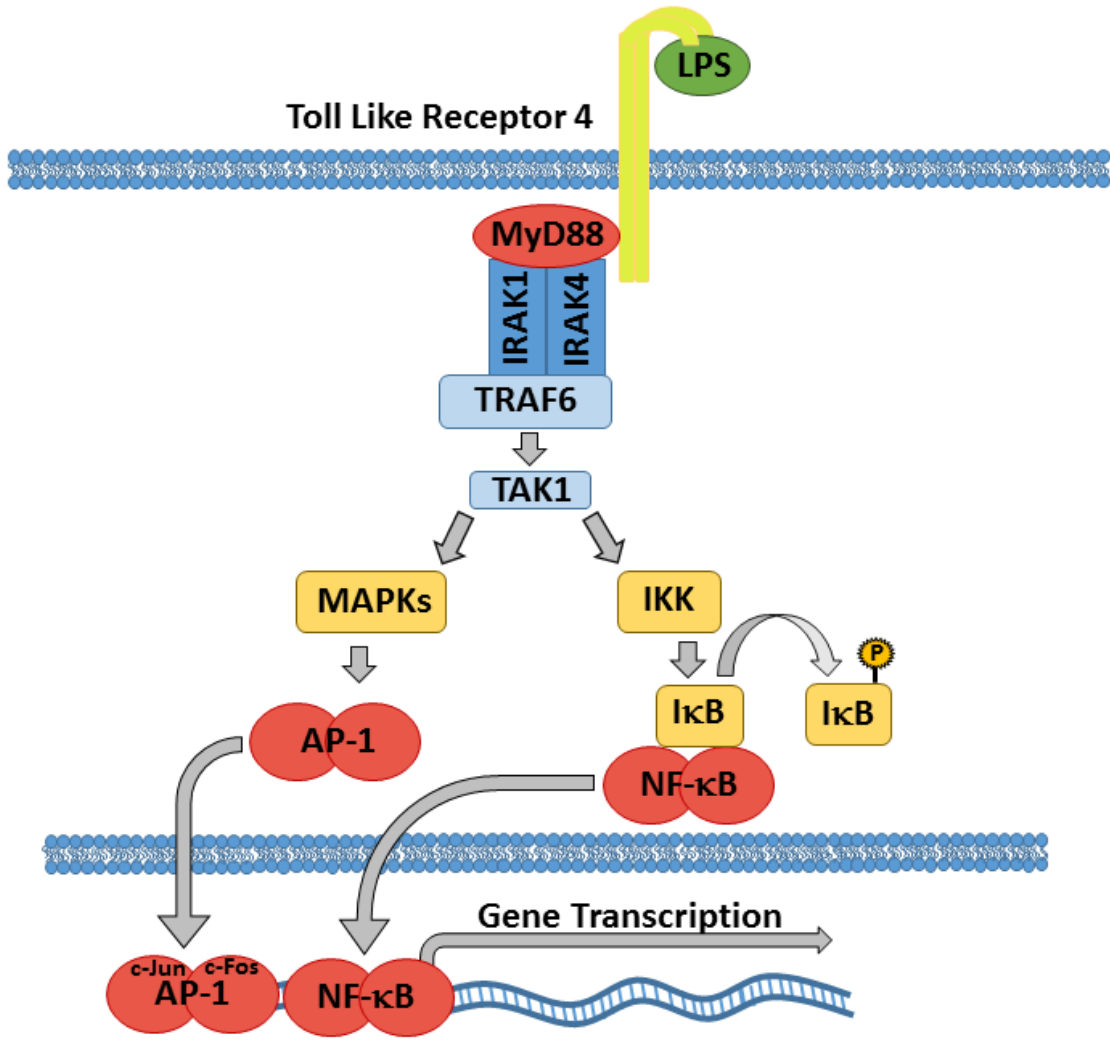


**Illustration 1: Overview of Toll Like Receptor 4 Signaling.**

with Th2 immune responses<sup>53,55</sup>.

As mentioned before these Alternatively Activated macrophages can be generated by stimulation with IL-4 or IL-13. Both of these cytokines involve signaling through the STAT6<sup>45,53</sup> as opposed to the STAT1 mediated signaling pathways that are activated in Classically Activated macrophages<sup>56,57</sup> (Illustration 2). While Classically Activated macrophages express iNOS and thus produce large amounts of nitric oxide, Alternatively Activated macrophages express arginase and produce urea<sup>44</sup>. AA-M $\phi$  have been implicated in protection against helminth and parasitic infections<sup>55</sup>. The molecules secreted by these macrophages have important roles in wound healing due to their anti-inflammatory, fibrotic, proliferative, and angiogenic activities<sup>58</sup>. Despite their protective role, these macrophages have been associated in several pathologies such as allergy and asthma.

### **1.3.3 M1/M2 Classification**

Mills and colleagues, while investigating the arginine metabolism of macrophages in mouse strains with Th1 and Th2 backgrounds, found that macrophages from these mice differed qualitatively in their ability to respond to the classic stimuli IFN- $\gamma$  or lipopolysaccharide (LPS). Hence they introduced a M1/M2 classification systems to mirror the Th1/Th2 classification system of T cells by Mossman and Coffmann<sup>59,60</sup>. Mills and colleagues went further and proposed that the M1/M2 dichotomy was an intrinsic property of macrophages associated with transitions from inflammation to healing. This would occur in the absence of an adaptive immune response and arose early in evolution<sup>60</sup>. Later the M1/M2 system was employed as a way of differentiating between the inflammatory,

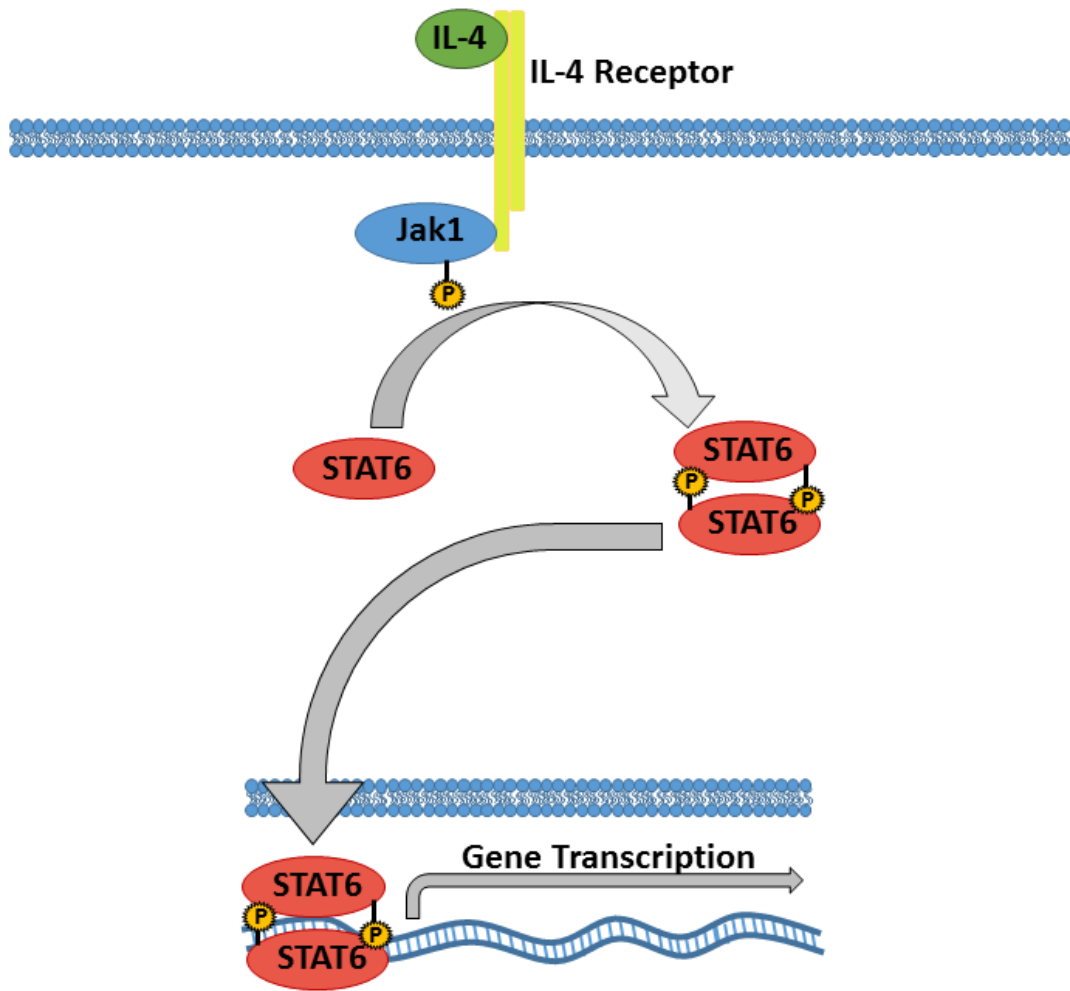


**Illustration 2: Overview of Interleukin-4 Signaling.**

IFN- $\gamma$ /LPS treated macrophages and the non-inflammatory IL-4 treated macrophages. The failure of AA-M $\phi$  to produce nitric oxide has been attributed to their induction of Arginase-1, which converts arginine to ornithine<sup>44,48</sup>. Consequently, Arg-1 has been used as a biomarker to identify AA-M $\phi$ , and several groups have mistakenly identified AA-M $\phi$  in tissue based on their expression of Arg-1. Subsequent demonstrations that multiple stimulated macrophages could produce Arg-1 revealed a fundamental confusion in the field that all non-M1 macrophages are AA-M $\phi$ <sup>61</sup>. This confusion led to the further classification of M2 macrophages into further subsets. At least three different subtypes of M2 macrophages have been defined: M2a macrophages that represent the conventional Alternatively Activated macrophages generated by addition of IL-4 or IL-13, M2b (immune complexes in combination with IL-1 $\beta$  or LPS) and M2c (IL-10, TGF- $\beta$  or glucocorticoids)<sup>62</sup>. Stimulation with G-CSF is a latest addition to these subtypes. The oversimplification of classifying macrophages other than Classically Activated macrophages as M2 macrophages has led to substantial confusion in the field of macrophage biology. First, researchers in the field get confused about which terminology to use and which markers define the subset of macrophages. Secondly, often the M1 and M2 macrophage coexist rather than being a distinct population and the occurrence of these subtypes is dependent on the activation signals in the microenvironment. Finally, it provides a false impression that a macrophage can exist only in one of the two states. This grey area in macrophage phenotypes and functions calls for a revision of macrophage nomenclature in order to create a global language for understanding different macrophage subsets.



### 1.3.4 Regulatory Activation (M2b)

The identification of macrophages with regulatory functions emerged from an unexpected observation that was made by stimulating macrophages in the presence of high-density immune complexes. This resulted in a unique cytokine response that was markedly different from that of Classically Activated macrophages<sup>63</sup>. Previous members of the Mosser lab observed that a combination of a TLR ligand with immune complexes resulted in macrophages that produce high levels of the anti-inflammatory cytokine IL-10 and little to no detectable IL-12<sup>44</sup>. This phenotype was in stark contrast to Classically Activated macrophages that produce high levels of IL-12 but relatively low levels of IL-10. Interestingly, the Regulatory macrophage retained the capability to induce IL-10 even when pretreated with IFN- $\gamma$ <sup>44</sup>. Additionally, stimulating macrophages with a TLR ligand and a secondary signals such as apoptotic bodies, prostaglandins or adenosine was capable of generated macrophages with an immunoregulatory phenotype<sup>40</sup>. The chemokine CCL1 was upregulated in Regulatory macrophages(R-M $\phi$ )<sup>46</sup> and similar to classical activation, the co-stimulatory molecules CD80/CD86 and MHC class II were also upregulated<sup>44</sup>. Interestingly, the high level of IL-10 production by R-M $\phi$  leads to Th2 biasing in T cells<sup>44</sup>. These immunoregulatory macrophages not only differed from Classically Activated macrophages but also from AA-M $\phi$ . While the AA-M $\phi$  participate in wound healing, the Regulatory macrophages appeared to limit tissue damage and did not appear to actively participate in the formation of the extracellular matrix.

The addition of a reprogramming second signal is central to the R-M $\phi$  phenotype. The signals reduce pro-inflammatory IL-12 production and increase anti-inflammatory IL-10 levels<sup>64,65</sup>. The binding of these secondary signals to their receptors causes activation of various signaling pathways. In the case of immune complex binding, there is activation of the Fc receptors which signal through Syk kinase<sup>66</sup>. The activation of Syk in turn activates high levels of the Map kinase, ERK<sup>67,68</sup> (Illustration 3). The activation of ERK results in the phosphorylation of histones associated with the *il-10* promoter, which makes the promoter more accessible to the transcription factors that induce *il-10* gene expression. The binding of adenosine and prostaglandin E<sub>2</sub> to G-protein coupled receptors causes increases in intracellular cAMP levels<sup>69-71</sup>. The increased cAMP level leads to activation of protein kinase A and subsequently to CREB transcription factor activation (Illustration 3). Additionally, G protein coupled receptor signaling leads to Ras activation with the end result being increased ERK activation. While these signaling pathways arise from different signaling proteins, they result in the induction of IL-10. Thus, although R-M $\phi$  shares some of the phenotypes of M1-M $\phi$  and AA-M $\phi$ , they are distinguished by exhibiting an immunoregulatory phenotype.

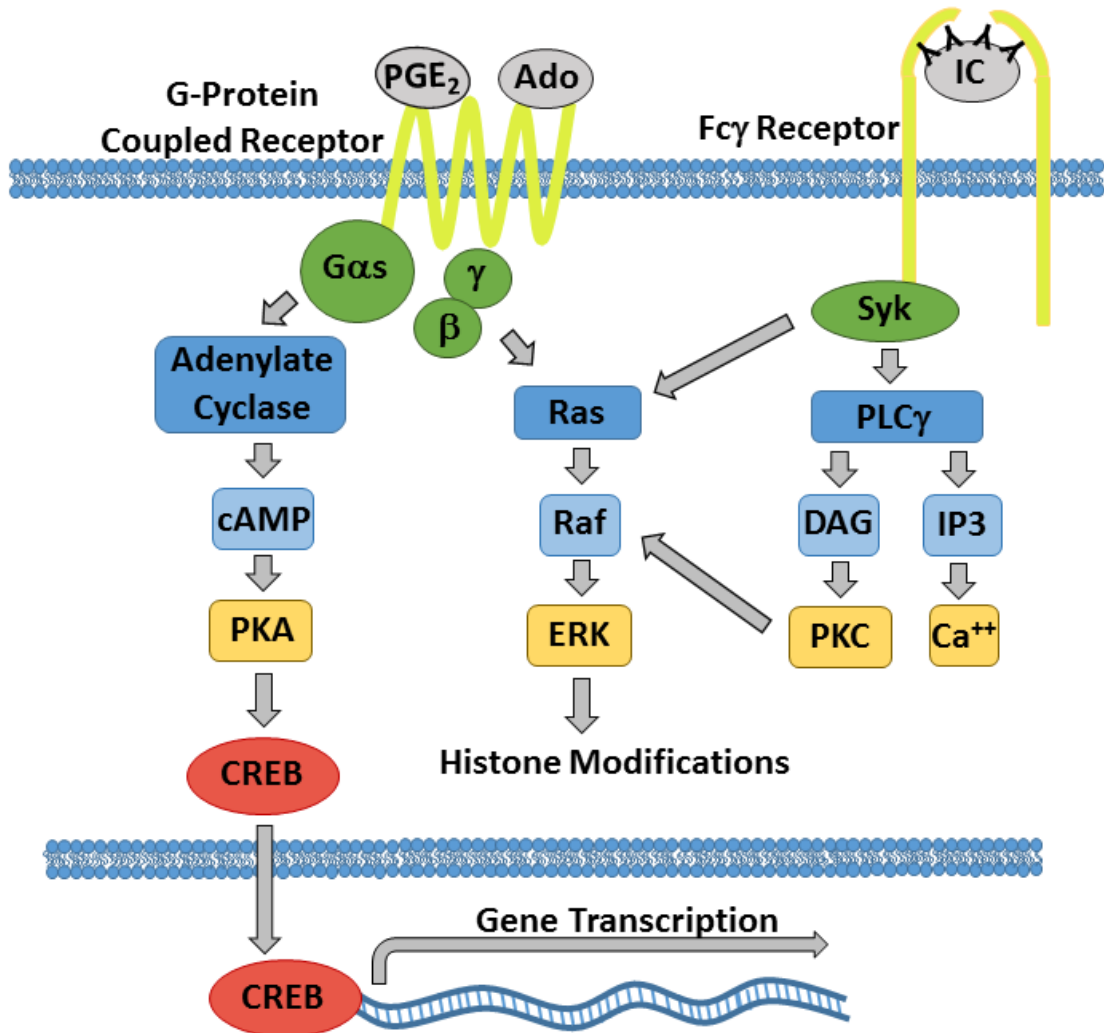


**Illustration 3: Overview of Receptor Signaling in Regulatory Activation.**

Despite the advances we made in understanding of these Regulatory macrophages, there are still many unknown aspects of these cells. The in vivo significance of this population in the context of a disease or an infection, the in vivo generation or occurrence of these cells and the markers that define regulatory activation are still poorly understood topics. This study aims at identifying stable markers to define R-M $\phi$  and their in vivo significance in an infection model.

### **1.3.5 Color Wheel**

As macrophage activation has become better understood, the need for a broader classification system became apparent. The linear M1/M2 was not capable of accommodating the macrophages with immunoregulatory abilities or those that arose from multiple cellular stimulations. The understanding that macrophages activation was no longer linear, led to our proposed color wheel model to be adopted (Illustration 4)<sup>40</sup>. This model allows the accommodation of the three distinct macrophage subpopulations: the Classically Activated macrophages/M1-M $\phi$ , the Alternatively Activated macrophages, and the Regulatory macrophages. Additionally, this color wheel scheme accounts for the existence of hybrid activation states that share phenotypic traits associated with multiple activation states. This model has helped us to understand the plasticity of macrophages, which the linear model of macrophage activation was unable to explain. Further, this model can accommodate the yet to be defined shades of activation resulting in a spectrum of macrophage populations and functions.

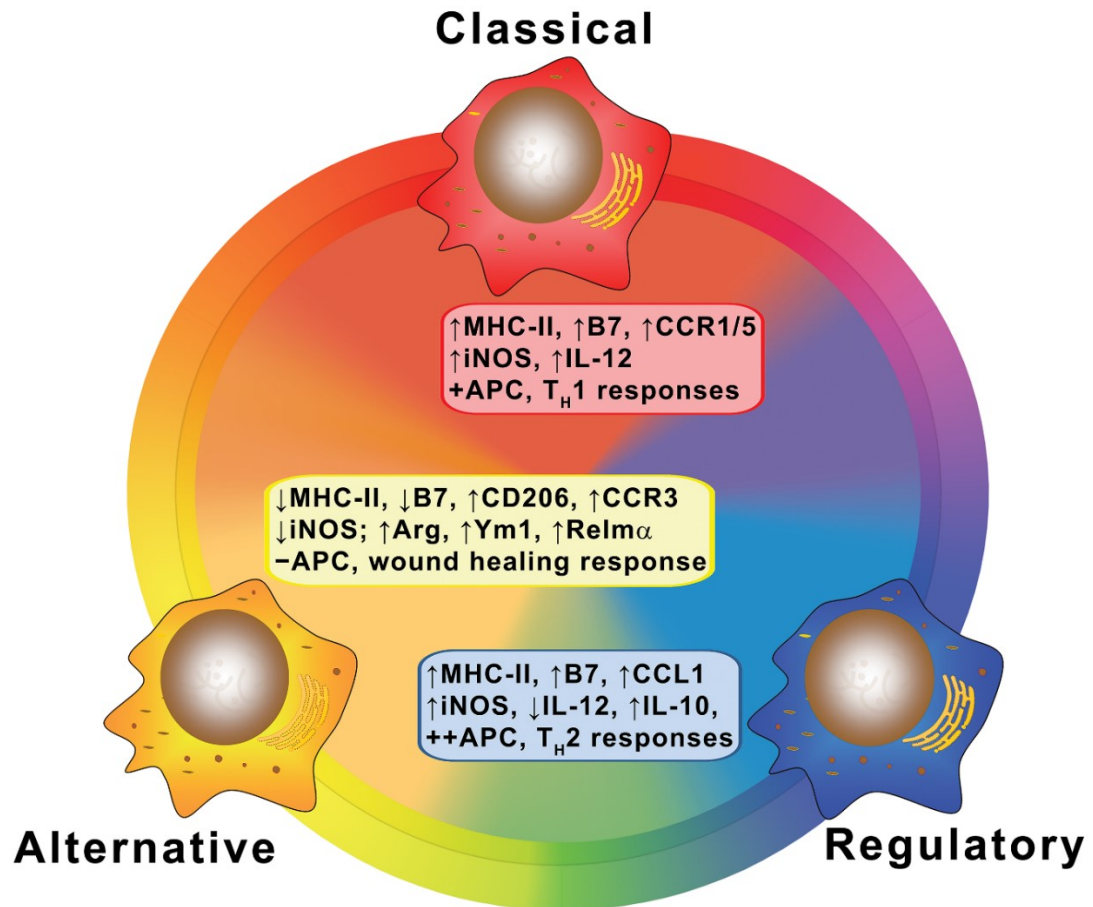


**Illustration 4: Color Wheel.** The three major macrophage subtypes and some of the biochemical and physiological properties of each.  $\uparrow\downarrow$  designated high or low expression in this subpopulation, related to the other three: ++, +, -, designates relative activity from high (++) to absent (-). Adapted from the *European Journal of Immunology*, “Regulatory macrophages: Setting the Threshold for Therapy”, 2011. **41**:2500.

## Chapter 2: Tools for Studying Macrophages

### 2.1 Studying at the DNA Level

#### 2.1.1 Background

All gene expression starts with the transcription of DNA into RNA. The sequences that make up the promoter region and the accessibility of these sites to transcription factors determine whether or not a gene will be expressed. The availability of genomic sequences has provided a new tool in studying gene expression. It is possible to analyze promoter sequences in an attempt to predict transcription factor binding sites<sup>72</sup>. Additionally, conserved patterns like start codons and splice junctions, can help identify previously undiscovered genes. The organization of DNA into nucleosomes provides a second level of regulation. The nucleosome is a histone-DNA complex that undergoes structural rearrangements to facilitate or inhibit transcription factor binding. The histone-histone or histone-DNA interactions together with the histone modifications elicit effects such as gene activation or gene repression<sup>73,74</sup>. The type of histone subunits, such as H1, H2A, H2B, H3 or H4 or their subtypes can have a direct effect on how they will be modified following signaling cascade activation<sup>75</sup>. Some of these modifications are long-lived and can be used as indicators of differentiation states of various cell types. The stable differentiation of T cells into Th1 or Th2 lineage is a good example of such long-lived epigenetic modifications<sup>76</sup>.

### **2.1.2 Experimental Applications**

The regulation of gene expression at the level of DNA was vital for the understanding of the “reprogramming signal” and the induction of IL-10 in Regulatory macrophages. Work by Lucas et al from the Mosser lab showed that ERK kinase activation following Fc $\gamma$ R ligation in R-M $\phi$  leads to chromatin modifications at the IL-10 locus<sup>67,77</sup>. Through chromatin immunoprecipitation assays (CHIP), the authors demonstrated that activation of ERK leads to the serine phosphorylation on histone H3 at the *il-10* gene, making the promoter more accessible to transcription factors<sup>67</sup>. Further work by Zhang et al., in the Mosser lab used CHIP assays and phosphorylation studies to explore the kinetics of histone modification. and showed that the histone phosphorylation and not acetylation was the proximal event to IL-10 induction<sup>77</sup>. Cao et al. from the Mosser lab utilized electrophoretic mobility shift assays and reporter assays to show that NF- $\kappa$ B1 (p50) homodimers can be transcriptional activators of IL-10.<sup>78</sup> These molecular methods were used by previous lab members to demonstrate the epigenetic and transcriptional modifications associated with Regulatory macrophages.

## **2.2 Studying at the RNA Level**

### **2.2.1 Background**

Studying the levels and kinetics of mRNA expression can help us to predict how the protein signature of these cells will be affected. Gene expression profiling assays have been a valuable tool in studying alterations in mRNA expression. The first high throughput technology to study gene expression profile was the DNA microarray. This technology

relied on the hybridization of labeled RNA to gene specific probes adhered to a substrate. The comparative analysis of label intensities allowed researchers to quantify the relative expression level of numerous genes in multiple samples<sup>79</sup>.

Recent advances in nucleotide sequencing have allowed for the development of a new technology known as RNA-seq (RNA sequencing) or WTSS (Whole Transcriptome Shotgun Sequencing). RNA-seq has revolutionized the way in which molecular biology research can be conducted. Researchers can now isolate total RNA from a cell and identify the origin of these transcripts through sequencing. RNA-seq provides wider coverage of the studied genes and provides a snapshot of the RNA expression in the studied cell types. RNA-seq technology helps us to identify previously unknown genes, micro RNAs and splice variants. All of these advances have made RNA-seq a powerful tool for studying gene expression in macrophages<sup>80</sup>.

Examining relative changes in RNA expression was made possible by real time PCR. A real time polymerase chain reaction is used to amplify and simultaneously detect or quantify a targeted cDNA molecule that have been synthesized from a RNA sample. Two common methods of quantitative real time PCR (qRT-PCR) are: (1) relative quantification that uses non-specific fluorescent dyes that intercalate with any double-stranded DNA, and (2) absolute quantification, which uses sequence-specific probes along with a fluorescent reporter<sup>81</sup>.



### **2.2.2 Experimental Applications**

To study the differences in the gene expression profile between CA-M $\phi$  and R-M $\phi$ , this lab previously utilized microarray analyses. The results of that data helped to first identify *tnfsf14* and *hb-egf* genes to be associated with regulatory activation<sup>44,82</sup>. To identify genes that were dependent on ERK activation, we performed microarray analysis in R-M $\phi$  pretreated with the MEK inhibitor U0126. From these unpublished results, we predicted that IL-33 was a MEK dependent regulatory marker in R-M $\phi$ . Attempts are underway to validate this finding.

To further characterize R-M $\phi$  and the markers associated with it, we had to take a better approach that would provide us a wider coverage of the genes studied. Therefore, in the study presented in this dissertation, we performed RNA-seq analyses on M1-M $\phi$  (LPS stimulation), AA-M $\phi$  (IL-4 stimulation) and Regulatory macrophages obtained from two different stimuli LPS stimulation paired with OVA-IC or adenosine. The results obtained from RNA-seq were validated using the qRT-PCR assays. The result of this study is to follow in the Results and Discussion section of this dissertation.

## **2.3 Studying at the Protein Level**

### **2.3.1 Background**

One of the most well established ways of characterizing macrophage activation states has been through the identification of secreted cytokines. The switch between IL-12 and IL-10 productions has been documented as the major change between CA-M $\phi$  and R-

M $\phi$ <sup>44</sup>. The cytokine measurements are usually obtained by Enzyme linked immunosorbent assay (ELISA) that utilizes a pair of antibodies targeted for each cytokine to be characterized. While ELISA remains the best way to quantify the protein levels, it limits the number of cytokines that can be examined at once. Another commonly used semi-quantitative method is western blotting which can detect a specific protein in a given sample.

The development of high throughput methods such as protein membrane arrays and multiplex assays has allowed researchers to examine several proteins in a single experiment. The membrane array is done by measuring the amount of protein that has hybridized to a nitrocellulose membrane spotted with multiple antibodies. Although this method helps for the initial screening of the proteins, it is only a semi-quantitative method. Multiplex assays, on the other hand, provide a quantitative tool that enables one to quantify several proteins in the sample by utilizing target specific fluorochrome conjugated beads. Multiparametric analysis at the cellular level was made possible with the advent of flow cytometry. The technique allows high throughput automated analysis of various parameters using lasers and fluorochromes. Flow cytometry is a widely used technique especially in the field of immunology and other fields of biology.

The advancements in mass spectrophotometry have enabled the identification of proteins present by analyzing their amino acid sequence composition. Researchers can fractionate cytosolic or membrane bound proteins and analyze their expression<sup>83</sup>. This technology might be limited in the ability to quantify the amounts of protein being made, but it could prove invaluable in the identification of novel biomarkers.

### **2.3.2 Experimental Applications**

For this study, I utilized ELISA, protein membrane array, multiplex assay and flow cytometry. ELISA was used to assess the cytokine levels in the supernatants of the stimulated macrophages. Protein membrane array was used to identify the proteins that are differentially regulated in R-M $\phi$  compared to other types. Flow cytometry was used to check if the high mRNA expression of some of the genes identified by RNA-seq analyses was translated at the protein level. Finally, multiplex assay was used to quantitate cytokine/chemokine levels secreted by human macrophages.

### **2.4 Research Objectives**

The previous work by members of the Mosser lab has laid the groundwork for our understanding of how the Regulatory macrophage is generated and how these cells respond during activation. The research described in this dissertation focuses on several important aspects of regulatory activation that have been poorly described. First, I will determine if adenosine and prostaglandin E<sub>2</sub> are capable of inducing regulatory activation in macrophages and will determine if all Regulatory macrophages have the same phenotype. Second, I will identify the core genes required for the immunoregulatory phenotype. This will serve to both identify new therapeutic targets, as well as help us to understand how the macrophage interacts with the immune system. Third, I will use the core genes to identify stable biomarkers that can be used to identify Regulatory macrophages. The ability to identify a macrophage's activation state in tissue would benefit countless diagnostic and therapeutic applications. Fourth, I will determine what role the Regulatory macrophage

plays in the disease endotoxemia. Finally, I will compare the various Regulatory macrophages to Alternatively Activated macrophages to determine if they share phenotypic similarities. This research will help us to better understand the mechanisms for regulatory activation and provide important information that will help in the classification of activated macrophage.

## Chapter 3: Comparative Analysis of Activated Macrophage Populations

### 3.2 Introduction

The plasticity of macrophages allows these cells to undergo dramatic alterations in their phenotype in response to diverse environmental stimuli<sup>40,84-88</sup>. This phenotypic heterogeneity of macrophages has led to a substantial degree of confusion in the field about how best to name these cells. This is not simply a semantic problem. A better understanding of the phenotypic alterations that macrophages undergo is necessary if we eventually hope to manipulate immune responses at the level of macrophages. Studies on macrophage heterogeneity can put us in a better position to generate macrophages with a predictable phenotype, to deplete one set of macrophages while preserving others, or to target drugs to individual subpopulations of macrophages.

The pioneering work of Gordon and colleagues in the 1990s helped to define two paradigmatic populations of macrophages, generally referred to as “Classical” *versus* “Alternative” but later termed M1 *versus* M2, or M(IFN- $\gamma$ ) *versus* M(IL-4)<sup>45,51,87,89</sup>. Exposing macrophages to IFN- $\gamma$  and TLR ligands results in an upregulation of inflammatory cytokines, an increased MHC class II and co-stimulatory molecule expression, and the production of antimicrobial products<sup>51,90-93</sup>. Cells exposed to IL-4, in contrast, fail to upregulate co-stimulatory molecules and MHC class II, are poor antigen presenting cells, and produce negligible amounts of nitric oxide. These cells express higher levels of chitinases and lectin-like receptors and are termed Alternatively Activated

macrophages (AA-M $\phi$ )<sup>51,94,95</sup>. The linear M1/M2 classification system remained the standard for describing macrophage activation states for nearly a decade. Gradually, investigators came to appreciate the limitations of this narrow classification system and attempted to expand the M2 classification to include macrophages that were treated with glucocorticoids, anti-inflammatory cytokines, extracts from tumors, apoptotic cells, immune complexes, or adenosine derivatives, to name a few.

A color wheel scheme was proposed to highlight the plasticity of macrophages<sup>40,96</sup>. This model placed an emphasis on the dynamic nature of macrophage activation and proposed that macrophages can readily transition from one activation state to another. Therefore certain tissue resident macrophages may not express clear phenotypic characteristics of a single population. In this study, we examine five different macrophage populations from different segments of the color wheel and demonstrate that macrophages treated with IL-4 are transcriptionally and phenotypically distinct from three macrophage populations with immunoregulatory phenotypes. We also show that although these three immunoregulatory macrophage populations can be distinguished from each other at the global transcriptome level, they all share a number of characteristics that endow them with immunoregulatory activity, including the reduced production of inflammatory cytokines and the secretion of growth and angiogenic factors. Therefore we loosely group them together as Regulatory macrophages (R-M $\phi$ ). We describe chemokine and cytokine signatures of R-M $\phi$  and demonstrate their functionality during inflammatory conditions.

### **3.3 Methods and Materials**

#### **3.3.1 Mice**

Five-week-old BALB/c mice were purchased from Charles River (Frederick, MD). Mice were used at 6-10 weeks of age as a source of bone marrow to culture bone marrow derived macrophages (BMDM). All mice were maintained in high-efficiency particulate air-filtered Thoren units (Thoren Caging Systems, Hazleton, PA) at the University of Maryland (College Park, MD) animal facility. All procedures were reviewed and approved by the University of Maryland Institutional Animal Care and Use Committee.

#### **3.3.2 Murine Macrophage Generation**

Bone marrow derived macrophages (BMDM) were obtained by flushing the femurs and tibiae of BALB/C mice, and plating the cells in petri dishes containing BMM medium (DMEM/F12 medium with 10% fetal bovine serum, 1% glutamine, 1% penicillin/streptomycin and supplemented with 15% L929 cell conditioned media (LCCM)). Cells were grown in a 37 °C incubator with 5% CO<sub>2</sub> and fed again with BMM/15% LCCM on day 3. For peritoneal macrophages, female mice were sacrificed and their peritoneal cavity was lavaged with cold 8-10 ml of PBS (Ca<sup>2+</sup>/Mg<sup>2+</sup> free). Cells obtained from 10-12 mice were pooled, washed, and suspended in DMEM/F12 medium supplemented with 10% FBS, glutamine, and antibiotics and plated in a 6 well plate at a density of 2x10<sup>6</sup> cells/ml. After overnight resting, the cells were stimulated with LPS, LPS+IC, LPS+adenosine, or IL-4 as indicated under the '*Cell Culture and Stimulation*' section. After 4 hours of stimulation, the medium was removed and the RNA was extracted

from the cells using the TRIzol-chloroform method according to the manufacturer's instructions. RNA-seq analyses were performed separately on three different sample sets obtained on different days.

### **3.3.3 Human Macrophage Culture**

Peripheral blood was collected from six healthy human volunteers and the mononuclear cells were separated by Ficoll-Hypaque density gradient centrifugation. The cells were incubated in 12 well tissue culture plates in the presence of plain RPMI medium (Gibco, Grand Island, NY) for two hours. The non-adherent cells were removed with four washes of HBSS. The adhered monocytes were cultured for a week in RPMI 1640 medium supplemented with 10% human AB serum (Life Technologies, Grand Island, NY) in the presence of 1% glutamine, 1% penicillin/streptomycin, and 50 ng/ml of M-CSF (Peprotech, Rocky Hill, NJ). The media was replaced with fresh media after 72 hours and 12 hours before stimulation. An additional wash to remove dead and non-adherent cells was carried out with HBSS before adding the fresh media for stimulation. All studies on human monocyte-derived macrophages were approved by the University of Maryland, Institutional Review Board (484966-2).

### **3.3.4 Cell Culture and Stimulation**

LPS treated macrophages were generated by adding 10 ng/ml ultra-pure LPS (Invivogen, San Diego, CA). Regulatory macrophages were obtained by stimulating BMDMs in the presence of 10 ng/ml LPS and one of the following “reprogramming” signals: high density immune complexes generated as previously described<sup>97</sup> by adding 1 µg OVA (Worthington Biochemical, Lakewood, NJ) to 120 µg anti-OVA (Polysciences,



Warrington, PA) in a volume of 21  $\mu$ l, 200  $\mu$ M PGE<sub>2</sub> (Cayman Chemical, Ann Arbor, MI), or 200 nM adenosine (Sigma-Aldrich, St. Louis, MO) (designated in the text as RM $\phi$ -IC, RM $\phi$ -PGE<sub>2</sub> and RM $\phi$ -Ado, respectively). Alternatively Activated macrophages were generated by adding 20 ng/ml mouse IL-4 (R&D Systems, Minneapolis, MN) to macrophages and designated AA-M $\phi$  in text. For RNA isolation, 2x10<sup>6</sup> BMDM (day 7-10) were stimulated in six well plates for 2-6 hours as indicated in the figures. For cytokine analyses of cell culture supernatants, 2.5x10<sup>5</sup> BMDM were placed in 48 well plates in a volume of 0.5 ml and stimulated for 12-16 hours. For the membrane protein array, 2x10<sup>6</sup> BMDM were stimulated for 12 hours in a six well plate in 1 ml of media. For the bioplex analyses, differentiated human macrophages were plated at a concentration of 5x10<sup>5</sup> macrophages/ 0.5 ml in 48 well plates and supernatants were collected after 24 hours. The supernatants were stored at -80 °C until assayed.

### **3.3.5 ELISA**

IL-12/23p40 and IL-10 levels were measured from cell-culture supernatants by sandwich ELISA method using antibodies purchased from BD Pharmingen (San Diego, CA) ([IL-12p40- C15.6 and C17.8], [IL-10- JES5-2A5 and JES5-16E3]) according to manufacturer's instructions. IL-1 $\beta$ , IL-6 and human IL-12/IL-23p40 levels were measured using Duoset ELISA kits (R&D systems, Minneapolis, MN), following manufacturer's instructions.

ELISA was performed by coating high bind plates with 100  $\mu$ l capture antibody in phosphate binding buffer overnight at 4 °C or at room temperature for 2 hours. Plates were

washed three times with ELISA wash buffer (PBS with 0.05% Tween20), followed by 200  $\mu$ l of blocking buffer (ELISA wash buffer + 10% FBS). After a 30 minute incubation at room temperature, plates were washed three times with ELISA wash buffer. Samples and serially diluted standards (typical diluted in RPMI with concentrations ranging from 4000 pg/ml to 15.625 pg/ml) were incubated in the wells overnight at 4 °C or at room temperature for 3 hours. Plates were washed three times with ELISA wash buffer, followed by a one hour incubation of detection antibody diluted in blocking buffer. Wells were washed four times with ELISA wash buffer, followed by the addition of 100  $\mu$ l of diluted streptavidin-AP or streptavidin-HRP in blocking buffer. Wells were washed five time and loaded with pNPP substrate or TMB substrate solution. Plates were developed for up to 30 minutes and HRP reactions were stopped with 0.2 M H<sub>2</sub>SO<sub>4</sub>. Optical densities were determined at 405 nm (pNPP substrate) or 450 nm (TMB substrate), with background readings taken at 595 nm.

### **3.3.6 Membrane Protein Array**

Mouse cytokine antibody array membranes (Proteome Profiler Antibody Array<sup>TM</sup> (Panel A), R&D systems, Minneapolis, MN) were used to assess the relative differences of 40 different cytokines and chemokines in the supernatants of various macrophage populations. The array was performed following manufacturer's instructions and the chemiluminescence was detected and the density was quantified using LAS-3000 Imaging systems from Fujifilm (Tokyo, Japan). The protein levels on each array were normalized

against a positive internal control provided with the array. Stimulation details can be found in the '*Cell Culture and Stimulation*' section.

### **3.3.7 Bioplex Assay**

The levels of cytokines/chemokines were measured from the supernatants of human macrophage cultures collected after 24 hours using the human magnetic Luminex screening assay (R&D systems, Minneapolis, MN). A 14-plex assay was carried out for the detection of secreted proteins following manufacturer's protocol. The samples were acquired in Magpix® and data was analyzed with the Luminex xPONENT software (Luminex Corporation, Austin, TX). The sample concentrations were calculated from the standard curves using five-parameter regression analyses. The obtained data was analyzed and plotted using Graphpad prism Version 6 software (Graphpad Software Inc, La Jolla, CA). Stimulation details can be found in the '*Cell Culture and Stimulation*' section.

### **3.3.8 RNA Isolation and cDNA Synthesis**

RNA was isolated from  $2 \times 10^6$  cells using TRIzol according the manufacturer's specifications. Complementary DNA (cDNA) was synthesized from 2 µg equivalent of RNA using cDNA synthesis kit (Invitrogen, Grand Island, NY), according to the manufacturer's instructions. Briefly, RNA was diluted up to 10.5 µl with nuclease free water, then 4 µl 5x cDNA buffer, 2 µl dNTP, 1 µl DTT, 1 µl RNaseOut, 1 µl Oligo dT<sub>20</sub>, and 0.5 µl Thermoscript RT was added. Transcription was carried out for 65° C for 5

minutes, 60 °C for 60 minutes, 85 °C for 5 minutes, then held at 37 °C. Followed by 1 µl of RNaseH, an incubation at 37 °C for 20 minutes and 179 µl to dilute the sample.

### **3.3.9 Conventional PCR**

PCR reactions were set up by adding 2 µl of diluted cDNA, 1 µl each of sense and anti-sense primers (5 pmols), 8.5 µl of nuclease free water and 12.5 µl of 2x PCR master mix (Fermentas, Pittsburgh, PA) for each reaction. PCR was carried out with denaturation for 95 °C for 5 minutes, DNA amplification for 30 cycles of 95 °C for 40 seconds, 58 °C for 40 seconds, 72 °C for 60 seconds, with a final extension at 72 °C for 7 minutes. Primers pairs that were used in this study are listed in **Table 1**.

**Table 1. Primer Pair Sequences**

Gene	Accession number	Primers (Amplicon Length)
<i>il-12p40</i>	NM_008352	5'-AAGACGTTTATGTTGTAGAGGTGGAC-3' (180) 5'-ACTGGCCAGGATCTAGAACTCTTT-3'
<i>il-10</i>	NM_010548	5'-GACTTTAAGGGTTACTTGGGTTGC-3' (190) 5'-TCTTATTTTCACAGGGGAGAAATCG-3'
<i>relm<math>\alpha</math></i>	NM_020509	5'-AATCCAGCTAACTATCCCTCCA-3' (103) 5'-CAGTAGCAGTCATCCCAGCA-3'
<i>ym1</i>	NM_009892	5'-AGGGTAATGAGTGGGTTGGT-3' (220) 5'-AGCTCCTCTCAATAAGGGCC-3'
<i>il-33</i>	NM_133775	5'-ATGGGAAGAAGCTGATGGTG-3' (150) 5'-CCGAGGACTTTTTGTGAAGG-3'
<i>flrt3</i>	NM_01172160	5'-TCTGGCTTATATGAGATGCTTGA-3' (197) 5'-GTCATGGCAACAAAAAGTGG-3'
<i>ccr1</i>	NM_009912	5'-AAGAGCCTGAAGCAGTGGAA-3' (204) 5'-CAGATTGTAGGGGGTCCAGA-3'
<i>gem</i>	NM_010276	5'-TTGAAGGCTATTGGGACCAG-3' (228) 5'-AACTCATGTGAACCCGAAGC-3'
<i>ildr1</i>	NM_134109	5'-CAAACCTGGCCTGAGGAGAAG-3' (164) 5'-AAGGCAGCTGGAACCTTGA-3'
<i>empl</i>	NM_010128	5'-CTCCCTTGTGGTCTTCGTGT-3' (163) 5'-GCTGCTGGAGTTGAAGTTCC-3'
<i>il-4il</i>	NM_010215	5'-AGCTTTGCAGAAGCCTTACG-3' (152) 5'-TGAGTGATCGACACCACAGG-3'
<i>ear11</i>	NM_053113	5'-CAACTCCGGCCAGTCATTAT-3' (234) 5'-TGACATGCAGTGCAAACAGA-3'
<i>cd209e</i>	NM_130905	5'-GGAGAATGGTACTGGCTGGA-3' (211) 5'-TGCAGAGAACGTCTGGTCAC-3'
<i>ndrg1</i>	NM_008681	5'-CATGAATGTGAACCCCTGTG-3' (213) 5'-CTGTTGTAGGCGCTGATGAA-3'
<i>klk9</i>	NM_028660	5'-GGATCTGAGCCTTGTTCCAG-3' (162) 5'-GAATCCTGCAGCATCCTCTC-3'
<i>dupl4</i>	NM_019819	5'-TGGGTGTTCCGGTTTAAGAG-3' (204) 5'-GAGCTCCTACTGCACCTGCT-3'
<i>hc</i>	NM_010406	5'-ACCAGATAAGCAGTGCACCA-3' (209) 5'-CAGTGGCTGATGTGATCCTG-3'
<i>tnfsf14</i>	NM_019418	5'-CTGCATCAACGTCTTGGAGA-3' (205) 5'-GATACGTCAAGCCCCTCAAG-3'

**Table 1. Primer Pair Sequences (Cont.)**

Gene	Accession number	Primers (Amplicon Length)
<i>cd244</i>	NM_018729	5'-AGTGCAAGCCTTCTGATTCC-3' (242) 5'-CTGCATGACACAGGATGAGG-3'
<i>lif</i>	NM_008501	5'-CTTGCTTGCTGGGTGTATGA-3' (171) 5'-GATCCCAGTCCCCTTAGCTC-3'
<i>xcr1</i>	NM_011798	5'-TCATCTTCACCGTCGTGGTA-3' (156) 5'-AGCAATGAGAGAAGGCCAAA-3'
<i>mid1</i>	NM_010797	5'-CCTCAGAGGACGAGTTCAGC-3' (205) 5'-TACTTGGTGCCACTTTGCAG-3'
<i>mospd4</i>	NR_045438	5'-GCCTCTTCCTGTTGTTCTGC-3' (175) 5'-CGGGCCATACTTCCAATAGA-3'
<i>gapdh</i>	NM_008084	5'-AAGGTCGGTGTGAACGGATTT-3' (155) 5'-AATTGCCGTGAGTGGAGTCATAC-3'

### 3.3.10 qRT-PCR

Relative quantification of RNA was done using SYBR-Green based quantitative real time PCR. The samples were run in Roche LightCycler® 480, in a 96 well plate. Each well contained 5 µl of diluted cDNA, 1 µl each of sense and anti-sense primers (5 pmol), 5.5 µl of nuclease free water and 12.5 µl of 2x go-Taq PCR master mix (Promega, Madison, WI). For data analysis, the comparative threshold cycle ( $C_T$ ) value for *gapdh* was used to calculate relative differences. The fold induction of RNA was calculated using  $2^{-(\Delta\Delta C_T)}$  method<sup>98</sup>.

### 3.3.11 RNA-seq Data Generation and Processing

Poly(A)-enriched cDNA libraries were generated using the Illumina TruSeq Sample Preparation kit (San Diego, CA). Paired end reads (100 bp) were obtained from the Illumina HiSeq 1500 platform. Trimmomatic<sup>99</sup> was used to remove any remaining Illumina adapter sequences from reads and to trim off bases with quality scores below 20. Sequence quality metrics were assessed using FastQC [<http://www.bioinformatics.babraham.ac.uk/projects/fastqc/>]. Reads were aligned to the *Mus musculus* genome (v. mm10/GRCm38) obtained from the UCSC genome browser (<http://genome.ucsc.edu>) using TopHat (v 2.0.10)<sup>100</sup>. Reads were allowed to map only to a single locus. The abundance of reads mapping to each gene feature was determined using HTSeq [<http://www-huber.embl.de/users/anders/HTSeq/>].

### **3.3.12 Data Quality Assessment and Differential Expression Analysis**

Multiple approaches were used to evaluate replicates and to visualize sample-sample distances, including Principal Component Analysis (PCA) and Euclidean distances-based hierarchical clustering. All components of the statistical pipeline, named cbcSEQ, can be accessed on GitHub (<https://github.com/kokrah/cbcSEQ/>). Non-expressed and weakly expressed genes were removed prior to differential expression analysis and a quartile normalization scheme was applied to all samples<sup>101</sup>. Limma (a Bioconductor package)<sup>102</sup> was used to conduct differential expression analyses following log<sub>2</sub> data transformation and the application of the voom<sup>103</sup> method. Experimental batch effects were adjusted for by including batch/experimental date as a covariate in the statistical model<sup>104</sup>. Differentially expressed genes were defined as genes with a Benjamini-Hochberg multiple-testing adjusted p value of < 0.05.

### **3.3.13 Ingenuity Pathway Analysis**

Ingenuity Pathway Analysis (IPA) software<sup>105</sup> was used to predict ‘Diseases and Functions’ and ‘Canonical Pathways’ associated with each macrophage population. The ‘Diseases and Functions’ associations were determined by comparing R-M $\phi$  to LPS stimulated (M1) macrophages. LPS treated and IL-4 treated macrophages were compared individually to resting macrophages. Canonical pathways were determined by comparing stimulated conditions to resting macrophages. Genes that exhibited less than a two-fold difference were excluded from the comparisons.



### **3.3.14 Macrophage Metabolism**

BALB/c bone marrow derived macrophages were plated in 48 well plates in 0.5 ml of BMM medium at a concentration of  $5 \times 10^5$  cells per ml. The five activated conditions were generated as described in the '*Cell Culture and Stimulation*' section. At 24 hours post stimulation, the media were collected and glucose levels were determined by using a Glucose Assay Kit (Sigma-Aldrich, St. Louis, MO) per the manufacturer's instructions. In the L-lactate experiment, cells were plated in a similar fashion, but the media were replaced with phenol red-free RPMI prior to stimulation. Cell culture supernatants were removed 8 hours post stimulation and L-lactate production was determined using L-lactate kit I (Eton Biosciences, San Diego, CA) per the manufacturer's instructions.

### **3.3.15 Flow Cytometry**

Surface expression of mouse CCR1 was detected using antibodies conjugated to the PE fluorochrome. Antibody was purchased from R&D Systems (Minneapolis, MN) and the staining was carried out in FACS buffer (1x PBS + 3% FBS) for 15 minutes. Expression was measured at 24 hours post-stimulation. Data acquisition was carried out using FACSCanto™ II (BD biosciences, Franklin Lakes, New Jersey) and the analyses were done using FlowJo version 10.

### **3.3.16 Lethal Endotoxin Challenge**

BALB/c BMDMs were plated in low bind 6 well plates and stimulated under various conditions. Cells were washed, pelleted at 300 g for 5 minutes, resuspended at  $1 \times 10^6$  cells/ 100  $\mu$ l PBS ( $\text{Ca}^{2+}$ / $\text{Mg}^{2+}$  free) and injected intraperitoneally into BALB/c mice.

Three hours after cell transplantation, mice were challenged with 10 mg/kg lethal dose of endotoxin (L2630, Sigma-Aldrich, St. Louis, MO). Survival of the mice was monitored and recorded for a week.

### **3.3.17 Statistics**

Non-parametric t-tests were performed to calculate the significance of the observed differences. A p value of <0.05 was considered to be significant for all analyses. The data in the graphs represent mean  $\pm$  standard error of the mean (SEM).

## **3.4 Results**

### **3.4.1 Cytokine and Chemokine Profiles of Immunoregulatory Macrophages**

To better understand the differences between Alternatively Activated macrophages (AA-M $\phi$ ) and Regulatory macrophages (R-M $\phi$ ), cytokine and chemokine profiles of five different stimulation conditions were examined and compared. The macrophages studied included M1 macrophages (M1-M $\phi$ ) treated with the TLR4 ligand LPS, Alternatively Activated macrophages that received IL-4 (AA-M $\phi$ ), and macrophages that were stimulated with LPS in the presence of three different “reprogramming” stimuli: immune complexes (RM $\phi$ -IC), prostaglandin E<sub>2</sub> (RM $\phi$ -PGE<sub>2</sub>), or adenosine (RM $\phi$ -Ado). The addition of these reprogramming signals to macrophages resulted in dramatic changes in their cytokine and chemokine expression. As expected, M1-M $\phi$  stimulated with LPS exhibited an inflammatory phenotype, secreting high IL-12/23p40, IL-1 $\beta$ , and IL-6 but low levels of IL-10 (Figure 1). Macrophages stimulated with LPS and reprogrammed with IC,

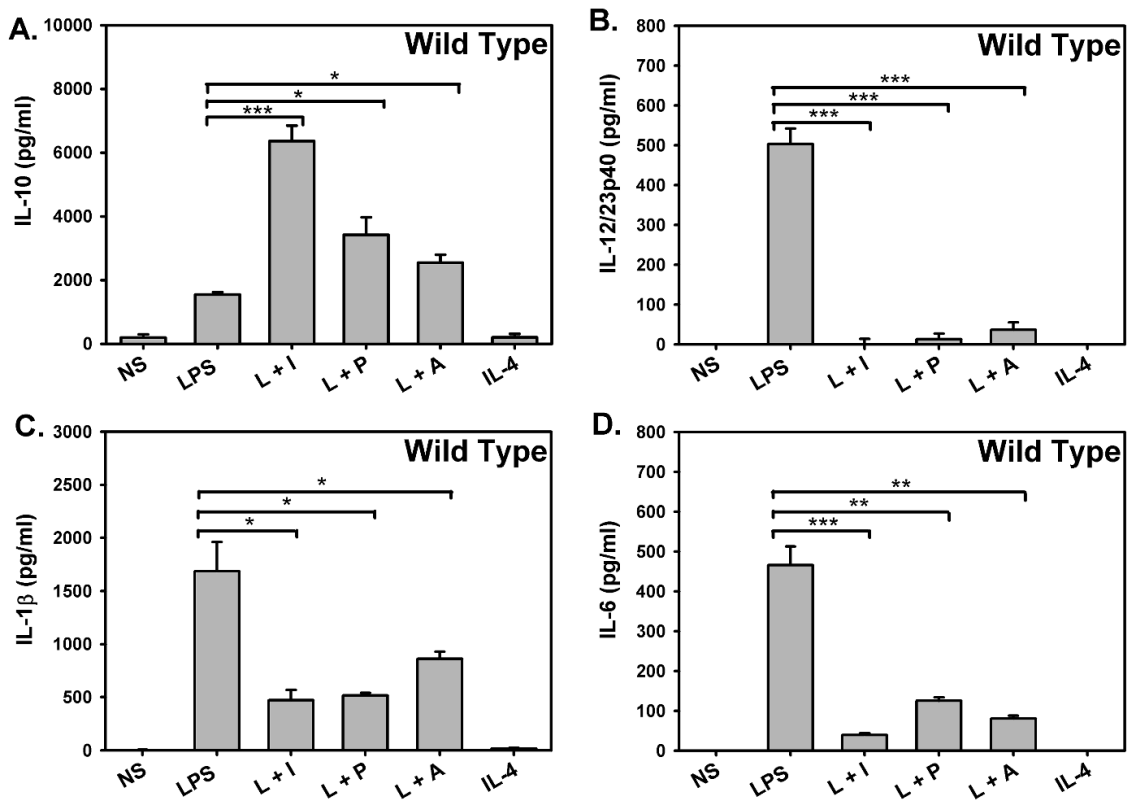


**Figure 1: Cytokine secretion by Regulatory macrophages.** BALB/c WT bone marrow derived macrophages were treated with 10 ng/ml LPS (L), a combination of LPS and 1 $\mu$ g of OVA opsonized with anti-OVA antibody (L+I), 200 nM PGE<sub>2</sub> (L+P), 200  $\mu$ M adenosine (L+A), or 20 ng/ml IL-4 for 16 hours. The levels of IL-10 (A), IL-12/23p40 (B), IL-1 $\beta$  (C) and IL-6 (D) were measured in their supernatants by ELISA. Error bars indicate Mean  $\pm$  SEM of three independent experiments. \*\*\*,  $p < 0.001$ . \*\*,  $p < 0.01$ . \*,  $p < 0.05$ .

PGE<sub>2</sub>, or Ado, were substantially less inflammatory. They secreted higher levels of IL-10, completely suppressed the production of IL-12/23p40, and partially suppressed IL-1 $\beta$  and IL-6 secretion (Figure 1). The importance of STAT6 signaling has been demonstrated to be important in the IL-4 mediated alternate activation of macrophages. To test if regulatory functions were also dependent on STAT6, macrophages from *stat6* knockout mice were challenged under the same stimulatory conditions. Macrophages from these mice exhibited a similar cytokine pattern as wild type (WT) mice when exposed to IC, PGE<sub>2</sub> or Ado, producing higher levels of immunoregulatory IL-10 and reduced levels of inflammatory cytokines IL-12/23p40, IL-1 $\beta$ , and IL-6, indicating that STAT6 signaling is dispensable for generating macrophages with an immunoregulatory phenotype (Figure 2). In contrast to R-M $\phi$  that produced high levels of cytokines, IL-4-treated AA-M $\phi$  produced little or no detectable amounts of the studied cytokines (Figure 1). RT-PCR analyses of AA-M $\phi$  from WT mice revealed high transcription of *relma* and *ym1*<sup>94</sup>, confirming that our IL-4 treatment had indeed generated AA-M $\phi$  (Figure 3). Macrophages from mice genetically deficient in *stat6* failed to transcribe *relma* and *ym1* in response to IL-4, as expected (Figure 3). This experiment helped to illustrate that the STAT6 signaling pathway that is required for alternative activation is dispensable in regulatory activation.

To gain a more global understanding of the cytokine/chemokine profile of activated macrophages, we performed a membrane array that looked at over 40 different cytokines and chemokines. The membrane arrays revealed an increased expression of G-CSF, CXCL13 and CCL1 as well as IL-10 in the R-M $\phi$ , relative to LPS or IL-4 treated M $\phi$  (Figure 4, 5). The chemokines CCL2 and CCL3 were downregulated by at least two-fold

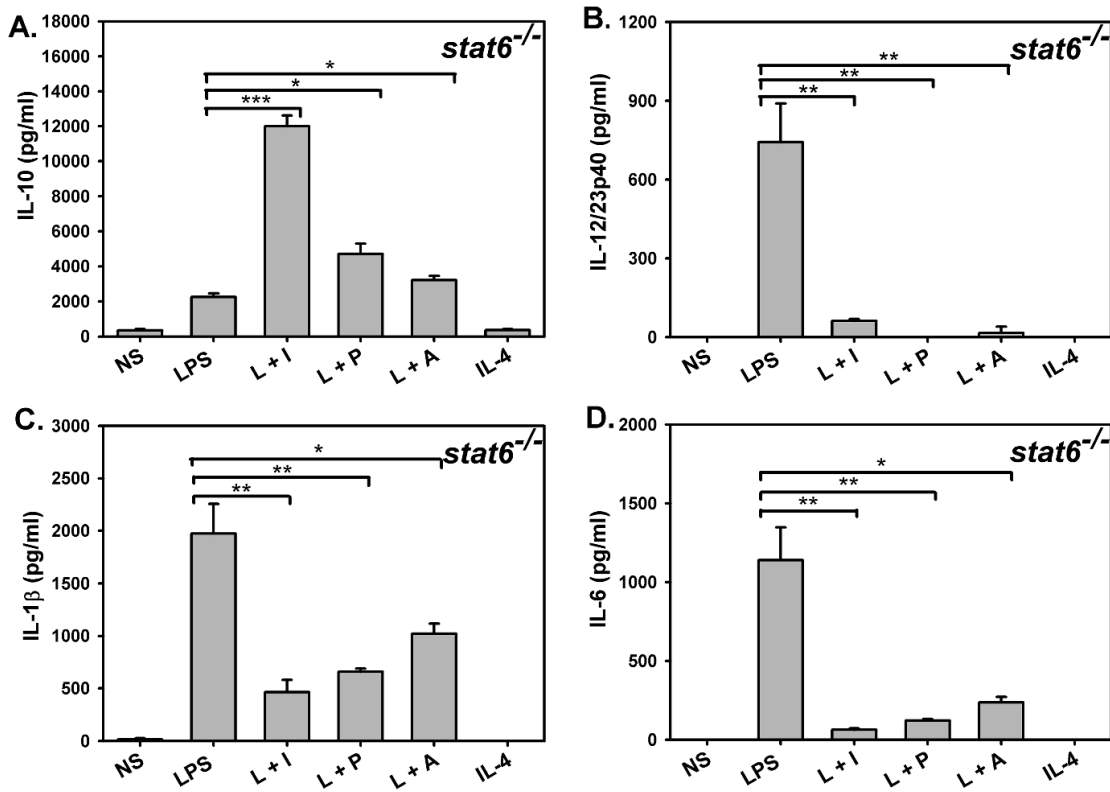


**Figure 2: Regulatory macrophage induction is independent of the STAT6 signaling pathway.** BALB/c *stat6*<sup>-/-</sup> bone marrow derived macrophages were treated with 10 ng/ml LPS (L), a combination of LPS and 1 μg of OVA opsonized with anti-OVA antibody (L+I), 200 nM PGE<sub>2</sub> (L+P), 200 μM adenosine (L+A), or 20 ng/ml IL-4 for 16 hours. The levels of IL-10 (A), IL-12/23p40 (B), IL-1β (C) and IL-6 (D) were measured in their supernatants by ELISA. Error bars indicate Mean ± SEM of three independent experiments. \*\*\*, p < 0.001. \*\*, p < 0.01. \*, p < 0.05.

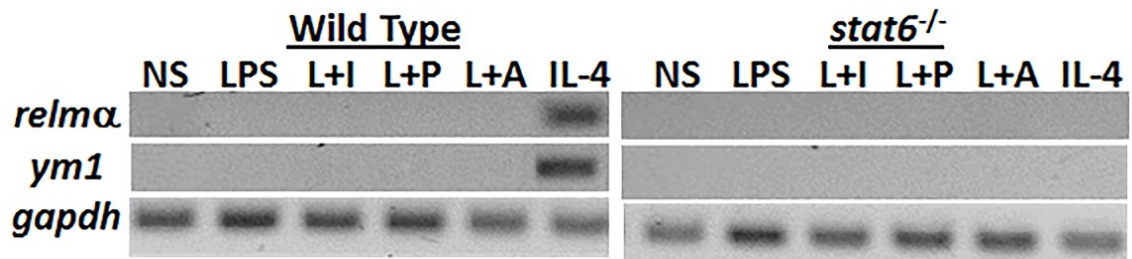


**Figure 3: Alternative Activated macrophage markers are dependent on the STAT6 signaling pathway.** BALB/c WT and *stat6*<sup>-/-</sup> bone marrow derived macrophages were treated with 10 ng/ml LPS (L), a combination of LPS and 1μg of OVA opsonized with anti-OVA antibody (L+I), 200 nM PGE<sub>2</sub> (L+P), 200 μM adenosine (L+A), or 20 ng/ml IL-4 for 4 hours before RNA isolation. The *gapdh* is used as the internal control.

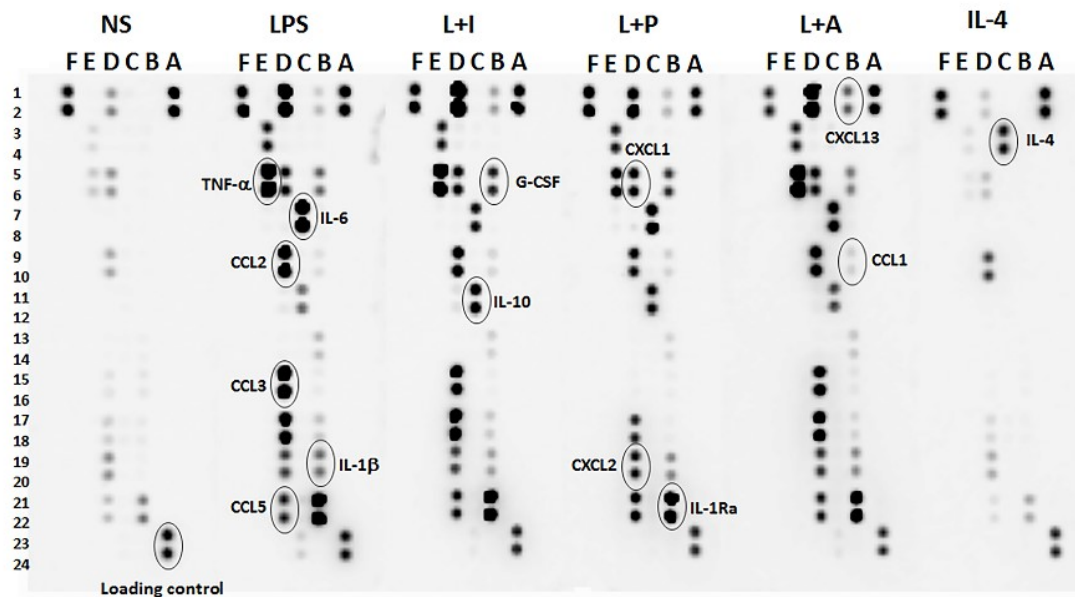


**Figure 4: Regulatory activation results in alterations of cytokine/chemokine profiles.** Chemokine and cytokine secretion by BMDMs was measured by a proteome profiler membrane antibody array. Supernatants from non-stimulated macrophages were compared to macrophages treated with 10 ng/ml LPS, a combination of LPS and 5 $\mu$ g of OVA opsonized with anti-OVA antibody (L+I), 200 nM PGE<sub>2</sub> (L+P), 200  $\mu$ M adenosine (L+A) or 20 ng/ml IL-4 for 12 hours. The proteins that are of interest to this study are indicated in circles and the letters and numbers are provided to identify the position of the analyte in the membrane. Pooled supernatants collected from three independent experiments were added to a single membrane for each condition. Experiment was performed with the help of Prabha Chandrasekaran.

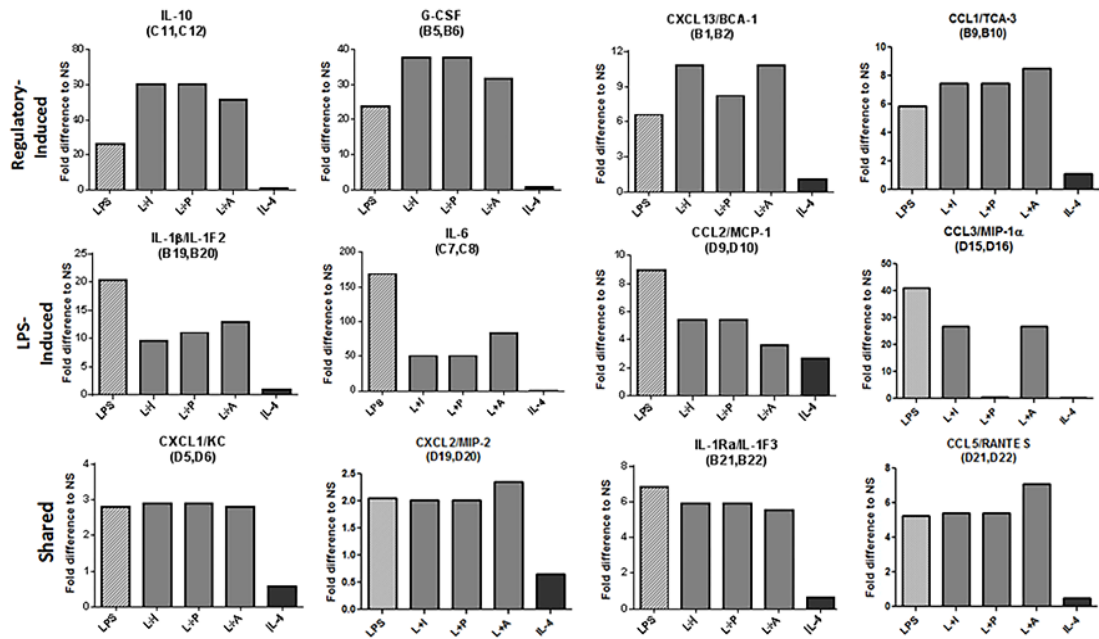


**Figure 5: Relative induction of cytokines/chemokines in activated macrophages.** Mean fold differences in chemiluminescent intensity of the duplicate samples for relevant analytes are compared to intensities from non-stimulated. The alphanumeric values within parentheses indicate their position in the membrane array. Expression values for each conditions were determined from a single membrane assay that was incubated with supernatants from three independent experiments. Experiment was performed with the help of Prabha Chandrasekaran.



in intensity in R-M $\phi$  (Figure 4, 5). All other cytokines and chemokines showed a similar intensity in both LPS treated M1-M $\phi$  and R-M $\phi$ . Most of the tested chemokines and cytokines showed little or no expression in AA-M $\phi$ , with the exception of CCL2, which was increased by two-fold over resting macrophages (Figure 4, 5). Together the data suggests that there are multiple ways to generate macrophages with immunoregulatory activity and that R-M $\phi$  exhibit a unique expression pattern of cytokines and chemokines that is clearly distinct from that of AA-M $\phi$ .

### 3.4.2 RNA-seq Analysis of Murine Macrophages

To further dissect the differences between the activation states of primary macrophages, we utilized high throughput RNA sequencing technology and generated RNA expression profiles for peritoneal macrophages stimulated under conditions similar to those used for bone marrow derived macrophages above. RNA expression levels of the cytokines *il-10*, *il-12/23p40* and *il-6* from peritoneal macrophages matched with the results we obtained for BMDM indicating that both macrophage populations are similarly capable of assuming a regulatory phenotype. Principal Component Analysis (PCA) revealed that AA-M $\phi$  cluster together with non-stimulated macrophages, whereas M1-M $\phi$ , RM $\phi$ -IC and RM $\phi$ -Ado align together along principal component 1 (the X axis), which accounts for a large majority of the variability observed between samples (>70%) (Figure 6A). Likewise, when Euclidean distance heat map analysis was used to visualize the relationships between the samples, IL-4 treated AA-M $\phi$  grouped closely with non-stimulated cells and the R-M $\phi$  clustered with LPS treated cells (Figure 6B). Thus the macrophages with

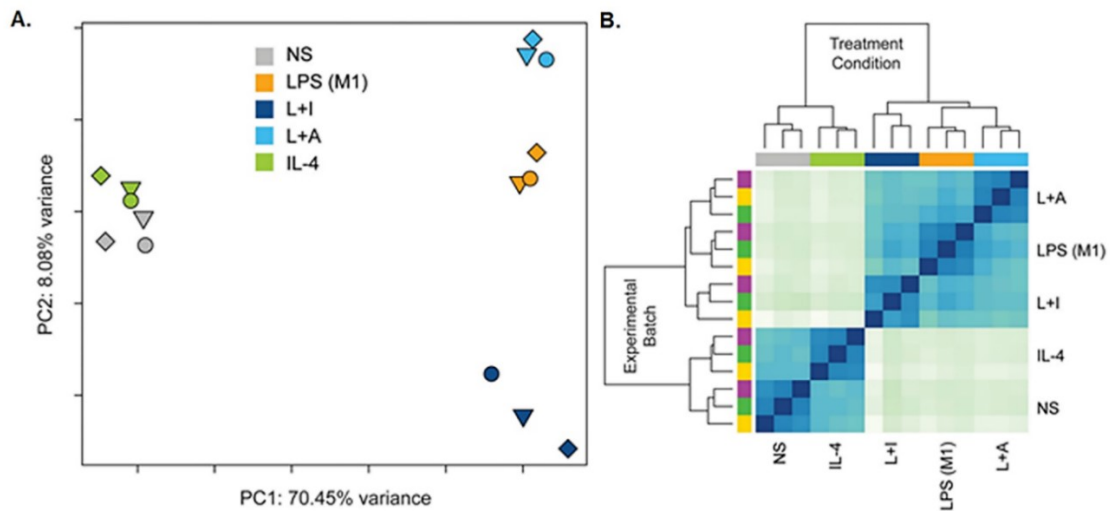


**Figure 6: Comparison of global RNA expression profiles of differentially activated macrophages.** RNA-sequencing was performed on an Illumina platform comparing non-stimulated (NS) murine macrophages and macrophages exposed to 10 ng/ml LPS, 10 ng/ml LPS and 5 $\mu$ g of OVA opsonized with anti-OVA antibody (L+I), 10 ng/ml LPS and 200  $\mu$ M adenosine (L+A) or 20 ng/ml IL-4. A principal components analysis (PCA) plot (**A**) and heat map of a hierarchical clustering analysis using the Euclidean distance metric (**B**) are shown. (**A**) In the PCA plot, each symbol represents an experimental sample with symbol color indicating macrophage treatment condition (gray = NS, orange = LPS, navy blue = L+I, medium blue = L+A, and green = IL-4) and symbol shape indicates batch. (**B**) Colors along the top of the heat map indicate the treatment condition (gray = NS, orange = LPS, navy blue = L+I, medium blue = L+A, and green = IL-4) and colors along the left side of the heat map indicate the batch/experimental date. This figure was generated through a collaboration with the El-Sayed lab by Laura Dillon.

immunoregulatory activity were transcriptionally distinct from IL-4-treated AA-M $\phi$ .

Differential expression analysis was used to generate lists of genes that were greater than two-fold different between each macrophage population and non-stimulated macrophages ( $p < 0.05$ ). The two populations of R-M $\phi$  (RM $\phi$ -IC and RM $\phi$ -Ado) shared a total of 182 upregulated genes that were not significantly upregulated in the M1-M $\phi$  or AA-M $\phi$  populations. This group of gene represents core immunoregulatory genes can help describe how Regulatory macrophages function. Interestingly, there were only 15 genes upregulated by both R-M $\phi$  and AA-M $\phi$ , which suggests that R-M $\phi$  and AA-M $\phi$  have little functional overlap (Figure 7A). Similarly there were 261 unique genes downregulated in both R-M $\phi$ , but not in other macrophages, but only 14 genes were mutually downregulated in R-M $\phi$  and AA-M $\phi$  (Figure 7B). The core genes that were upregulated in R-M $\phi$  have the potential to be used as biomarkers for defining macrophages with immunoregulatory activity, and they may also provide further insight into the functions and phenotype of R-M $\phi$ . It should be noted that the two populations of R-M $\phi$  showed some transcriptional diversity when compared. There were 385 genes were upregulated and 398 were downregulated in RM $\phi$ -IC. Similarly, 283 genes were upregulated and 314 genes were downregulated uniquely in RM $\phi$ -Ado (Figure 7A, 7B). These genes might explain how macrophages can tailor an immune response to combat a specific pathogen and provide important insights into macrophage functions.

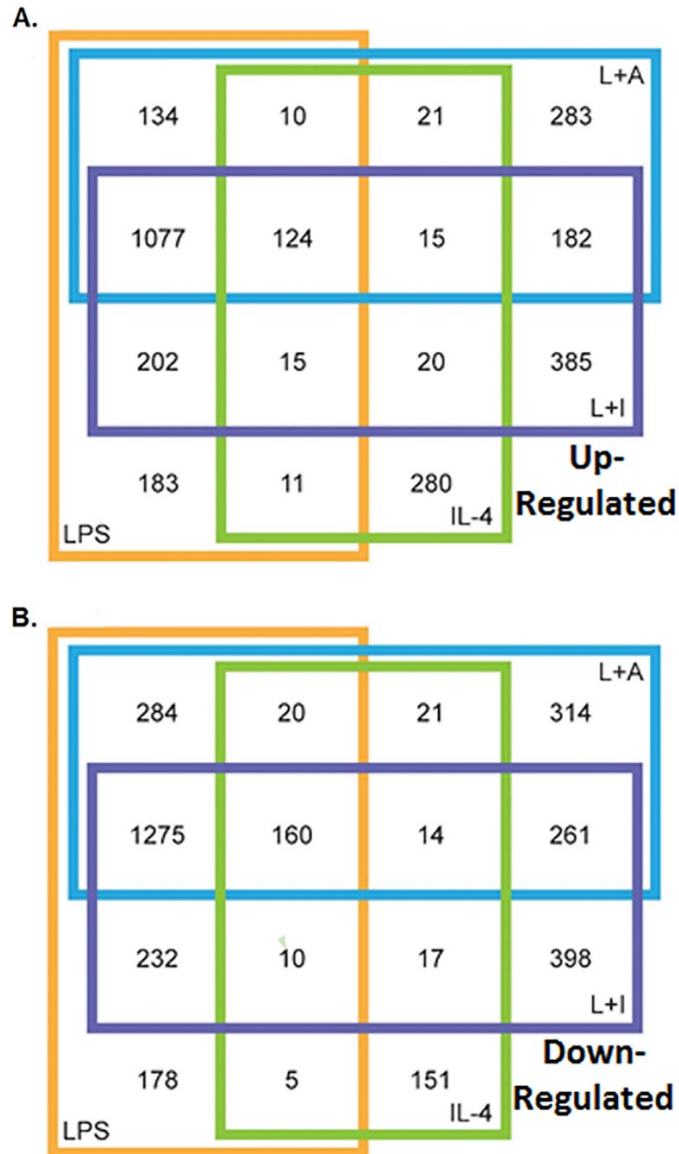


**Figure 7: Four way Venn diagrams of genes differentially expressed following activation.** Overlap of differentially expressed genes upregulated (**A**) or downregulated (**B**) by greater than 2-fold relative to non-stimulated macrophages are displayed in Venn diagrams. Each large colored square represents the treatment condition (orange = LPS, navy blue = L+I, medium blue = L+A, and green = IL-4). This figure was generated through a collaboration with the El-Sayed lab by Laura Dillon.

### 3.4.3 Differentially Expressed Genes

Alternatively Activated macrophages and Regulatory macrophages are often grouped as the subset of M2-M $\phi$ <sup>45,55</sup>. However, our cytokine/chemokine profile, PCA, and heat map analyses shows that these macrophages are indeed different. To identify the genes that define each population, we analyzed the differentially expressed genes in each of the subsets. The first step to identify the genes that showed the highest level of upregulation in each condition. The expression values are expressed as log<sub>2</sub> and were calculated by comparing the expression value in the stimulated condition to the non-stimulated condition. The top 100 genes for LPS (Table 2), LPS+immune complexes (Table 3), LPS+adenosine (Table 4) and IL-4 (Table 5) treatments are listed below. We see that cytokines like IL-6, IL-19, IL-12 and IL-23 are some of the most highly upregulated genes associated with LPS treatment. Additionally, our previously defined markers for murine AA-M $\phi$ , including *ym1(chi3l3)* & *relm $\alpha$ (retnla)* were confirmed by our RNA-seq analyses<sup>94</sup>. These tables are helpful in understanding the global changes that occur following the various stimulation, but make it difficult to compare gene expression levels in multiple parallel populations.

Once we have the identified genes that were important for the various activation phenotypes, it was possible to identify genes that had a two-fold difference over the other populations. The top 25 genes that were induced in AA-M $\phi$  relative to all other stimulation conditions are listed in Table 6. These genes help to define alternative activation and the functions associated with these macrophages. To help remove LPS associated genes, we selected genes that showed a two-fold upregulation in R-M $\phi$  compared to M1-M $\phi$  and

**Table 2: Top 100 Upregulated Genes In LPS Treated Macrophages**

	Symbol	Name	(log <sub>2</sub> )
1	<i>u90926</i>	cDNA sequence U90926	11.02
2	<i>csf3</i>	colony stimulating factor 3 (granulocyte)	11.01
3	<i>nos2</i>	nitric oxide synthase 2 inducible	10.02
4	<i>mmp3</i>	matrix metalloproteinase 3	9.70
5	<i>il6</i>	interleukin 6	9.62
6	<i>il19</i>	interleukin 19	9.26
7	<i>il23a</i>	interleukin 23 alpha subunit p19	8.84
8	<i>il1f6</i>	interleukin 1 family member 6	8.75
9	<i>csf2</i>	colony stimulating factor 2 (granulocyte-macrophage)	8.74
10	<i>tpbpa</i>	trophoblast specific protein alpha	8.70
11	<i>lipg</i>	lipase endothelial	8.70
12	<i>saa1</i>	serum amyloid A 1	8.49
13	<i>ccl4</i>	chemokine (C-C motif) ligand 4	8.32
14	<i>ptgs2</i>	prostaglandin-endoperoxide synthase 2	8.12
15	<i>steap4</i>	STEAP family member 4	8.12
16	<i>il1b</i>	interleukin 1 beta	8.10
17	<i>ccl7</i>	chemokine (C-C motif) ligand 7	8.08
18	<i>il12b</i>	interleukin 12b	7.87
19	<i>slamf1</i>	signaling lymphocytic activation molecule family member 1	7.86
20	<i>lif</i>	leukemia inhibitory factor	7.69
21	<i>4732419C18Rik</i>	RIKEN cDNA 4732419C18 gene	7.68
22	<i>has1</i>	hyaluronan synthase 1	7.64
23	<i>saa2</i>	serum amyloid A 2	7.50
24	<i>hunk</i>	hormonally upregulated Neu-associated kinase	7.47
25	<i>lcn2</i>	lipocalin 2	7.46
26	<i>osmr</i>	oncostatin M receptor	7.39
27	<i>il1a</i>	interleukin 1 alpha	7.38
28	<i>ccl5</i>	chemokine (C-C motif) ligand 5	7.32
29	<i>adamts4</i>	a disintegrin-like and metalloproteinase with thromb. mo. 4	7.26
30	<i>gm14047</i>	predicted gene 14042	7.12
31	<i>nid2</i>	nidogen 2	7.04
32	<i>hdc</i>	histidine decarboxylase	7.04
33	<i>cxcl1</i>	chemokine (C-X-C motif) ligand 1	6.99
34	<i>7530420F21Rik</i>	RIKEN cDNA 7530420F21 gene	6.96
35	<i>ccl3</i>	chemokine (C-C motif) ligand 3	6.94

	Symbol	Table 2(Cont.): Top 100	(log <sub>2</sub> )
36	<i>rnd1</i>	Rho family GTPase 1	6.85
37	<i>mt2</i>	metallothionein 2	6.78
38	<i>gjal</i>	gap junction protein alpha 1	6.75
39	<i>armcx4</i>	armadillo repeat containing X-linked 4	6.70
40	<i>trim30c</i>	tripartite motif-containing 30C	6.69
41	<i>gm16292</i>	predicted gene 16286	6.67
42	<i>oasl1</i>	2'-5' oligoadenylate synthetase-like 1	6.64
43	<i>ch25h</i>	cholesterol 25-hydroxylase	6.64
44	<i>areg</i>	Amphiregulin	6.63
45	<i>plat</i>	plasminogen activator tissue	6.56
46	<i>shisa3</i>	shisa homolog 3	6.55
47	<i>ccl2</i>	chemokine (C-C motif) ligand 2	6.50
48	<i>erich2</i>	glutamate rich 2	6.49
49	<i>urah</i>	urate (5-hydroxyiso-) hydrolase	6.38
50	<i>uppl</i>	uridine phosphorylase 1	6.31
51	<i>gm16685</i>	predicted gene 16685	6.26
52	<i>rhov</i>	ras homolog gene family member U	6.21
53	<i>sptssb</i>	serine palmitoyltransferase small subunit B	6.20
54	<i>phlda1</i>	pleckstrin homology-like domain family A member 1	6.18
55	<i>il22</i>	interleukin 22	6.17
56	<i>inhba</i>	inhibin beta-A	6.16
57	<i>gm14023</i>	predicted gene 14023	6.13
58	<i>ereg</i>	Epiregulin	6.13
59	<i>ifit1</i>	interferon-induced protein with tetratricopeptide repeats 1	6.11
60	<i>nt5c1a</i>	5'-nucleotidase cytosolic IA	6.10
61	<i>krt222</i>	keratin 222	6.09
62	<i>gm4955</i>	predicted gene 4955	6.07
63	<i>inhbb</i>	inhibin beta-B	6.06
64	<i>calcr</i>	calcitonin receptor	6.05
65	<i>rsad2</i>	radical S-adenosyl methionine domain containing 2	6.04
66	<i>car4</i>	carbonic anhydrase 4	6.04
67	<i>gm11435</i>	predicted gene 11435	6.03
68	<i>isg15</i>	ISG15 ubiquitin-like modifier	6.03
69	<i>ambp</i>	alpha 1 microglobulin/bikunin	5.98
70	<i>dusp2</i>	dual specificity phosphatase 2	5.98

Symbol	Table 2(Cont.): Top 100	(log <sub>2</sub> )
71	<i>ppp1r3g</i> protein phosphatase 1 regulatory (inhibitor) subunit 3G	5.93
72	<i>gm5483</i> predicted gene 5483	5.93
73	<i>timp1</i> tissue inhibitor of metalloproteinase 1	5.92
74	<i>ifitm7</i> interferon induced transmembrane protein 7	5.91
75	<i>hbegf</i> heparin-binding EGF-like growth factor	5.89
76	<i>olf1r56</i> olfactory receptor 56	5.88
77	<i>gm26667</i> predicted gene 26667	5.88
78	<i>il1rn</i> interleukin 1 receptor antagonist	5.86
79	<i>gm26584</i> predicted gene 26584	5.83
80	<i>cxcl10</i> chemokine (C-X-C motif) ligand 10	5.82
81	<i>gm13822</i> predicted gene 13822	5.77
82	<i>cdh6</i> cadherin 6	5.77
83	<i>mx2</i> myxovirus (influenza virus) resistance 2	5.77
84	<i>gcnt2</i> glucosaminyl (N-acetyl) transferase 2 I-branching enzyme	5.76
85	<i>edn1</i> endothelin 1	5.75
86	<i>tnfsf15</i> tumor necrosis factor (ligand) superfamily member 15	5.71
87	<i>sele</i> selectin endothelial cell	5.67
88	<i>etnk2</i> ethanolamine kinase 2	5.65
89	<i>mbd3l2</i> methyl-CpG binding domain protein 3-like 2	5.58
90	<i>adora2b</i> adenosine A2b receptor	5.47
91	<i>cxcl2</i> chemokine (C-X-C motif) ligand 2	5.47
92	<i>alpk2</i> alpha-kinase 2	5.47
93	<i>tarm1</i> T cell-interacting activating receptor on myeloid cells 1	5.44
94	<i>gm26687</i> predicted gene 26687	5.42
95	<i>il12a</i> interleukin 12a	5.42
96	<i>fst</i> Follistatin	5.41
97	<i>stfa3</i> stefin A3	5.41
98	<i>tmtc2</i> transmembrane and tetratricopeptide repeat containing 2	5.41
99	<i>il27</i> interleukin 27	5.38
100	<i>draxin</i> dorsal inhibitory axon guidance protein	5.37

The top 100 genes that were upregulated following treatment with LPS. Values were determined by calculating the induction over the non-stimulated condition and are expressed as a log<sub>2</sub> value.



**Table 3: Top 100 Upregulated Genes In LPS+Immune Complex Treated Macrophages**

	Symbol	Name	(log <sub>2</sub> )
1	<i>csf3</i>	colony stimulating factor 3 (granulocyte)	11.61
2	<i>ccl7</i>	chemokine (C-C motif) ligand 7	10.52
3	<i>ccl4</i>	chemokine (C-C motif) ligand 4	9.31
4	<i>u90926</i>	cDNA sequence U90926	9.29
5	<i>il6</i>	interleukin 6	8.86
6	<i>lif</i>	leukemia inhibitory factor	8.80
7	<i>ptgs2</i>	prostaglandin-endoperoxide synthase 2	8.74
8	<i>ccl2</i>	chemokine (C-C motif) ligand 2	8.66
9	<i>slamf1</i>	signaling lymphocytic activation molecule family member 1	8.50
10	<i>illf6</i>	interleukin 1 family member 6	8.47
11	<i>csf2</i>	colony stimulating factor 2 (granulocyte-macrophage)	8.37
12	<i>saal</i>	serum amyloid A 1	8.13
13	<i>il10</i>	interleukin 10	8.10
14	<i>mmp3</i>	matrix metalloproteinase 3	7.94
15	<i>il1b</i>	interleukin 1 beta	7.78
16	<i>nos2</i>	nitric oxide synthase 2 inducible	7.67
17	<i>gm26584</i>	predicted gene 26584	7.57
18	<i>steap4</i>	STEAP family member 4	7.53
19	<i>il19</i>	interleukin 19	7.52
20	<i>cxcl1</i>	chemokine (C-X-C motif) ligand 1	7.47
21	<i>il23a</i>	interleukin 23 alpha subunit p19	7.47
22	<i>inhba</i>	inhibin beta-A	7.42
23	<i>illa</i>	interleukin 1 alpha	7.36
24	<i>tpbpa</i>	trophoblast specific protein alpha	7.34
25	<i>lipg</i>	lipase endothelial	7.29
26	<i>ccl3</i>	chemokine (C-C motif) ligand 3	7.26
27	<i>ch25h</i>	cholesterol 25-hydroxylase	7.14
28	<i>has1</i>	hyaluronan synthase1	7.04
29	<i>areg</i>	Amphiregulin	6.89
30	<i>osmr</i>	oncostatin M receptor	6.80
31	<i>illrn</i>	interleukin 1 receptor antagonist	6.79
32	<i>samd11</i>	sterile alpha motif domain containing 11	6.69
33	<i>urah</i>	urate (5-hydroxyiso-) hydrolase	6.68
34	<i>7530420F21Rik</i>	RIKEN cDNA 7530420F21 gene	6.63
35	<i>armcx4</i>	armadillo repeat containing X-linked 4	6.59

	Symbol	Table 3(Cont.): Top 100	(log <sub>2</sub> )
36	<i>g530011O06Rik</i>	RIKEN cDNA G530011O06 gene	6.56
37	<i>isg15</i>	ISG15 ubiquitin-like modifier	6.54
38	<i>kctd4</i>	potassium channel tetramerisation domain containing 4	6.51
39	<i>mt2</i>	metallothionein 2	6.47
40	<i>oasl1</i>	2'-5' oligoadenylate synthetase-like 1	6.44
41	<i>pdpn</i>	Podoplanin	6.36
42	<i>trim30c</i>	tripartite motif-containing 30C	6.35
43	<i>stfa3</i>	stefin A3	6.34
44	<i>gm21742</i>	predicted gene 21742	6.31
45	<i>ildr1</i>	immunoglobulin-like domain containing receptor 1	6.30
46	<i>gm14023</i>	predicted gene 14023	6.28
47	<i>mbd3l2</i>	methyl-CpG binding domain protein 3-like 2	6.27
48	<i>gm26667</i>	predicted gene 26667	6.26
49	<i>htra4</i>	htrA serine peptidase 4	6.25
50	<i>gm15726</i>	predicted gene 15726	6.23
51	<i>ppp1r3g</i>	protein phosphatase 1 regulatory (inhibitor) subunit 3G	6.21
52	<i>saa2</i>	serum amyloid A 2	6.20
53	<i>hbegf</i>	heparin-binding EGF-like growth factor	6.19
54	<i>niacr1</i>	niacin receptor 1	6.18
55	<i>flrt3</i>	fibronectin leucine rich transmembrane protein 3	6.16
56	<i>gm21857</i>	predicted gene 21857	6.15
57	<i>gm14047</i>	predicted gene 14047	6.12
58	<i>gm21748</i>	predicted gene 21748	6.09
59	<i>gm5483</i>	predicted gene 5483	6.06
60	<i>cxcl2</i>	chemokine (C-X-C motif) ligand 2	6.04
61	<i>sphk1</i>	sphingosine kinase 1	6.01
62	<i>erich2</i>	glutamate rich 2	6.00
63	<i>gm15247</i>	predicted gene 15247	6.00
64	<i>xcr1</i>	chemokine (C motif) receptor 1	6.00
65	<i>cd209a</i>	CD209a antigen	6.00
66	<i>rsad2</i>	radical S-adenosyl methionine domain containing 2	5.93
67	<i>gm16292</i>	predicted gene 16286	5.93
68	<i>ereg</i>	Epiregulin	5.92
69	<i>gjal</i>	gap junction protein alpha 1	5.86
70	<i>gm3513</i>	predicted gene 3513	5.85

	Symbol	Table 3(Cont.): Top 100	(log <sub>2</sub> )
71	<i>phlda1</i>	pleckstrin homology-like domain family A member 1	5.85
72	<i>gm21860</i>	predicted gene 21860	5.83
73	<i>gng4</i>	guanine nucleotide binding protein (G protein) gamma 4	5.82
74	<i>il33</i>	interleukin 33	5.81
75	<i>uppl1</i>	uridine phosphorylase 1	5.79
76	<i>tnf</i>	tumor necrosis factor	5.78
77	<i>edn1</i>	endothelin 1	5.73
78	<i>aw011738</i>	expressed sequence AW011738	5.72
79	<i>f3</i>	coagulation factor III	5.70
80	<i>gm26687</i>	predicted gene 26687	5.69
81	<i>gm16685</i>	predicted gene 16685	5.69
82	<i>gcnt2</i>	glucosaminyl (N-acetyl) transferase 2 I-branching enzyme	5.67
83	<i>car4</i>	carbonic anhydrase 4	5.65
84	<i>gm4955</i>	predicted gene 4955	5.63
85	<i>gm5416</i>	predicted gene 5416	5.61
86	<i>ccl5</i>	chemokine (C-C motif) ligand 5	5.60
87	<i>gdf15</i>	growth differentiation factor 15	5.58
88	<i>1600029D21Rik</i>	RIKEN cDNA 1600029D21 gene	5.57
89	<i>gfpt2</i>	glutamine fructose-6-phosphate transaminase 2	5.54
90	<i>ifit1</i>	interferon-induced protein with tetratricopeptide repeats 1	5.53
91	<i>gm13822</i>	predicted gene 13822	5.50
92	<i>nt5c1a</i>	5'-nucleotidase cytosolic IA	5.42
93	<i>timp1</i>	tissue inhibitor of metalloproteinase 1	5.40
94	<i>adamts4</i>	a disintegrin-like and metalloproteinase with thromb. mo 4	5.38
95	<i>ckap2l</i>	cytoskeleton associated protein 2-like	5.38
96	<i>ndrg1</i>	N-myc downstream regulated gene 1	5.38
97	<i>gm8818</i>	predicted pseudogene 8818	5.36
98	<i>itga2</i>	integrin alpha 2	5.35
99	<i>alpk2</i>	alpha-kinase 2	5.31
100	<i>drd1a</i>	dopamine receptor D1A	5.27

The top 100 genes that were upregulated following treatment with LPS+immune complexes. Values were determined by calculating the induction over the non-stimulated condition and are expressed as a log<sub>2</sub> value.

**Table 4: Top 100 Upregulated Genes In LPS+Adenosine Treated Macrophages**

	Symbol	Name	(log <sub>2</sub> )
1	<i>u90926</i>	cDNA sequence U90926	10.83
2	<i>csf3</i>	colony stimulating factor 3 (granulocyte)	10.15
3	<i>csf2</i>	colony stimulating factor 2 (granulocyte-macrophage)	9.61
4	<i>sele</i>	selectin endothelial cell	9.57
5	<i>il33</i>	interleukin 33	9.13
6	<i>nos2</i>	nitric oxide synthase 2 inducible	9.11
7	<i>il19</i>	interleukin 19	9.00
8	<i>has1</i>	hyaluronan synthase1	8.87
9	<i>lif</i>	leukemia inhibitory factor	8.79
10	<i>steap4</i>	STEAP family member 4	8.73
11	<i>il6</i>	interleukin 6	8.73
12	<i>lipg</i>	lipase endothelial	8.53
13	<i>gm14047</i>	predicted gene 14042	8.31
14	<i>tpbpa</i>	trophoblast specific protein alpha	8.28
15	<i>saal</i>	serum amyloid A 1	8.18
16	<i>ccl7</i>	chemokine (C-C motif) ligand 7	8.18
17	<i>ptgs2</i>	prostaglandin-endoperoxide synthase 2	8.13
18	<i>il1f6</i>	interleukin 1 family member 6	7.98
19	<i>mmp3</i>	matrix metalloproteinase 3	7.89
20	<i>urah</i>	urate (5-hydroxyiso-) hydrolase	7.86
21	<i>adamts4</i>	a disintegrin-like and metalloproteinase with thromb. mo.4	7.82
22	<i>4732419C18Rik</i>	RIKEN cDNA 4732419C18 gene	7.67
23	<i>il23a</i>	interleukin 23 alpha subunit p19	7.66
24	<i>areg</i>	Amphiregulin	7.63
25	<i>il1b</i>	interleukin 1 beta	7.57
26	<i>7530420F21Rik</i>	RIKEN cDNA 7530420F21 gene	7.53
27	<i>osmr</i>	oncostatin M receptor	7.51
28	<i>ereg</i>	Epiregulin	7.42
29	<i>plat</i>	plasminogen activator tissue	7.36
30	<i>hc</i>	hemolytic complement	7.35
31	<i>il1a</i>	interleukin 1 alpha	7.32
32	<i>dusp14</i>	dual specificity phosphatase 14	7.31
33	<i>gjal</i>	gap junction protein alpha 1	7.31
34	<i>gfpt2</i>	glutamine fructose-6-phosphate transaminase 2	7.31
35	<i>ccl4</i>	chemokine (C-C motif) ligand 4	7.27

	Symbol	Table 4(Cont.): Top 100	(log <sub>2</sub> )
36	<i>tpbg</i>	trophoblast glycoprotein	7.27
37	<i>nid2</i>	nidogen 2	7.26
38	<i>ifi202b</i>	interferon activated gene 202B	7.20
39	<i>nptx2</i>	neuronal pentraxin 2	7.06
40	<i>cxcl1</i>	chemokine (C-X-C motif) ligand 1	7.00
41	<i>slamf1</i>	signaling lymphocytic activation molecule family member 1	6.99
42	<i>rnd1</i>	Rho family GTPase 1	6.90
43	<i>klk9</i>	kallikrein related-peptidase 9	6.80
44	<i>hdc</i>	histidine decarboxylase	6.79
45	<i>hunk</i>	hormonally upregulated Neu-associated kinase	6.77
46	<i>slco2b1</i>	solute carrier organic anion transporter family member 2b1	6.75
47	<i>erich2</i>	glutamate rich 2	6.72
48	<i>gzmb</i>	granzyme B	6.72
49	<i>inhba</i>	inhibin beta-A	6.61
50	<i>saa2</i>	serum amyloid A 2	6.58
51	<i>hist1h3e</i>	histone cluster 1 H3e	6.51
52	<i>gm4847</i>	predicted gene 4847	6.50
53	<i>gm16292</i>	predicted gene 16286	6.49
54	<i>1600029D21Rik</i>	RIKEN cDNA 1600029D21 gene	6.49
55	<i>flrt3</i>	fibronectin leucine rich transmembrane protein 3	6.48
56	<i>trim30c</i>	tripartite motif-containing 30C	6.45
57	<i>ccl2</i>	chemokine (C-C motif) ligand 2	6.41
58	<i>gm5483</i>	predicted gene 5483	6.38
59	<i>phlda1</i>	pleckstrin homology-like domain family A member 1	6.37
60	<i>rhov</i>	ras homolog gene family member U	6.35
61	<i>sptssb</i>	serine palmitoyltransferase small subunit B	6.34
62	<i>lcn2</i>	lipocalin 2	6.28
63	<i>mt2</i>	metallothionein 2	6.26
64	<i>il10</i>	interleukin 10	6.26
65	<i>gm5416</i>	predicted gene 5416	6.25
66	<i>uppl1</i>	uridine phosphorylase 1	6.23
67	<i>etnk2</i>	ethanolamine kinase 2	6.20
68	<i>tnfaip6</i>	tumor necrosis factor alpha induced protein 6	6.18
69	<i>ifitm7</i>	interferon induced transmembrane protein 7	6.17
70	<i>nptx1</i>	neuronal pentraxin 1	6.13

	Symbol	Table 4(Cont.): Top 100	(log <sub>2</sub> )
71	<i>gm26584</i>	predicted gene 26584	6.12
72	<i>tmtc2</i>	transmembrane and tetratricopeptide repeat containing 2	6.10
73	<i>ccl5</i>	chemokine (C-C motif) ligand 5	6.10
74	<i>penk</i>	Preproenkephalin	6.04
75	<i>gm14023</i>	predicted gene 14023	6.02
76	<i>arc</i>	activity regulated cytoskeletal-associated protein	5.98
77	<i>tnfrsf9</i>	tumor necrosis factor receptor superfamily member 9	5.98
78	<i>drd1a</i>	dopamine receptor D1A	5.95
79	<i>ckap2l</i>	cytoskeleton associated protein 2-like	5.91
80	<i>niacr1</i>	niacin receptor 1	5.91
81	<i>illrn</i>	interleukin 1 receptor antagonist	5.89
82	<i>gm8818</i>	predicted pseudogene 8818	5.88
83	<i>inhbb</i>	inhibin beta-B	5.88
84	<i>gcnt2</i>	glucosaminyl (N-acetyl) transferase 2 I-branching enzyme	5.86
85	<i>hist1h4c</i>	histone cluster 1 H4c	5.85
86	<i>gm26667</i>	predicted gene 26667	5.85
87	<i>hbegf</i>	heparin-binding EGF-like growth factor	5.83
88	<i>adora2b</i>	adenosine A2b receptor	5.82
89	<i>dusp2</i>	dual specificity phosphatase 2	5.81
90	<i>pxdc1</i>	PX domain containing 1	5.76
91	<i>gm26687</i>	predicted gene 26687	5.75
92	<i>gm13889</i>	predicted gene 13889	5.74
93	<i>gdnf</i>	glial cell line derived neurotrophic factor	5.70
94	<i>tslp</i>	thymic stromal lymphopoietin	5.70
95	<i>il22</i>	interleukin 22	5.68
96	<i>stfa3</i>	stefin A3	5.65
97	<i>timp1</i>	tissue inhibitor of metalloproteinase 1	5.65
98	<i>trem1</i>	triggering receptor expressed on myeloid cells 1	5.63
99	<i>shisa3</i>	shisa homolog 3	5.61
100	<i>ccl3</i>	chemokine (C-C motif) ligand 3	5.61

The top 100 genes that were upregulated following treatment with LPS+adenosine. Values were determined by calculating the induction over the non-stimulated condition and are expressed as a log<sub>2</sub> value.

**Table 5: Top 100 Upregulated Genes In IL-4 Treated Macrophages**

	Symbol	Name	(log <sub>2</sub> )
1	<i>chi3l3</i>	checkpoint with forkhead and ring finger domains	8.60
2	<i>itgb3</i>	integrin beta 3	6.69
3	<i>cd209e</i>	CD209e antigen	6.49
4	<i>flt1</i>	FMS-like tyrosine kinase 1	6.26
5	<i>serpina3g</i>	serine (or cysteine) peptidase inhibitor clade A member 3G	6.11
6	<i>gm8221</i>	predicted gene 8221	6.11
7	<i>ear11</i>	eosinophil-associated ribonuclease A family member 11	5.89
8	<i>slc7a2</i>	solute carrier family 7 member 2	5.69
9	<i>pdcd1lg2</i>	programmed cell death 1 ligand 2	5.68
10	<i>chi3l4</i>	checkpoint with forkhead and ring finger domains	5.61
11	<i>cdh1</i>	cadherin 1	5.44
12	<i>tmem26</i>	transmembrane protein 26	5.25
13	<i>il4i1</i>	interleukin 4 induced 1	5.08
14	<i>il31ra</i>	interleukin 31 receptor A	5.04
15	<i>cish</i>	cytokine inducible SH2-containing protein	4.97
16	<i>peg10</i>	paternally expressed 10	4.96
17	<i>tslp</i>	thymic stromal lymphopietin	4.94
18	<i>apol7c</i>	apolipoprotein L 7c	4.93
19	<i>mrc1</i>	mannose receptor C type 1	4.91
20	<i>ccl7</i>	chemokine (C-C motif) ligand 7	4.78
21	<i>ddx4</i>	DEAD (Asp-Glu-Ala-Asp) box polypeptide 4	4.71
22	<i>socs1</i>	suppressor of cytokine signaling 1	4.69
23	<i>retna</i>	resistin like alpha	4.69
24	<i>gatm</i>	glycine amidinotransferase	4.66
25	<i>en2</i>	engrailed 2	4.55
26	<i>hbegf</i>	heparin-binding EGF-like growth factor	4.54
27	<i>mgl2</i>	macrophage galactose N-acetyl-galactosamine specific lectin 2	4.54
28	<i>ccl12</i>	chemokine (C-C motif) ligand 12	4.46
29	<i>insrr</i>	insulin receptor-related receptor	4.44
30	<i>irf4</i>	interferon regulatory factor 4	4.32
31	<i>lipn</i>	lipase family member N	4.27
32	<i>batf3</i>	basic leucine zipper transcription factor ATF-like 3	4.25
33	<i>tuba8</i>	tubulin alpha 8	4.07
34	<i>gm26584</i>	predicted gene 26584	4.03
35	<i>adc</i>	arginine decarboxylase	3.98

	Symbol	Table 5 (Cont.): Top 100	(log <sub>2</sub> )
36	<i>alox15</i>	arachidonate 15-lipoxygenase	3.88
37	<i>apol7b</i>	apolipoprotein L 7b	3.83
38	<i>car4</i>	carbonic anhydrase 4	3.81
39	<i>rab3il1</i>	RAB3A interacting protein (rabin3)-like 1	3.77
40	<i>il20rb</i>	interleukin 20 receptor beta	3.65
41	<i>dixdc1</i>	DIX domain containing 1	3.64
42	<i>nrg1</i>	neuregulin 1	3.62
43	<i>tfr</i>	transferrin receptor	3.58
44	<i>slc30a4</i>	solute carrier family 30 (zinc transporter) member 4	3.58
45	<i>plekhf1</i>	pleckstrin homology domain containing family F member 1	3.52
46	<i>klf4</i>	kruppel-like factor 4 (gut)	3.49
47	<i>gm6116</i>	predicted gene 6116	3.47
48	<i>prps1</i>	phosphoribosyl pyrophosphate synthetase 1	3.43
49	<i>ch25h</i>	cholesterol 25-hydroxylase	3.43
50	<i>pcyox1l</i>	prenylcysteine oxidase 1 like	3.39
51	<i>scimp</i>	SLP adaptor and CSK interacting membrane protein	3.36
52	<i>b3gnt7</i>	betaGal beta-1 3-N-acetylglucosaminyltransferase 7	3.32
53	<i>cd83</i>	CD83 antigen	3.32
54	<i>btbd11</i>	BTB (POZ) domain containing 11	3.29
55	<i>ccl24</i>	chemokine (C-C motif) ligand 24	3.24
56	<i>hid1</i>	HID1 domain containing	3.22
57	<i>htr2a</i>	5-hydroxytryptamine (serotonin) receptor 2A	3.21
58	<i>atp8b1</i>	ATPase class I type 8B member 1	3.15
59	<i>6430571L13Rik</i>	RIKEN cDNA 6430571L13 gene	3.13
60	<i>slc14a1</i>	solute carrier family 14 (urea transporter) member 1	3.12
61	<i>rhoj</i>	ras homolog gene family member J	3.02
62	<i>sdc4</i>	syndecan 4	3.00
63	<i>dnah12</i>	dynein axonemal heavy chain 12	2.98
64	<i>apol7e</i>	apolipoprotein L 7e	2.97
65	<i>pxdc1</i>	PX domain containing 1	2.97
66	<i>rasgrp1</i>	RAS guanyl releasing protein 1	2.96
67	<i>lad1</i>	Ladinin	2.94
68	<i>na</i>	NA	2.93
69	<i>fgf2</i>	fibroblast growth factor 2	2.91
70	<i>tbc1d4</i>	TBC1 domain family member 4	2.85



	Symbol	Table 5 (Cont.): Top 100	(log <sub>2</sub> )
71	<i>ms4a8a</i>	membrane-spanning 4-domains subfamily A member 8A	2.85
72	<i>tarm1</i>	T cell-interacting activating receptor on myeloid cells 1	2.85
73	<i>rgl1</i>	ral guanine nucleotide dissociation stimulator -like 1	2.83
74	<i>itgal</i>	integrin alpha 1	2.82
75	<i>ramp3</i>	receptor (calcitonin) activity modifying protein 3	2.82
76	<i>cd209a</i>	CD209a antigen	2.80
77	<i>amica1</i>	adhesion molecule interacts with CXADR antigen 1	2.80
78	<i>p2ry1</i>	purinergic receptor P2Y G-protein coupled 1	2.78
79	<i>fncl7</i>	fibronectin type III domain containing 7	2.76
80	<i>wnt2</i>	wingless-related MMTV integration site 2	2.75
81	<i>bcar3</i>	breast cancer anti-estrogen resistance 3	2.73
82	<i>2810055G20Rik</i>	RIKEN cDNA 2810055G20 gene	2.71
83	<i>ido2</i>	indoleamine 2 3-dioxygenase 2	2.70
84	<i>ptpro</i>	protein tyrosine phosphatase receptor type O	2.69
85	<i>arg1</i>	arginase liver	2.68
86	<i>cyp1b1</i>	cytochrome P450 family 1 subfamily b polypeptide 1	2.68
87	<i>flrt3</i>	fibronectin leucine rich transmembrane protein 3	2.67
88	<i>olfm1</i>	olfactomedin 1	2.65
89	<i>adcy3</i>	adenylate cyclase 3	2.65
90	<i>uppl</i>	uridine phosphorylase 1	2.63
91	<i>ccl2</i>	chemokine (C-C motif) ligand 2	2.63
92	<i>cd40</i>	CD40 antigen	2.60
93	<i>fyn</i>	Fyn proto-oncogene	2.56
94	<i>egr2</i>	early growth response 2	2.56
95	<i>pald1</i>	phosphatase domain containing paladin 1	2.55
96	<i>sfrp1</i>	secreted frizzled-related protein 1	2.52
97	<i>serpina3f</i>	serine (or cysteine) peptidase inhibitor clade A member 3F	2.52
98	<i>fchsd2</i>	FCH and double SH3 domains 2	2.51
99	<i>tll11</i>	tubulin tyrosine ligase-like family member 11	2.51
100	<i>flrt2</i>	fibronectin leucine rich transmembrane protein 2	2.49

The top 100 genes that were upregulated following treatment with IL-4. Values were determined by calculating the induction over the non-stimulated condition and are expressed as a log<sub>2</sub> value.

**Table 6. Top 25 Genes Uniquely Induced Following IL-4 Stimulation**

	Symbol	Name	(log <sub>2</sub> )
1	<i>chi3l3</i>	checkpoint with forkhead and ring finger domains	8.60
2	<i>itgb3</i>	integrin beta 3	6.69
3	<i>cd209e</i>	CD209e antigen	6.49
4	<i>flt1</i>	FMS-like tyrosine kinase 1	6.26
5	<i>serpina3g</i>	serine (or cysteine) peptidase inhibitor clade A member 3G	6.11
6	<i>gm8221</i>	predicted gene 8221	6.11
7	<i>ear11</i>	eosinophil-associated ribonuclease A family member 11	5.89
8	<i>pdc1lg2</i>	programmed cell death 1 ligand 2	5.68
9	<i>chi3l4</i>	checkpoint with forkhead and ring finger domains	5.61
10	<i>cdh1</i>	cadherin 1	5.44
11	<i>tmem26</i>	transmembrane protein 26	5.25
12	<i>il4i1</i>	interleukin 4 induced 1	5.08
13	<i>il31ra</i>	interleukin 31 receptor A	5.04
14	<i>apol7c</i>	apolipoprotein L 7c	4.93
15	<i>mrc1</i>	mannose receptor C type 1	4.91
16	<i>ddx4</i>	DEAD (Asp-Glu-Ala-Asp) box polypeptide 4	4.71
17	<i>retnla</i>	resistin like alpha	4.69
18	<i>gatm</i>	glycine amidinotransferase	4.66
19	<i>en2</i>	engrailed 2	4.55
20	<i>mgl2</i>	macrophage galactose N-acetyl-galactosamine specific lectin 2	4.54
21	<i>insrr</i>	insulin receptor-related receptor	4.44
22	<i>irf4</i>	interferon regulatory factor 4	4.32
23	<i>lipn</i>	lipase family member N	4.27
24	<i>batf3</i>	basic leucine zipper transcription factor ATF-like 3	4.25
25	<i>tuba8</i>	tubulin alpha 8	4.07

The top 25 genes that were induced following IL-4 treatment. All of these genes have at least a two-fold upregulation over LPS, LPS+immune complex and LPS+adenosine treated expression levels. Values were determined by calculating the induction over the non-stimulated condition and are expressed as a log<sub>2</sub> value.

considered these to be immunoregulatory genes. As expected, IL-10 was one of the first few on the list with the immune regulatory functions (Table 7). For the first time we gaining a comprehensive understanding of the core genes shared between differentially activated Regulatory macrophage populations. Among this list, was 26 genes had no known function (Table 8). These genes helps to highlight the fact that macrophage activation responses have not been fully describe and that there may be important factors yet to be discovered.

#### **3.4.4 Activated ‘Diseases and Function’ Identified by IPA Analysis**

The Ingenuity Pathway Analysis (IPA) platform was used to identify differences in ‘Diseases and Functions’ associations between the two R-M $\phi$  and the LPS treated M1-M $\phi$ . The attributes most closely associated with RM $\phi$ -IC were development of blood vessels, the proliferation of liver cells and the development of tumors (Figure 8A). As expected, RM $\phi$ -IC downregulated myeloid cells activation and the induction of T<sub>H</sub>1-associated functions (Figure 8A). The RM $\phi$ -Ado shared vascularization functions with RM $\phi$ -IC and reduced anti-microbial responses (Figure 8B). This IPA analysis helped confirm that one of the primary functions of R-M $\phi$  is to limit immune responses and help to repair tissue that has been damaged. The previously reported functions associated with LPS stimulation<sup>44,106-108</sup> were confirmed by our RNA-seq and IPA analysis and includes the activation of strong inflammatory immune responses (Figure 9A). AA-M $\phi$  appeared to be associated with maintaining connective tissue and general tissue development (Figure 9B), thus agreeing with previously described phenotypes for these cells<sup>53,55</sup>. The IPA analysis of these data clearly demonstrate that R-M $\phi$  have functions that are distinct from AA-M $\phi$ .

**Table 7. Genes Induced Following Regulatory Activation**

	Symbol	Name	L+I (log <sub>2</sub> )	L+A (log <sub>2</sub> )
1	<i>lif</i>	leukemia inhibitory factor	8.80	8.79
2	<i>il10</i>	interleukin 10	8.10	6.26
3	<i>il1r1</i>	immunoglobulin-like domain containing receptor 1	6.30	4.25
4	<i>flrt3</i>	fibronectin leucine rich transmembrane protein 3	6.16	6.48
5	<i>xcr1</i>	chemokine (C motif) receptor 1	6.00	4.79
6	<i>il33</i>	interleukin 33	5.81	9.13
7	<i>ckap2l</i>	cytoskeleton associated protein 2-like	5.38	5.91
8	<i>ndrg1</i>	n-myc downstream regulated gene 1	5.38	5.05
9	<i>itga2</i>	integrin alpha 2	5.35	4.95
10	<i>gem</i>	GTP binding protein	5.24	4.28
11	<i>mid1</i>	midline 1	5.05	3.65
12	<i>odc1</i>	ornithine decarboxylase structural 1	5.05	5.58
13	<i>hepha1l</i>	hephaestin-like 1	5.03	5.12
14	<i>gdnf</i>	glial cell line derived neurotrophic factor	4.94	5.70
15	<i>klk9</i>	kallikrein related-peptidase 9	4.60	6.80
16	<i>dusp14</i>	dual specificity phosphatase 14	4.59	7.31
17	<i>gprc5a</i>	g protein-coupled receptor family C group 5 member A	4.44	3.76
18	<i>tmem88</i>	transmembrane protein 88	4.37	5.04
19	<i>hrc</i>	histidine rich calcium binding protein	4.20	2.68
20	<i>nptx2</i>	neuronal pentraxin 2	3.84	7.06
21	<i>dusp10</i>	dual specificity phosphatase 10	3.72	3.52
22	<i>hc</i>	hemolytic complement	3.59	7.35
23	<i>cdk6</i>	cyclin-dependent kinase 6	3.27	2.89
24	<i>tmem236</i>	transmembrane protein 236	3.26	3.35
25	<i>fam71f2</i>	family with sequence similarity 71 member F2	3.19	4.30

The top 25 genes that were induced following LPS+immune complex treatment and LPS+adenosine treatment. All of these genes have at least a two-fold upregulation over both the LPS treated and IL-4 treated expression levels. Values were determined by calculating the induction over the non-stimulated condition and are expressed as a log<sub>2</sub> value.

**Table 8. Shared Predicted Genes Induced Following Regulatory Activation**

Ref #	Symbol	Name	L+I (log <sub>2</sub> )	L+A (log <sub>2</sub> )
1	<i>gm21742</i>	predicted gene 21742	6.31	4.61
2	<i>gm15726</i>	predicted gene 15726	6.23	4.63
3	<i>gm21857</i>	predicted gene 21857	6.15	4.74
4	<i>gm21748</i>	predicted gene 21748	6.09	3.91
5	<i>gm15247</i>	predicted gene 15247	6.00	4.47
6	<i>gm3513</i>	predicted gene 3513	5.85	3.78
7	<i>gm21860</i>	predicted gene 21860	5.83	3.91
8	<i>gm8818</i>	predicted pseudogene 8818	5.36	5.88
9	<i>gm22748</i>	predicted gene 22748	4.76	4.46
10	<i>gm14636</i>	predicted gene 14636	4.49	3.22
11	<i>gm8174</i>	predicted gene 8174	4.33	5.09
12	<i>gm26603</i>	predicted gene 26603	4.22	3.21
13	<i>gm7120</i>	predicted gene 7120	4.10	1.71
14	<i>gm26772</i>	predicted gene 26772	3.63	2.30
15	<i>gm6611</i>	predicted gene 6611	3.42	3.60
16	<i>gm13889</i>	predicted gene 13889	3.05	5.74
17	<i>gm11870</i>	predicted gene 11870	2.61	2.72
18	<i>gm17709</i>	predicted gene 17709	2.59	2.24
19	<i>gm9797</i>	predicted pseudogene 9797	2.48	1.40
20	<i>gm16596</i>	predicted gene 16596	2.21	1.87
21	<i>gm16310</i>	predicted gene 16310	2.19	3.38
22	<i>gm24357</i>	predicted gene 24357	1.56	1.32
23	<i>gm21769</i>	predicted gene 21769	1.49	1.56
24	<i>gm9982</i>	predicted gene 9982	1.42	1.29
25	<i>gm26767</i>	predicted gene 26767	1.40	1.39
26	<i>gm16184</i>	predicted gene 16184	1.24	1.14

The 26 predicted genes/pseudogenes that were induced following LPS+immune complex treatment and LPS+adenosine treatment. All of these genes have at least a two-fold up-regulation over both the LPS treated and IL-4 treated expression levels. Values were determined by calculating the induction over the non-stimulated condition and are expressed as a log<sub>2</sub> value.

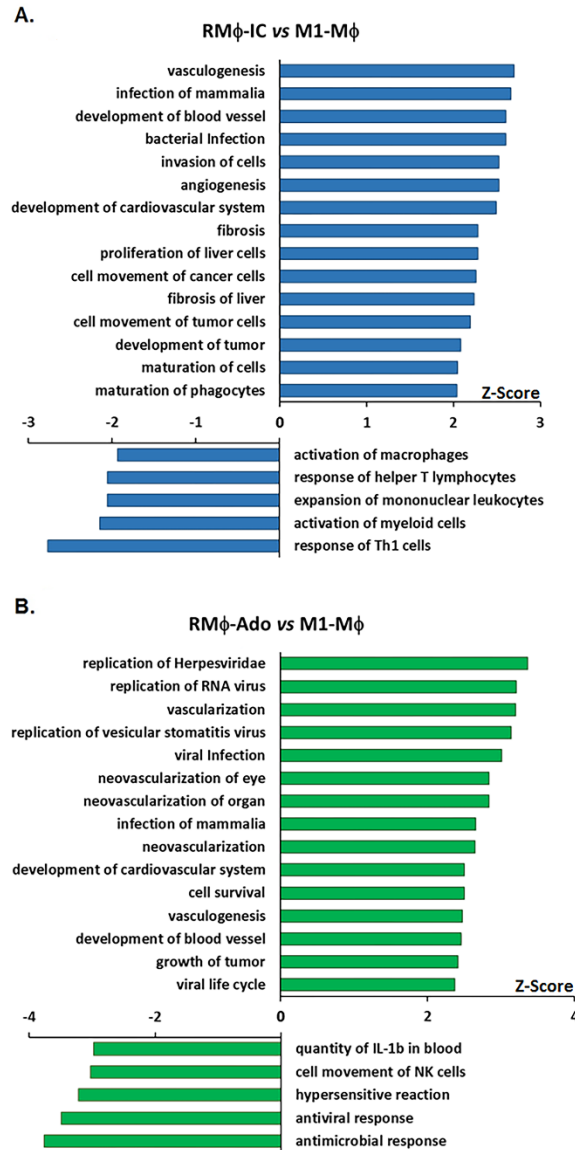


**Figure 8: Top activated and repressed ‘Diseases and Function’ associated with regulatory activation in macrophages.** The changes associated with ‘Diseases and Functions’ in R-M $\phi$  were predicted by Ingenuity pathway analysis program. Genes that showed a changed in L+I (A) or L+A (B) of at least two-fold when compared to M1-M $\phi$  were selected to identify pathways associated with regulatory functions. Fold changes were uploaded to IPA and the ‘Diseases and Functions’ predicted to be altered based on a significant z-score were selected for these graphs. A z-score above 1.65 (activated) or below -1.65 (inhibited) is considered statistically significant. Figure was generated with the help of Bess Dalby.

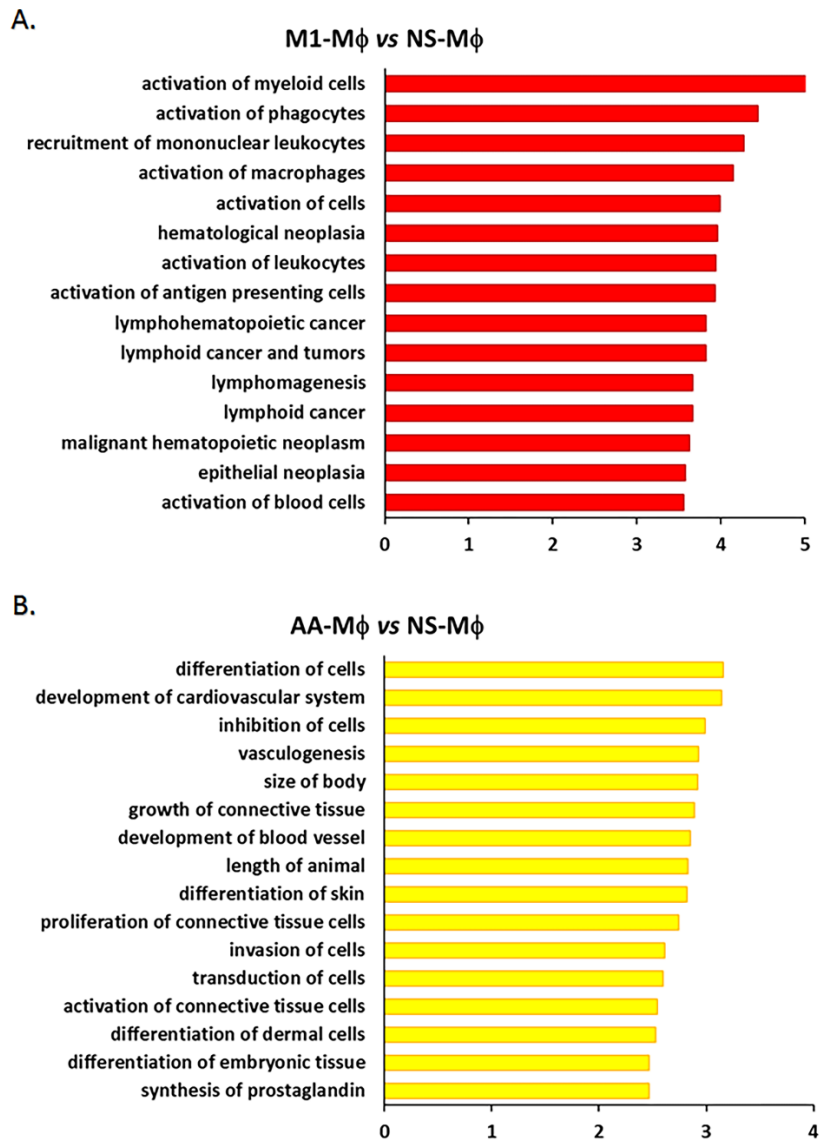


**Figure 9: Top 15 activated ‘Diseases and Function’ associated with M1 and Alternatively Activated macrophages.** Top 15 activated pathways associated with ‘Diseases and Functions’ predicted by Ingenuity Pathway Analysis Program are shown for M1-M $\phi$  (A) and AA-M $\phi$  (B). Data is expressed as a Z-score which was generated by comparing the stimulated conditions to the non-stimulated resting macrophages. A Z-score of 1.65 or greater indicates statistical significance. Figure was generated with the help of Bess Dalby.

### **3.4.5 Metabolism in Regulatory Activation is Similar to that of LPS Treated Cells**

Several studies have identified metabolic alterations among the various macrophage activation states<sup>109-111</sup>. Applying IPA to the RNA-seq data identified several metabolic changes that occurred in both LPS stimulated M1-M $\phi$  and R-M $\phi$ , but not in IL-4 treated AA-M $\phi$  (Table 9). To confirm the metabolic differences predicted by IPA, the consumption of glucose and the production of L-lactate was experimentally determined. Glucose consumption by the three R-M $\phi$  populations was comparable to M1-M $\phi$ , and much higher than IL-4-treated AA-M $\phi$  which was comparable to non-stimulated cells (Figure 10A). Similarly, the secretion of L-lactate, a metabolic product of the fermentation pathway, was higher in M1-M $\phi$  and R-M $\phi$  relative to IL-4 treated AA-M $\phi$  (Figure 10B). These results suggest that R-M $\phi$  share metabolic similarities with LPS treated M1-M $\phi$  and are distinct from AA-M $\phi$ . Additionally, it indicated that changes in metabolism might be involved in cellular responses required for the combat of pathogens.



**Table 9: Metabolic Pathways Identified by IPA Analysis (Z-score)**

Canonical Pathways related to energy metabolism	LPS	L+I	L+A	IL-4
Pentose phosphate pathway (Oxidative branch)	2.54	2.37	2.42	0.73
Pentose phosphate pathway	2.43	2.20	2.26	0.44
Fatty acid $\beta$ -oxidation I	1.82	2.46	3.12	0.00
Glycogen degradation II	1.89	1.70	2.53	0.00
Glycogen degradation III	2.19	1.33	2.79	0.00
Gluconeogenesis I	1.66	3.73	1.06	0.21
Oleate biosynthesis II (animals)	0.85	1.77	1.82	0.00
Glycolysis I	1.12	3.51	0.97	0.00

The top energy metabolism related canonical pathways that shows significant upregulation in at least one of the four conditions analyzed by RNA-seq. Numbers are expressed as the Z-score which was generated from a Fisher's Exact test when comparing stimulated to non-stimulated macrophages. Numbers that had a Z-score of at least 1.65( $p < 0.05$ ) are considered significant. Table was generated by Bess Dalby.

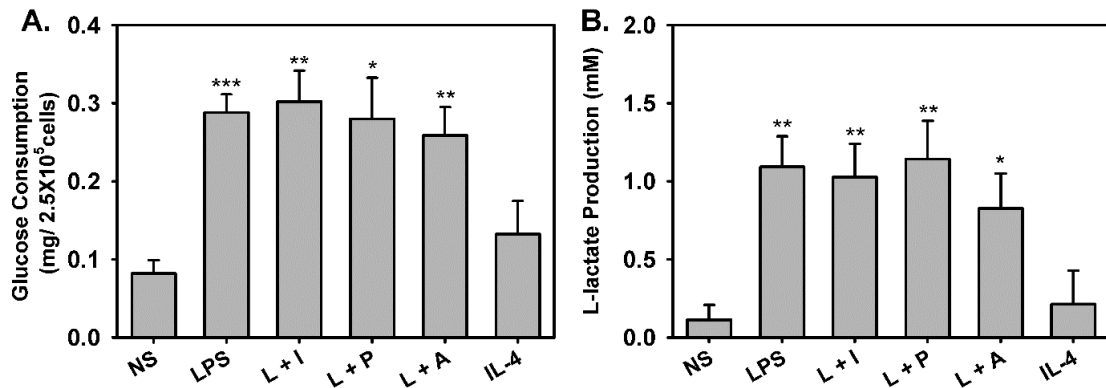


**Figure 10: Glucose and lactate production in Regulatory macrophages.** BMDMs were left unstimulated or stimulated with 10 ng/ml LPS, a combination of LPS and 1 $\mu$ g of OVA opsonized with anti-OVA antibody (L+I), 200 nM PGE<sub>2</sub> (L+P), 200  $\mu$ M adenosine (L+A), or 20 ng/ml IL-4 for 24 hours. **(A)** Glucose consumption was determined 24 hours post stimulation by an enzymatic assay as described in materials and methods. **(B)** L-lactate concentrations in the supernatants were obtained 8 hours post stimulation by utilizing the NADH-coupled enzyme reaction that reduces tetrazolim salt to formazan which is measured at an absorbance of 490 nm. Error bars indicate Mean  $\pm$  SEM of four independent experiments. Statistics were determined by comparing the various activation conditions to the non-stimulated condition. \*\*\*,  $p < 0.001$ . \*\*,  $p < 0.01$ . \*,  $p < 0.05$ . Figure was generated with the help of Bess Dalby.

### 3.4.6 Identification of Candidate Biomarkers

To validate the RNA-seq analyses, qRT-PCR was performed to examine several regulatory and AA-M $\phi$  associated genes. Activation states were confirmed through the examination of well-established markers (Figure 11). Among the tested genes, the mRNA levels of *il-33*, *flrt3*, and *ccr1* were induced in all regulatory conditions, but not by LPS or IL-4 stimulation (Figure 12). The mutual upregulation of these cells in Regulatory macrophages suggests that these genes play an important roles in the immunoregulatory phenotype. These studies were repeated in the *stat6*<sup>-/-</sup> mice to determine if their inductions was independent of STAT6 signaling. The induction profiles were indeed similar to those observed in the wild type mice (Figure 13). Thus, these genes represent potential biomarkers for R-M $\phi$ .

Additionally, genes were found to be associated with a single stimulatory conditions. Some genes were induced in individual regulatory populations but not shared by all three R-M $\phi$ . For example, mRNAs encoding *gem*, *ildr1*, and *empl* were induced in RM $\phi$ -IC, but not in RM $\phi$ -PGE<sub>2</sub>/RM $\phi$ -Ado (Figure 14). The unique induction of these genes suggests that not all Regulatory macrophages are the same, but rather are related by a group of core genes. Similarly, the mRNA expression of *il-4i1*, *earl1* and *cd209e* was specifically induced in AA-M $\phi$  (Figure 15). The fact that not of these genes were associated with regulatory activation suggests that the function of AA-M $\phi$  is distinct from R-M $\phi$ . Like before, these genes were tested to determine if they were dependent on STAT6 signaling. As expected, the genes associated with immune complex stimulations were STAT6

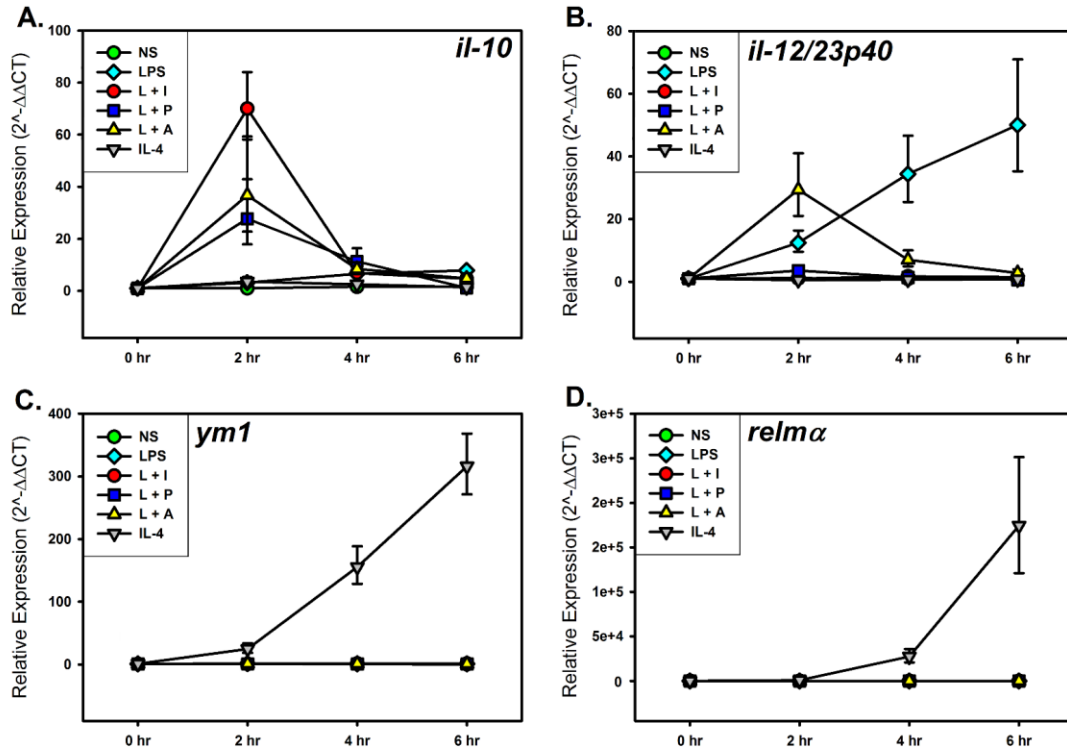


**Figure 11: Induction profiles of control genes in activated macrophages.** Real time-PCR analyses were performed at indicated time points on cDNA obtained from WT BALB/c BMDMs, which were left unstimulated or stimulated with 10 ng/ml LPS, a combination of LPS and 5 $\mu$ g of OVA opsonized with anti-OVA antibody (L+I), 200 nM PGE<sub>2</sub> (L+P), 200  $\mu$ M adenosine (L+A) or 20 ng/ml IL-4. Graphs for *il-10* (A), *il-12/23p40* (B), *ym1* (C), and *relm $\alpha$*  (D) are shown. Each data point represents mean value  $\pm$  SEM from duplicate values of four separate experiments.

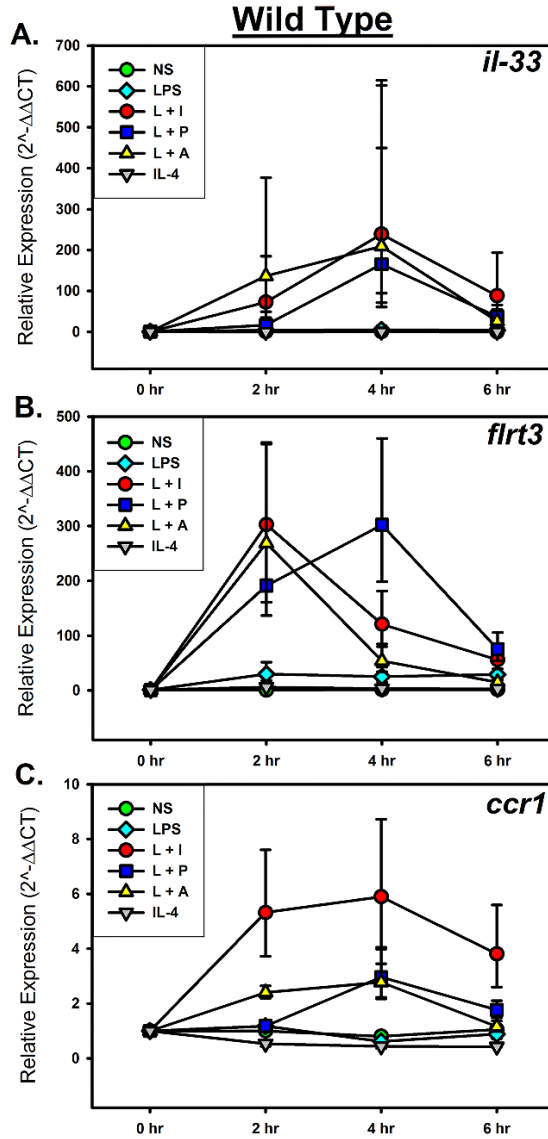


**Figure 12: Induction profiles of regulatory genes in activated macrophages.** Real time-PCR analyses were performed at indicated time points on cDNA obtained from BALB/c WT BMDMs, which were left unstimulated or stimulated with 10 ng/ml LPS, a combination of LPS and 5 $\mu$ g of OVA opsonized with anti-OVA antibody (L+I), 200 nM PGE<sub>2</sub> (L+P), 200  $\mu$ M adenosine (L+A) or 20 ng/ml IL-4. Graphs for *il-33* (A), *flrt3* (B), and *ccr1* (C) are shown. Each data point represents mean value  $\pm$  SEM from duplicate values of four separate experiments.

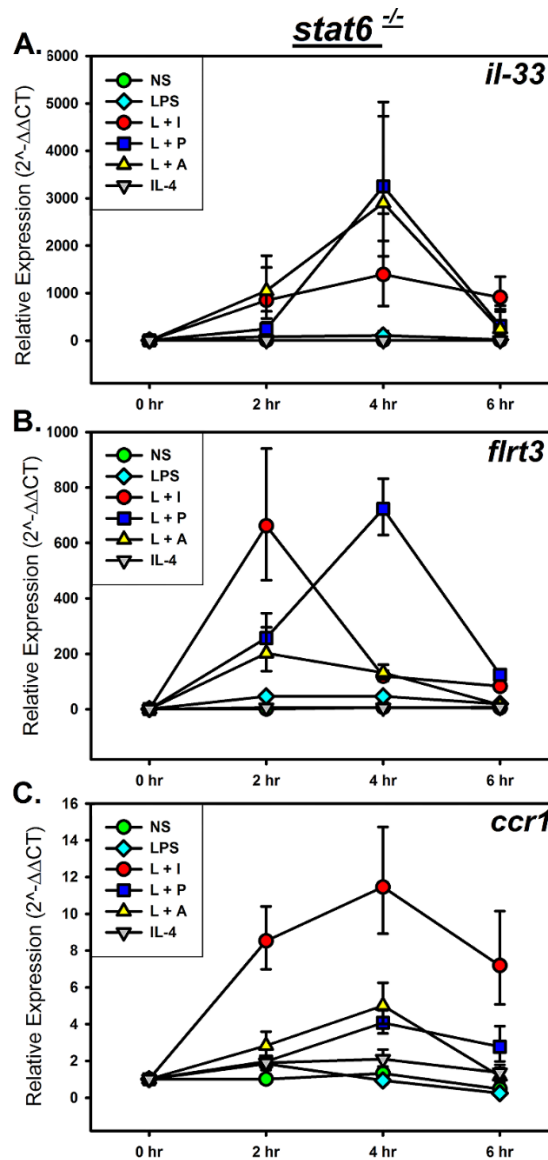


**Figure 13: Induction profiles of regulatory genes in activated macrophages is independent of STAT6 signaling.** Real time-PCR analyses were performed at indicated time points on cDNA obtained from BALB/c *stat6*<sup>-/-</sup> BMDMs, which were left unstimulated or stimulated with 10 ng/ml LPS, a combination of LPS and 5 $\mu$ g of OVA opsonized with anti-OVA antibody (L+I), 200 nM PGE<sub>2</sub> (L+P), 200  $\mu$ M adenosine (L+A) or 20 ng/ml IL-4. Graphs for *il-33* (A), *flrt3* (B), and *ccr1* (C) are shown. Each data point represents mean value  $\pm$  SEM from duplicate values of four separate experiments.

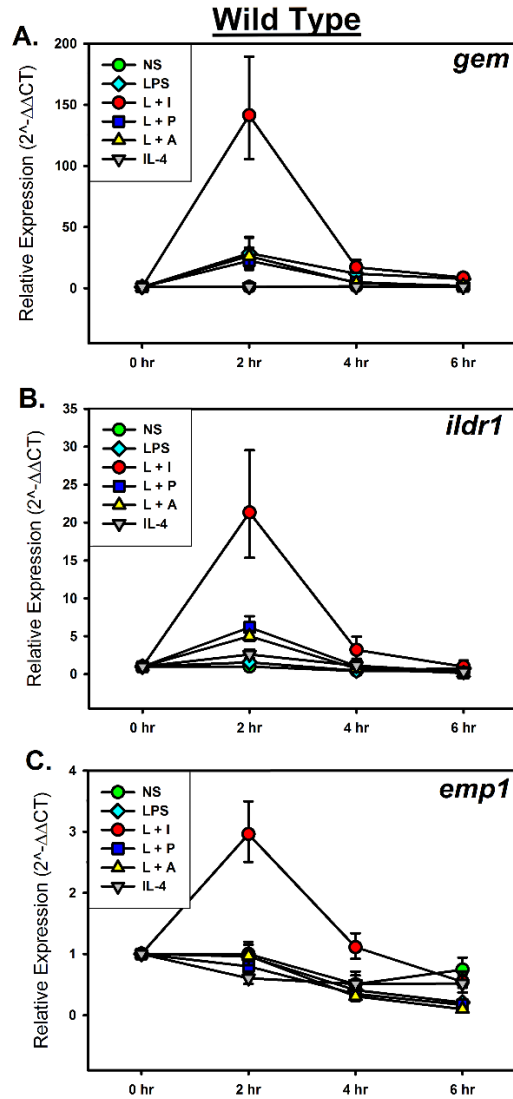


**Figure 14: Induction profiles of immune complex induced genes in activated macrophages.** Real time-PCR analyses were performed at indicated time points on cDNA obtained from BALB/c WT BMDMs, which were left unstimulated or stimulated with 10 ng/ml LPS, a combination of LPS and 5 $\mu$ g of OVA opsonized with anti-OVA antibody (L+I), 200 nM PGE<sub>2</sub> (L+P), 200  $\mu$ M adenosine (L+A) or 20 ng/ml IL-4. Graphs for *gem* (A), *ildir1* (B), and *emp1* (C) are shown. Each data point represents mean value  $\pm$  SEM from duplicate values of four separate experiments.

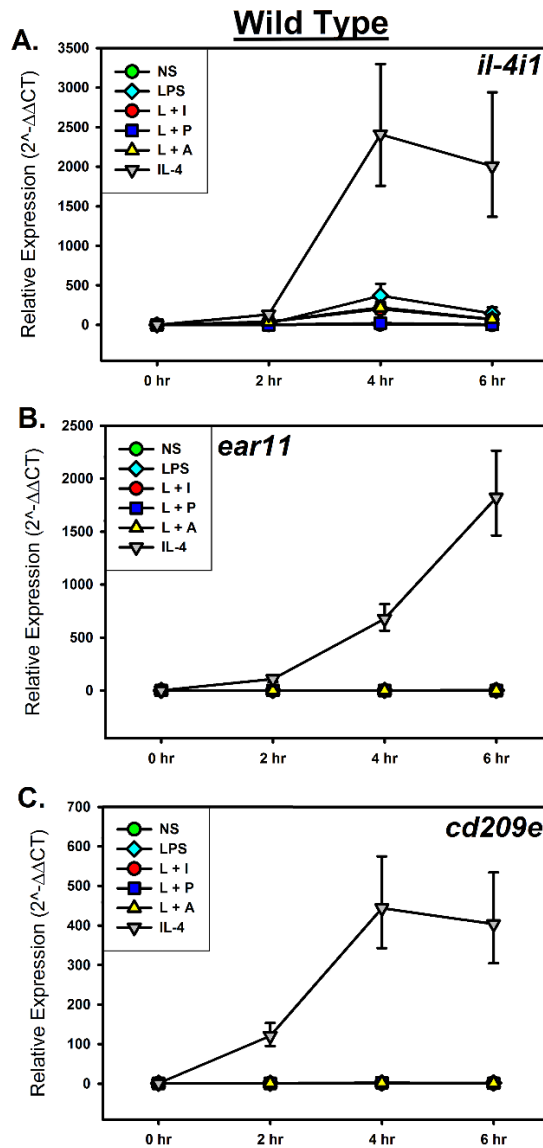


**Figure 15: Induction profiles of IL-4 induced genes in activated macrophages.** Real time-PCR analyses were performed at indicated time points on cDNA obtained from BALB/c WT BMDMs, which were left unstimulated or stimulated with 10 ng/ml LPS, a combination of LPS and 5 $\mu$ g of OVA opsonized with anti-OVA antibody (L+I), 200 nM PGE<sub>2</sub> (L+P), 200  $\mu$ M adenosine (L+A) or 20 ng/ml IL-4. Graphs for *il-4i1* (A), *ear11* (B), and *cd209e* (C) are shown. Each data point represents mean value  $\pm$  SEM from duplicate values of four separate experiments.



independent, but the genes associated with IL-4 stimulation were STAT6 dependent (Figure 16). This helps to highlight a fundamental difference in how these genes are induced and how they help to define the different activation states.

There were additional qRT-PCR validations performed on genes found in Table 7. Genes that showed increased expression for at least one regulatory condition were *ndrg1*, *klk9*, *dusp14*, *hc*, *tnfsf14* and *cd244* (Figure 17). Analysis of *lif*, *xcr1*, *mid1*, and *mospd4* revealed that these genes were not associated with regulatory conditions or were below the level of detection (Figure 18). The failed validation of these genes could indicate differences in how bone marrow derived and peritoneal macrophages regulate gene expression.

#### **3.4.7 Detecting Candidate Biomarkers on the Protein Level**

Chemokine receptors form an important component of immune responses and the polarized macrophages subsets exhibit differences in their surface chemokine receptor expression<sup>46</sup>. To correlate transcription with surface protein levels, we performed flow cytometric analysis of CCR1 surface expression on the different macrophage populations. There was a 3-4 fold increase in mean fluorescent intensity (MFI) observed in all of the R-M $\phi$ , with only a 2 fold induction in the LPS treated cells and no induction in IL-4 treated cells (Figure 19). Thus, CCR1 represents a potential biomarker for R-M $\phi$  and suggests that Regulatory macrophages can be identified through analysis of their surface markers.

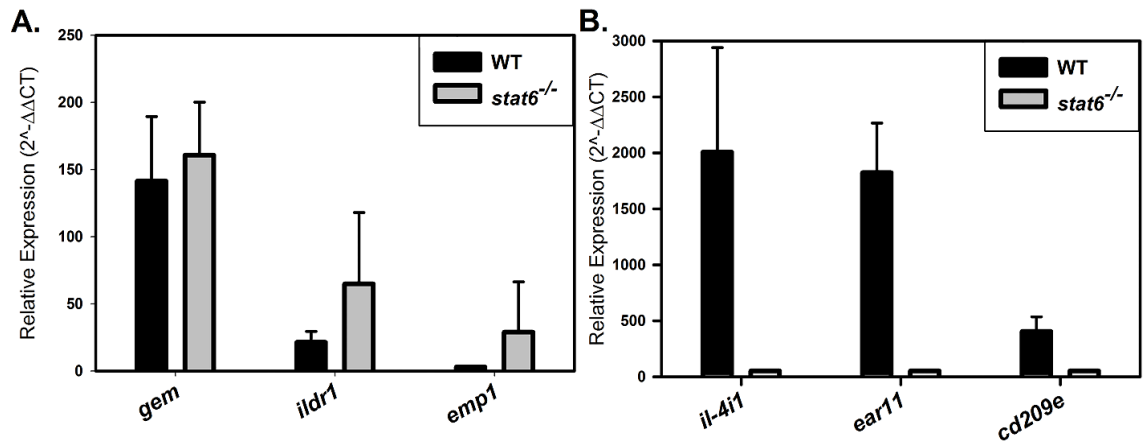


**Figure 16: Induction of immune complex induced genes is independent of STAT6 signaling in activated macrophages.** Real time-PCR analyses of immune complex induced genes (A) and IL-4 induced (B) genes were performed at 2 hours and 6 hours, respectively. BALB/c WT and *stat6*<sup>-/-</sup> BMDMs were stimulated LPS and 5 $\mu$ g of OVA opsonized with anti-OVA antibody or 20 ng/ml IL-4. Relative expression was determined by a comparison with non-stimulated cells. Each error bar represents mean value  $\pm$  SEM from duplicate values of four separate experiments.

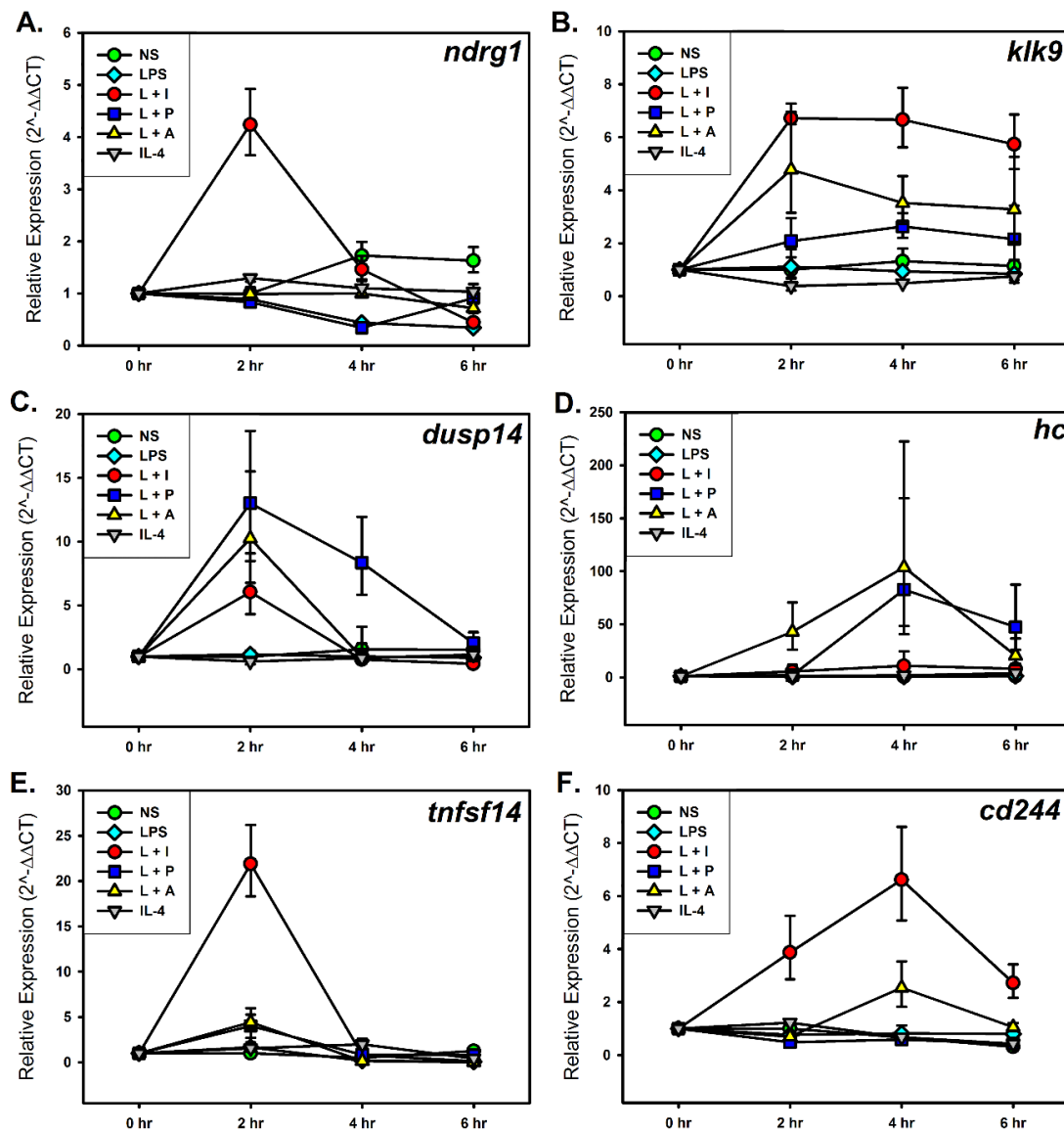


**Figure 17: Validation of regulatory gene candidates in activated macrophages.** Real time-PCR analyses were performed at indicated time points on cDNA obtained from WT BALB/c BMDMs, which were left unstimulated or stimulated with 10 ng/ml LPS, a combination of LPS and 5 $\mu$ g of OVA opsonized with anti-OVA antibody (L+I), 200 nM PGE<sub>2</sub> (L+P), 200  $\mu$ M adenosine (L+A) or 20 ng/ml IL-4. Graphs for *ndrg1* (A), *klk9* (B), *dusp14* (C), *hc* (D), *tnfsf14* (E), and *cd244* (F) are shown. Each data point represents mean value  $\pm$  SEM from duplicate values of four separate experiments.

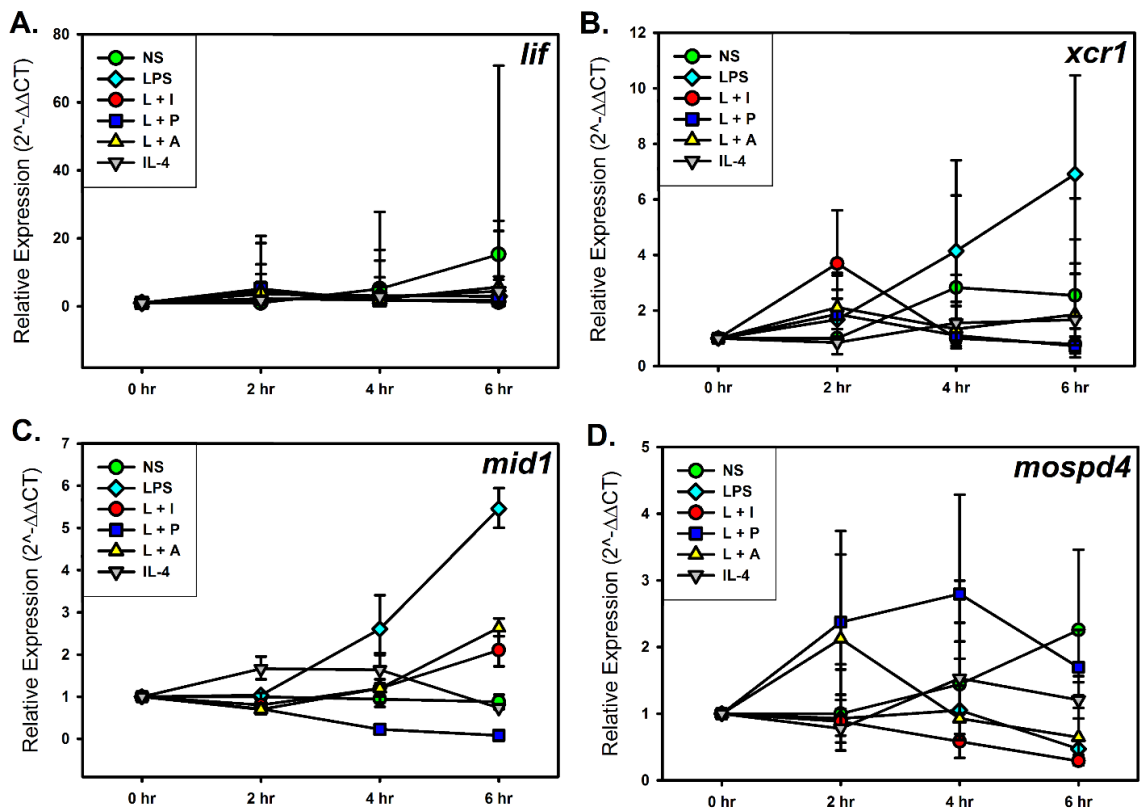


**Figure 18: Failed validation of regulatory gene candidates in activated macrophages.** Real time-PCR analyses were performed at indicated time points on cDNA obtained from WT BALB/c BMDMs, which were left unstimulated or stimulated with 10 ng/ml LPS, a combination of LPS and 5 $\mu$ g of OVA opsonized with anti-OVA antibody (L+I), 200 nM PGE<sub>2</sub> (L+P), 200  $\mu$ M adenosine (L+A) or 20 ng/ml IL-4. Graphs for *lif* (A), *xcr1* (B), *mid1* (C), and *mospd4* (D) are shown. Each data point represents mean value  $\pm$  SEM from duplicate values of four separate experiments.

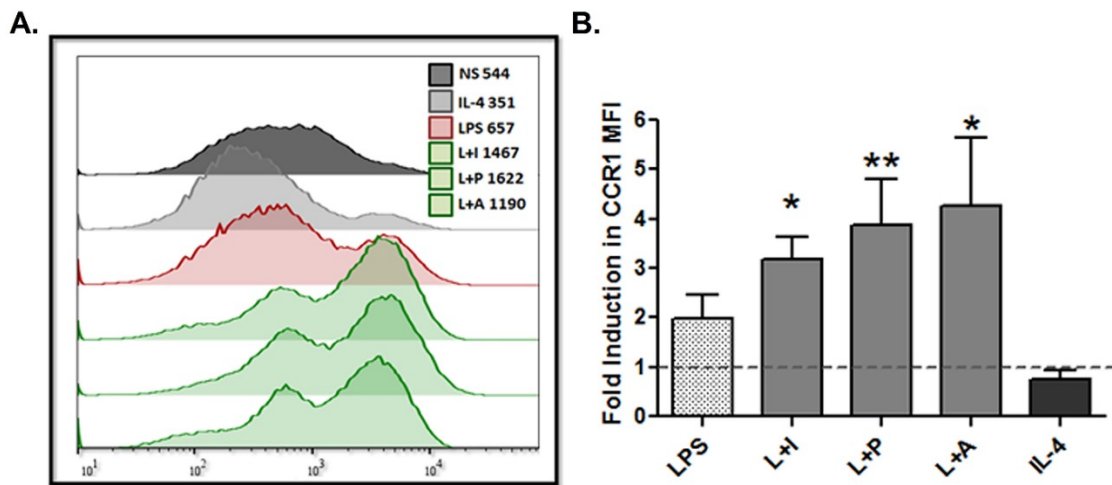


**Figure 19: CCR1 expression is associated with regulatory activation of macrophages.** BALB/c WT BMDMs, which were left unstimulated or stimulated with 10 ng/ml LPS, a combination of LPS and 5 $\mu$ g of OVA opsonized with anti-OVA antibody (L+I), 200 nM PGE<sub>2</sub> (L+P), 200  $\mu$ M adenosine (L+A) or 20 ng/ml IL-4. Surface expression of CCR1 was assessed by flow cytometry using a PE-conjugated antibody after 24 hours of stimulation. A representative histogram (A) and the fold induction in CCR1 mean fluorescence intensity (MFI) over non-stimulated cells is represented from five separate experiments (B) are shown here. The mean values are represented with SEM and statistics were determined through a comparison to the LPS condition. \*, \*\* represents p < 0.05, 0.01, respectively. This figure was generated with the help of Prabha Chandrasekaran and Arup Sarkar.

### **3.4.8 Regulatory Activation Offers Protection from Lethal Endotoxin Challenge**

The production of IL-10 by the macrophage has been identified as an important component in sparing mice from lethal endotoxemia<sup>112,113</sup>. We hypothesized that the R-M $\phi$  should offer protection against lethal endotoxin challenge. To test this, we adoptively transferred the various R-M $\phi$  and AA-M $\phi$  into the peritoneum of mice, followed by intraperitoneal injection of a lethal dose of LPS (endotoxin). All three R-M $\phi$  populations provided some level of protection to mice receiving endotoxin. Mice that received RM $\phi$ -IC showed a 90% survival, whereas mice that received RM $\phi$ -PGE<sub>2</sub> or RM $\phi$ -Ado showed survival rates of 70% and 50%, respectively. In contrast, 80% of mice receiving resting unstimulated M $\phi$  succumbed to lethal endotoxemia. Parallel groups of mice receiving a transfer of IL-4-treated AA-M $\phi$  were not protected from lethal endotoxemia, and in fact did slightly worse than mice receiving resting macrophages (Figure 20A). The mice that received RM $\phi$ -IC had a 90% survival rate, regardless of whether the macrophages that were transferred were from WT or *stat6* KO mice (Figure 20B). Thus, the ability to provide protection from lethal endotoxin challenge highlights a major functional difference between the R-M $\phi$  and IL-4-treated AA-M $\phi$ .

### **3.4.9 Cytokine Expression Profile of Human Macrophages**

To extend our observations from mouse to human, we stimulated human monocyte derived macrophages from six different healthy human donors with the same conditions used for mouse BMDM and assessed the cytokine levels in the supernatants. The results showed that there were some differences in the responses of the human macrophages to the

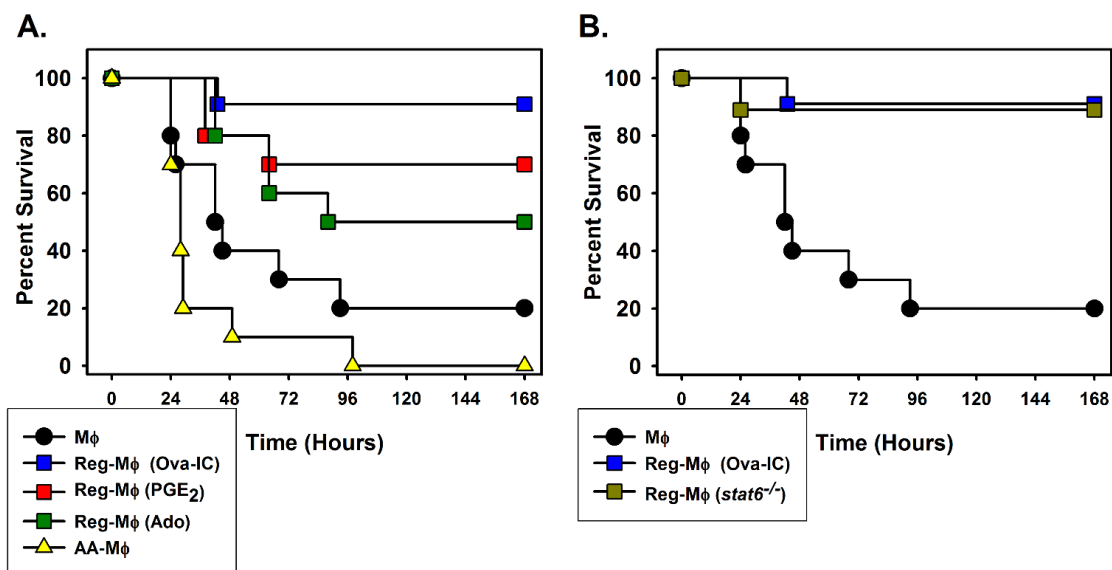


**Figure 20: Regulatory macrophages provide protection from lethal endotoxemia. (A)** BALB/c mice received  $1 \times 10^6$  resting non-stimulated macrophages (M $\phi$  filled circles) intraperitoneally or macrophages stimulated in vitro with LPS and  $5 \mu\text{g}$  of OVA opsonized with anti-OVA antibody (blue squares),  $200 \text{ nM}$  PGE<sub>2</sub> (red squares),  $200 \mu\text{M}$  adenosine (green squares) or  $20 \text{ ng/ml}$  IL-4 (yellow triangles), three hours prior to challenge with a lethal dose of endotoxin ( $10 \text{ mg/kg}$ ). The survival of the mice was recorded every eight hours over the next week. **(B)** A similar survival experiment was carried out in WT mice that received  $1 \times 10^6$  LPS+IC macrophages from WT (blue squares) or *stat6*<sup>-/-</sup> (dark yellow squares) mice prior to endotoxin challenge. Each graph represents data of two independent experiments with 10 mice each experiment for each condition. The data from the control group and WT RM $\phi$ -IC were shared between the two graphs.

“reprogramming” stimulations when compared to their mouse counterparts. Whereas the RM $\phi$ -IC and RM $\phi$ -Ado show upregulation of IL-10, G-CSF was only significant in RM $\phi$ -IC. The other regulatory conditions did not show any observable differences compared to LPS stimulated macrophages (Figure 21A, 21B). The inhibition of LPS induced inflammatory cytokines IL-12/23p40 and TNF- $\alpha$  was observed for RM $\phi$ -Ado and RM $\phi$ -PGE<sub>2</sub> but not for RM $\phi$ -IC (Figure 21C, 21D). Interestingly, as observed with the mouse macrophages, the LPS induced production of IL-6 was significantly inhibited under all tested regulatory conditions in human macrophages (Figure 21E). The levels of IL-1 $\beta$  were unaffected by the presence of any of the regulatory signals in human macrophage (Figure 21F). These results demonstrate that regulatory signals are inducible in human macrophages and when induced, they have distinct cytokine signatures that differentiate them from M1-M $\phi$  and AA-M $\phi$ .

### **3.5 Discussion**

It has been suggested that there are many potential reprogramming signals that can change the phenotype of stimulated macrophages. In earlier reports, we demonstrated that macrophages stimulated with TLR ligands in the presence of high density immune complexes assumed immunoregulatory functions by dampening inflammatory cytokine production and turning on IL-10 secretion<sup>97,114</sup>. We know now that the induction of R-M $\phi$  required two concurrent signals; one to activate the transcription factors necessary for cytokine production and the second to “reprogram” the cell to secrete immunoregulatory cytokines. We investigated whether secondary signals like adenosine and prostaglandin E<sub>2</sub>



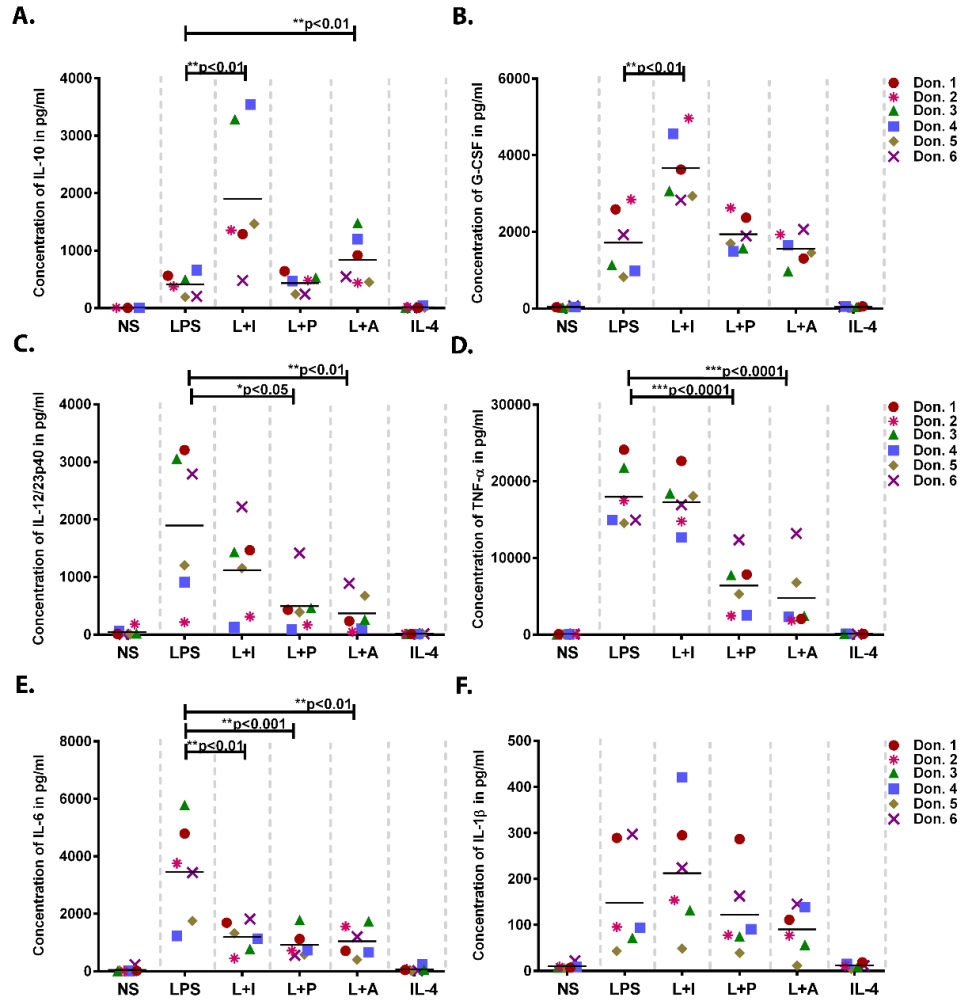


**Figure 21: Cytokine profiles of human macrophages under regulatory stimulation conditions.** Human monocyte-derived macrophages were cultured at the concentration of  $5 \times 10^5$  cells/ 500  $\mu$ L of medium in the presence of M-CSF and were left unstimulated or stimulated with 10 ng/ml LPS (L), a combination of LPS and 5 $\mu$ g of OVA opsonized with anti-OVA antibody (L+I), 200 nM PGE<sub>2</sub> (L+P), 200  $\mu$ M adenosine (L+A), or 20 ng/ml IL-4 for 24 hours. The levels of all indicated cytokines except IL-12/23p40 were measured using a bioplex assay (A-D, F). IL-12/23p40 levels were measured using a sandwich ELISA kit (E). The horizontal bar represents the mean value and the asterisks represent the significance of the observed values compared to LPS treated cells. Figure was generated with the help of Prabha Chandrasekaran.

were capable of inducing macrophages with an immunoregulatory functions. We demonstrated that all of these macrophages exhibit common characteristics, such as the production of high levels of immunomodulatory cytokines, including IL-10, and the secretion of reduced levels of inflammatory cytokines, such as IL-1 $\beta$ , IL-6, and IL-12/23. This change in cytokine profile is important because it has a direct impact on how immune responses develop and on disease clearance. Additionally, these cells produced higher levels of transcripts for cell growth and angiogenic factors as determined by RNA-seq analysis. IPA analysis revealed that R-M $\phi$  are closely associated with cell growth and proliferation regardless of whether they were induced with immune complexes or adenosine. Thus, it is likely that all R-M $\phi$  contribute to the maintenance of homeostasis by dampening immune responses and promoting cellular repair.

The classification of macrophages has become increasingly more complex and controversial. Although there is a reasonable consensus as to what constitutes M1-M $\phi$ , there remains a substantial degree of confusion regarding what constitutes the so-called M2-M $\phi$ . The original grouping of all macrophages that were not M1-M $\phi$  into the M2 category was instructional because it fostered the idea that not all stimulated macrophages are the same. However, it has also led to the misconception that all M2-M $\phi$  are similar, and this does not appear to be the case. In this work, we demonstrate that R-M $\phi$  are quite distinct from IL-4 treated AA-M $\phi$  with respect to metabolism and disease modulation. We also demonstrate that macrophages with potent immunoregulatory activity can be generated via a STAT6-independent mechanism. Confusion regarding the various

macrophage populations has delayed attempts to deplete specific macrophage subpopulations or to target drugs to one subset or another.

Previous work by the Mosser lab has demonstrated that Regulatory macrophages produce high levels of nitric oxide following stimulation<sup>44</sup>. This is in direct contrast to AA-M $\phi$  that fail to produce nitric oxide upon activation. The failure of AA-M $\phi$  to produce nitric oxide has been attributed to their induction of Arginase-1, which converts arginine to ornithin<sup>44,48</sup>. Consequently, Arg-1 has been used as a biomarker to identify AA-M $\phi$ , and several groups have mistakenly identified AA-M $\phi$  in tissue based exclusively on their expression of Arg-1. It is now known that multiple macrophages populations can produce Arg-1 following activation<sup>61,87</sup>. While the use of Arg-1 as a biomarker remains controversial, the lack of nitric oxide by AA-M $\phi$  provides evidence that R-M $\phi$  and AA-M $\phi$  display fundamental differences in their arginine metabolism.

Other research groups have implicated metabolic reprogramming as an important factor in the polarization of macrophages into M1 and M2 phenotype<sup>115,116</sup>. It has been reported that metabolic pathways shift to anaerobic glycolysis in M1-M $\phi$  and to oxidative glucose metabolism in M2-M $\phi$ <sup>109</sup>. To determine if our macrophage populations showed differences in glucose metabolism, we utilized a glucose consumption and L-lactate production assays. We demonstrated that R-M $\phi$  undergo enhanced glycolysis and produce L-lactate similarly to M1-M $\phi$ . This observation may not be surprising since both M1 and R-M $\phi$  are stimulated with LPS, but it does reveal that the reprogramming signals that so dramatically alter cytokine production do not alter general cellular metabolism. The AA-

M $\phi$  show minimal increases in glucose consumption and low levels of L-lactate production. These cells showed more metabolic similarities with the non-stimulated cells, than they did with the R-M $\phi$ . Our IPA analyses of metabolic pathways in R-M $\phi$  confirm that these macrophages resemble M1-M $\phi$  and are clearly distinct from AA-M $\phi$ . The differences associated with metabolism are just one example that helps to disprove the belief that all non-M1-M $\phi$  are M2-M $\phi$ .

The immunomodulatory effects of IL-10 appear to be most pronounced at the level of antigen presenting cells. Therefore, the high levels of IL-10 production from R-M $\phi$  suggests that macrophages themselves are the main regulators of macrophage activation, and that this is a primary function of R-M $\phi$ . Interleukin-10 has been previously shown to inhibit IFN- $\gamma$  and TNF- $\alpha$  production and offer protection during experimental endotoxemia<sup>112,117,118</sup>. Hence, we hypothesized that the R-M $\phi$  would confer protection in experimental sepsis models in mice. The administration of R-M $\phi$  increased the survival of mice during endotoxemia, whereas the addition of AA-M $\phi$  did not. In our experiments, the addition of IL-4 treated macrophages actually increased mortality. This experiment provided evidence that the generation of R-M $\phi$  and AA-M $\phi$  in disease can have a polarize effect on the outcome of disease. Additionally, this supports the idea that the selective depletion of a single macrophage population can have a direct effect on disease progression. It has previously been shown that IL-4 treatment of macrophages can augment their production of IL-12<sup>119,120</sup> and this observation may explain why IL-4 treated macrophage caused increased mortality in this model. The role of IL-4 in LPS induced

endotoxin shock has not been clearly defined. However, in a *S. aureus* triggered sepsis and an arthritis model, the survival of *il-4* deficient mice was dependent on the genetic background of the mice<sup>121</sup>. The results from our studies clearly demonstrate that R-M $\phi$  and AA-M $\phi$  have different functions, reaffirming that these macrophages should not be considered part of the same class.

To address whether IL-4 or STAT6 signaling was a requisite for regulatory macrophage functions, we studied cytokine production from macrophages from *stat6*<sup>-/-</sup> mice stimulated under immunoregulatory conditions. Signaling through STAT6 was previously demonstrated to be important for the anti-inflammatory properties of IL-4<sup>57,122</sup> and for the generation of AA-M $\phi$ .<sup>122</sup> In our hands, macrophages from *stat6* deficient mice failed to induce *ym1* and *relm $\alpha$*  expression as previously reported<sup>122</sup>. The *stat6* deficient macrophages retained their ability to induction of anti-inflammatory IL-10 and the down regulation of pro-inflammatory IL-12, IL-1 $\beta$  and IL-6 following regulatory activation. Additionally, *stat6* deficient macrophages that were stimulated with immune complexes were capable of protecting mice from lethal endotoxin challenge. From this, we concluded that STAT6 signaling was dispensable for the generation of R-M $\phi$ . The fact that regulatory activation is independence from STAT6 signaling has demonstrate that there is no overlap with the pathways required for alternative activation. This supports the idea that the classification of R-M $\phi$  and AA-M $\phi$  as subset of M2-M $\phi$  is both inaccurate and misleading.

It is our belief that a transcriptomic analysis would be the most appropriate way of comparing regulatory and alternative activation. RNA-seq analysis of various human<sup>123</sup>

and mouse<sup>124</sup> macrophage subsets has been previously reported and have helped to highlight the differences in activated macrophage. Through PCA and heat map analysis we demonstrated that Regulatory macrophages and Alternatively Activated macrophages are characterized by very different transcriptomes. While the Regulatory macrophages cluster with the LPS treated macrophages, the Alternatively Activated macrophages clustered with non-stimulated cells. Additionally, our analysis revealed that AA-M $\phi$  were predicted to be involved in cell differentiation and elongation, whereas R-M $\phi$  were predicted to promote cell growth, angiogenesis, and repair. This shows that Regulatory and Alternatively Activated macrophages are not only different in the number of genes that they induce, but in their overall functionality.

The generation of transcriptomic profiles allowed us to identify every gene response for the observed activation phenotypes. We compiled a list of genes that was associated with Alternatively Activated macrophages and began to realize that most of these genes were absent from the Regulatory macrophage profiles. Most of the genes that we report to be specifically upregulated in AA-M $\phi$  agree with previously published reports<sup>124</sup>. To further our analysis we identified the transcripts produced by R-M $\phi$  that were absent in AA-M $\phi$ . This approach was undertaken to identify a “core transcriptome” that would define macrophages with an immunoregulatory phenotype. We identified some 182 genes that were uniquely upregulated in R-M $\phi$ , relative to other macrophage populations, including resting, M1, and AA-M $\phi$ . We believe that these genes are responsible for the immunoregulatory function of Regulatory macrophages and that by studying these genes

it will be possible to better understand how these macrophages function. In addition to examining differences in the transcripts produced by AA-M $\phi$  relative to R-M $\phi$ , our analysis also examined similarities among transcripts produced by the different R-M $\phi$  populations. This helped us realize that while Regulatory macrophages can be transcriptomically different from one another, they share a set of core genes that is responsible for their immunoregulatory functions.

The plasticity of macrophages have made it difficult to study this cells in tissue. We recently demonstrated that M1-M $\phi$  gradually transition into R-M $\phi$  following stimulation<sup>61</sup>, and this transition makes it difficult to establish a baseline biomarker expression level from which to compare. Furthermore, the “reprogramming” signals that induce R-M $\phi$  affect the chromatin associated with regulatory transcripts<sup>67,77</sup>, making it difficult to use promoter-reporter mice. Recently, our attempts to utilize *il-33* reporter mice as an indicator of regulatory activation failed<sup>125</sup>. We assume that the epigenetic modifications that lead to transcript expression in R-M $\phi$  are not preserved in these reporter mice. The need for reliable protein biomarkers for R-M $\phi$  remains of the utmost importance. This work identified that the chemokine receptor CCR1 was upregulated at both the mRNA and protein levels in R-M $\phi$ , and this upregulation occurred independent of STAT6 expression. Thus CCR1 represents a potential biomarker for R-M $\phi$ . Attempts to identify R-M $\phi$  in tissue based on CCR1 expression are underway. This chemokine receptor has been implicated in immune regulatory functions in inflammatory and infections

models<sup>126,127</sup>. How this receptor affects the migratory pattern of R-M $\phi$  is of future interest to us.

In conclusion, this study has demonstrated that R-M $\phi$  are distinct from AA-M $\phi$ . In fact, R-M $\phi$  are transcriptionally more closely related to M1-M $\phi$ , but they distinguish themselves from the latter by a relatively small and unique set of transcripts and immune regulatory functions. Although there are subtle differences in the gene expression patterns and cytokine/chemokine responses among the differently generated Regulatory macrophage, it should be appreciated that these macrophages are biochemically and functionally related, and distinct from M1-M $\phi$  and AA-M $\phi$ . Hence we recommend considering Regulatory macrophages as a separate macrophage population, and not as a subset of M2-M $\phi$ .



## Chapter 4: Conclusions

The research conducted in this dissertation has helped us to gain a better understanding of the Regulatory macrophage. We have demonstrated that Regulatory macrophages can be generated by simultaneously adding a TLR ligand and a secondary reprogramming signal such as immune complexes, adenosine or prostaglandin E<sub>2</sub>. The addition of these secondary signals causes a dampening of the pro-inflammatory cytokines IL-12, IL-1 $\beta$  and IL-6, while inducing the production of anti-inflammatory IL-10. This immunoregulatory phenotype observed in macrophages can be attributed to a group of core immunoregulatory genes that is shared between the regulatory conditions. These immunoregulatory genes are not limited to, but include *il-33*, *flrt3*, and *ccr1*, since these genes were found to be strongly induced in response to regulatory inducers, but failed to be induced with LPS or IL-4 treatments. Additional studies on CCR1 surface expression confirmed that increases in this chemokine receptor can be associated with regulatory activation. While the plasticity and auto-regulatory mechanisms associated with macrophages have made studying their activation states difficult, we believe that we have found a stable surface marker that can be used for characterization. Although more than one marker will be required to accurately describe a macrophages activation state, the expression of CCR1 has provides a new marker for identification of macrophages with immunoregulatory activity.

This work also provided evidence that Regulatory macrophages and Alternatively Activated macrophages show key phenotypic differences. An induction of IL-10 and a

dampening of pro-inflammatory cytokines was associated with regulatory activation, while alternative activation produced little to no detective cytokines. Regulatory macrophages showed increased glucose consumption and L-lactate production upon activation, which was similar to the M1 macrophages that had been stimulated with LPS alone. The Alternatively Activated macrophages showed only a slight increase in metabolism and remained similar to non-stimulated cells. The induction of immunoregulatory genes in Regulatory macrophages was shown to be independent of STAT6 signaling. Conversely, the genes associated with alternative activation were found to be dependent on STAT6 signaling and failed to be induced in the absence of STAT6. Finally, the Regulatory macrophages provided protection against lethal endotoxin challenge, while Alternatively Activated macrophages exacerbated the onset of disease symptoms leading to increased mortality. The fact that Alternatively Activated macrophages and Regulatory macrophages lack common markers, arise from vastly different stimuli, and behave differently in endotoxin challenge model, help to supports the idea that these cells were wrongly classified together as a subset of M2 macrophages. This dissertation suggests that a new classification system is required to more accurately describe the various activation states of macrophages.

## Chapter 5: Future Directions

### Continued Studies at the DNA Level

Further studies are underway in the Mosser lab on Regulatory macrophages. Promoter analyses are being conducted to identify transcription factor binding sites associated with genes that are induced or repressed following regulatory activation. The expression data from the RNA-seq analysis in combination with known promoter sequences will help to identify transcription factors associated with immunoregulatory genes. Identification of these binding sites will enable a genome wide search for genes with these promoter characteristics. The RNA-seq analyses identified mRNA transcripts of genes with unknown functions. This predicted gene set might contain important components of the immune regulation response. The over expression of these genes or their knockdown with siRNA can be used to ascertain the function of these yet to be characterized proteins. This may lead to the discovery of important regulators of the immune response. Additionally, the overexpression of *il-33*, *flrt3*, and *ccr1* could be examined in inflammatory disease models to determine if their expression level has a direct effect on the immunoregulatory activity of Regulatory macrophages.

### Continued Studies at the RNA Level

The RNA-seq analysis for this study was carried out at single time point, i.e 4 hours after stimulation. By expanding the time points in our RNA-seq analysis it may be possible to identify important genes that were overlooked in our original analysis. Additionally, the

plasticity of macrophages and the strength of activation signals cannot be overlooked. Hence to understand long term effects of these stimulations, transcriptomic profiles should be generated at multiple time points. Similarly, the addition of regulatory inducers at suboptimum concentrations can reduce the production of pro-inflammatory cytokines, but fail to induce anti-inflammatory cytokines. The addition of a time component and signal strength component would suggest that a three dimensional transcriptomic model might be the most accurate way of quantifying macrophage activation. The development of a three dimensional model would benefit researchers in several ways. First, it would allow researchers to more accurately characterize macrophages that have been isolated at different stages of disease progression. This would reflect how long the macrophage had been stimulated and the relative concentration of stimuli in the environment. Second, a model of this nature could be adapted to reflect cells that had undergone multiple stimulation events. Finally, a model of this nature would easily be able to accommodate newly described activation states. The development of a detailed three dimensional model will take years of transcriptomic analysis, but a model of this nature might be required if we hope to fully understand macrophage activation.

It is important to point out that there are several experiments that would immediately increase our understanding of macrophage activation. First, only about twenty of the immunoregulatory genes have been validated through qRT-PCR in this study. The other potential candidate genes identified in our primary analysis are to be screened as biomarkers for Regulatory macrophages. Second, performing RNA-seq analysis on macrophages stimulated with LPS+PGE<sub>2</sub> would enable us to apply a stricter criteria to the

“core regulatory genes”. This has the potential to identify the gene responsible for the immunoregulatory phenotype. Third, using qRT-PCR to validate the genes uniquely expressed in the individual regulatory condition. These genes may allow macrophages to generate stimulation-specific responses required for the elimination of diverse pathogens. Studying them will allow us to better understand the subtle differences among R-M $\phi$ . Finally, the development of a customized Nanostring platform would aid researchers in identifying a macrophage’s activation state. This would provide a quick and cost effective method for understanding how macrophages are effecting tissue microenvironments. This may provide important clues to understanding how macrophage activation affects disease progression and resolution. These four experiments are currently underway and should yield results in the near future.

### **Continued Studies at the Protein Level**

While the measurement of RNA concentration is great for early activation time points, the short period of time required for gene transcription can limit the window for detection. Additionally, variations in RNA stability and translational regulation can affect the observed protein levels. Therefore the identified mRNA markers are currently being validated at the protein expression level to identify suitable markers for murine R-M $\phi$ . Members of the Mosser lab are working to perform proteomic analysis on human macrophages exposed to different activation conditions. This is in an attempt to identify protein biomarkers and to identify proteins with functional significance. The identification of several stable human macrophage biomarkers would greatly advance the field of

macrophage biology and therapeutics. In cases of cancer, the anti-inflammatory and angiogenic nature of Regulatory macrophages could result in increased tumor growth. The selective depletion of this immunoregulatory macrophages could allow Classically Activated macrophage to product the pro-inflammatory environment needed for tumor destruction. Conversely, the removal of Classically Activated macrophages in cases of autoimmunity or autoinflammatory diseases would make it easier for Regulatory macrophages to limit inflammation and alleviate disease symptoms. The manipulation of macrophage populations can provide a new avenue for the treatment of various diseases.

## Bibliography

1. Ricklin D, Lambris JD. Complement-targeted therapeutics. *Nat Biotechnol.* 2007;25(11):1265-1275.
2. Bohlsón SS, O'Conner SD, Hulsebus HJ, Ho MM, Fraser DA. Complement, c1q, and c1q-related molecules regulate macrophage polarization. *Front Immunol.* 2014;5:402.
3. Markiewski MM, DeAngelis RA, Lambris JD. Complexity of complement activation in sepsis. *J Cell Mol Med.* 2008;12(6A):2245-2254.
4. Skattum L, van Deuren M, van der Poll T, Truedsson L. Complement deficiency states and associated infections. *Mol Immunol.* 2011;48(14):1643-1655.
5. Veerhuis R, Nielsen HM, Tenner AJ. Complement in the brain. *Mol Immunol.* 2011;48(14):1592-1603.
6. Leffler J, Bengtsson AA, Blom AM. The complement system in systemic lupus erythematosus: an update. *Ann Rheum Dis.* 2014;73(9):1601-1606.
7. Janeway CA, Medzhitov R. Innate immune recognition. *Annu Rev Immunol.* 2002;20:197-216.
8. Picard C, Casanova JL, Puel A. Infectious diseases in patients with IRAK-4, MyD88, NEMO, or I $\kappa$ B $\alpha$  deficiency. *Clin Microbiol Rev.* 2011;24(3):490-497.

9. Sheshachalam A, Srivastava N, Mitchell T, Lacy P, Eitzen G. Granule protein processing and regulated secretion in neutrophils. *Front Immunol.* 2014;5:448.
10. Galli SJ, Borregaard N, Wynn TA. Phenotypic and functional plasticity of cells of innate immunity: macrophages, mast cells and neutrophils. *Nat Immunol.* 2011;12(11):1035-1044.
11. Kolaczkowska E, Kubes P. Neutrophil recruitment and function in health and inflammation. *Nat Rev Immunol.* 2013;13(3):159-175.
12. Futosi K, Fodor S, Mócsai A. Neutrophil cell surface receptors and their intracellular signal transduction pathways. *Int Immunopharmacol.* 2013;17(3):638-650.
13. Brinkmann V, Reichard U, Goosmann C, et al. Neutrophil extracellular traps kill bacteria. *Science.* 2004;303(5663):1532-1535.
14. Feghali CA, Wright TM. Cytokines in acute and chronic inflammation. *Front Biosci.* 1997;2:d12-26.
15. Rothenberg ME, Owen WF, Silberstein DS, Soberman RJ, Austen KF, Stevens RL. Eosinophils cocultured with endothelial cells have increased survival and functional properties. *Science.* 1987;237(4815):645-647.
16. Acharya KR, Ackerman SJ. Eosinophil granule proteins: form and function. *J Biol Chem.* 2014;289(25):17406-17415.
17. Rothenberg ME, Hogan SP. The eosinophil. *Annu Rev Immunol.* 2006;24:147-174.



18. Cadman ET, Thyse KA, Bearder S, et al. Eosinophils are important for protection, immunoregulation and pathology during infection with nematode microfilariae. *PLoS Pathog.* 2014;10(3):e1003988.
19. Slifman NR, Loegering DA, McKean DJ, Gleich GJ. Ribonuclease activity associated with human eosinophil-derived neurotoxin and eosinophil cationic protein. *J Immunol.* 1986;137(9):2913-2917.
20. Siracusa MC, Kim BS, Spergel JM, Artis D. Basophils and allergic inflammation. *J Allergy Clin Immunol.* 2013;132(4):789-801; quiz 788.
21. Suzukawa M, Iikura M, Koketsu R, et al. An IL-1 cytokine member, IL-33, induces human basophil activation via its ST2 receptor. *J Immunol.* 2008;181(9):5981-5989.
22. Karasuyama H, Yamanishi Y. Basophils have emerged as a key player in immunity. *Curr Opin Immunol.* 2014;31C:1-7.
23. Jenkins SJ, Hume DA. Homeostasis in the mononuclear phagocyte system. *Trends Immunol.* 2014;35(8):358-367.
24. Geissmann F, Jung S, Littman DR. Blood monocytes consist of two principal subsets with distinct migratory properties. *Immunity.* 2003;19(1):71-82.
25. Ziegler-Heitbrock L, Ancuta P, Crowe S, et al. Nomenclature of monocytes and dendritic cells in blood. *Blood.* 2010;116(16):e74-80.
26. Serbina NV, Kuziel W, Flavell R, Akira S, Rollins B, Pamer EG. Sequential MyD88-independent and -dependent activation of innate immune responses to intracellular bacterial infection. *Immunity.* 2003;19(6):891-901.

27. Samstein M, Schreiber HA, Leiner IM, Susac B, Glickman MS, Pamer EG. Essential yet limited role for CCR2<sup>+</sup> inflammatory monocytes during Mycobacterium tuberculosis-specific T cell priming. *Elife*. 2013;2:e01086.
28. Peters W, Cyster JG, Mack M, et al. CCR2-dependent trafficking of F4/80<sup>dim</sup> macrophages and CD11c<sup>dim</sup>/intermediate dendritic cells is crucial for T cell recruitment to lungs infected with Mycobacterium tuberculosis. *J Immunol*. 2004;172(12):7647-7653.
29. Auffray C, Fogg D, Garfa M, et al. Monitoring of blood vessels and tissues by a population of monocytes with patrolling behavior. *Science*. 2007;317(5838):666-670.
30. Nahrendorf M, Swirski FK, Aikawa E, et al. The healing myocardium sequentially mobilizes two monocyte subsets with divergent and complementary functions. *J Exp Med*. 2007;204(12):3037-3047.
31. Carlin LM, Stamatiades EG, Auffray C, et al. Nr4a1-dependent Ly6C<sup>(low)</sup> monocytes monitor endothelial cells and orchestrate their disposal. *Cell*. 2013;153(2):362-375.
32. Trombetta ES, Mellman I. Cell biology of antigen processing in vitro and in vivo. *Annu Rev Immunol*. 2005;23:975-1028.
33. Fu C, Jiang A. Generation of tolerogenic dendritic cells via the E-cadherin/beta-catenin-signaling pathway. *Immunol Res*. 2010;46(1-3):72-78.

34. Mildner A, Jung S. Development and function of dendritic cell subsets. *Immunity*. 2014;40(5):642-656.
35. Reizis B, Bunin A, Ghosh HS, Lewis KL, Sisirak V. Plasmacytoid dendritic cells: recent progress and open questions. *Annu Rev Immunol*. 2011;29:163-183.
36. Nizzoli G, Krietsch J, Weick A, et al. Human CD1c<sup>+</sup> dendritic cells secrete high levels of IL-12 and potently prime cytotoxic T-cell responses. *Blood*. 2013;122(6):932-942.
37. Kohyama M, Ise W, Edelson BT, et al. Role for Spi-C in the development of red pulp macrophages and splenic iron homeostasis. *Nature*. 2009;457(7227):318-321.
38. Davies LC, Jenkins SJ, Allen JE, Taylor PR. Tissue-resident macrophages. *Nat Immunol*. 2013;14(10):986-995.
39. Taylor PR, Martinez-Pomares L, Stacey M, Lin HH, Brown GD, Gordon S. Macrophage receptors and immune recognition. *Annu Rev Immunol*. 2005;23:901-944.
40. Mosser DM, Edwards JP. Exploring the full spectrum of macrophage activation. *Nat Rev Immunol*. 2008;8(12):958-969.
41. Muzio M, Mantovani A. Toll-like receptors. *Microbes Infect*. 2000;2(3):251-255.
42. Kawasaki T, Kawai T. Toll-like receptor signaling pathways. *Front Immunol*. 2014;5:461.

43. MACKANESS GB. Cellular resistance to infection. *J Exp Med.* 1962;116:381-406.
44. Edwards JP, Zhang X, Frauwirth KA, Mosser DM. Biochemical and functional characterization of three activated macrophage populations. *J Leukoc Biol.* 2006;80(6):1298-1307.
45. Martinez FO, Gordon S. The M1 and M2 paradigm of macrophage activation: time for reassessment. *F1000Prime Rep.* 2014;6:13.
46. Mantovani A, Sica A, Sozzani S, Allavena P, Vecchi A, Locati M. The chemokine system in diverse forms of macrophage activation and polarization. *Trends Immunol.* 2004;25(12):677-686.
47. Hansen G, Hercus TR, McClure BJ, et al. The structure of the GM-CSF receptor complex reveals a distinct mode of cytokine receptor activation. *Cell.* 2008;134(3):496-507.
48. Hesse M, Modolell M, La Flamme AC, et al. Differential regulation of nitric oxide synthase-2 and arginase-1 by type 1/type 2 cytokines in vivo: granulomatous pathology is shaped by the pattern of L-arginine metabolism. *J Immunol.* 2001;167(11):6533-6544.
49. Flodström M, Eizirik DL. Interferon-gamma-induced interferon regulatory factor-1 (IRF-1) expression in rodent and human islet cells precedes nitric oxide production. *Endocrinology.* 1997;138(7):2747-2753.
50. Mackaness GB. Resistance to intracellular infection. *J Infect Dis.* 1971;123(4):439-445.

51. Stein M, Keshav S, Harris N, Gordon S. Interleukin 4 potently enhances murine macrophage mannose receptor activity: a marker of alternative immunologic macrophage activation. *J Exp Med.* 1992;176(1):287-292.
52. Doyle AG, Herbein G, Montaner LJ, et al. Interleukin-13 alters the activation state of murine macrophages in vitro: comparison with interleukin-4 and interferon-gamma. *Eur J Immunol.* 1994;24(6):1441-1445.
53. Gordon S, Martinez FO. Alternative activation of macrophages: mechanism and functions. *Immunity.* 2010;32(5):593-604.
54. Loke P, Nair MG, Parkinson J, Guiliano D, Blaxter M, Allen JE. IL-4 dependent alternatively-activated macrophages have a distinctive in vivo gene expression phenotype. *BMC Immunol.* 2002;3:7.
55. Martinez FO, Helming L, Gordon S. Alternative activation of macrophages: an immunologic functional perspective. *Annu Rev Immunol.* 2009;27:451-483.
56. Ohmori Y, Hamilton TA. Requirement for STAT1 in LPS-induced gene expression in macrophages. *J Leukoc Biol.* 2001;69(4):598-604.
57. Ohmori Y, Hamilton TA. STAT6 is required for the anti-inflammatory activity of interleukin-4 in mouse peritoneal macrophages. *J Biol Chem.* 1998;273(44):29202-29209.
58. Martin P, Leibovich SJ. Inflammatory cells during wound repair: the good, the bad and the ugly. *Trends Cell Biol.* 2005;15(11):599-607.

59. Mosmann TR, Coffman RL. Heterogeneity of cytokine secretion patterns and functions of helper T cells. *Adv Immunol.* 1989;46:111-147.
60. Mills CD. M1 and M2 Macrophages: Oracles of Health and Disease. *Crit Rev Immunol.* 2012;32(6):463-488.
61. Cohen HB, Briggs KT, Marino JP, Ravid K, Robson SC, Mosser DM. TLR stimulation initiates a CD39-based autoregulatory mechanism that limits macrophage inflammatory responses. *Blood.* 2013;122(11):1935-1945.
62. Martinez FO, Sica A, Mantovani A, Locati M. Macrophage activation and polarization. *Front Biosci.* 2008;13:453-461.
63. Sutterwala FS, Noel GJ, Salgame P, Mosser DM. Reversal of proinflammatory responses by ligating the macrophage Fcγ receptor type I. *J Exp Med.* 1998;188(1):217-222.
64. Anderson CF, Mosser DM. A novel phenotype for an activated macrophage: the type 2 activated macrophage. *J Leukoc Biol.* 2002;72(1):101-106.
65. Anderson CF, Gerber JS, Mosser DM. Modulating macrophage function with IgG immune complexes. *J Endotoxin Res.* 2002;8(6):477-481.
66. Yi YS, Son YJ, Ryou C, Sung GH, Kim JH, Cho JY. Functional roles of Syk in macrophage-mediated inflammatory responses. *Mediators Inflamm.* 2014;2014:270302.
67. Lucas M, Zhang X, Prasanna V, Mosser DM. ERK activation following macrophage FcγR ligation leads to chromatin modifications at the IL-10 locus. *J Immunol.* 2005;175(1):469-477.

68. Ng SW, Nelson C, Parekh AB. Coupling of Ca(2+) microdomains to spatially and temporally distinct cellular responses by the tyrosine kinase Syk. *J Biol Chem.* 2009;284(37):24767-24772.
69. Xaus J, Mirabet M, Lloberas J, et al. IFN-gamma up-regulates the A2B adenosine receptor expression in macrophages: a mechanism of macrophage deactivation. *J Immunol.* 1999;162(6):3607-3614.
70. Aronoff DM, Canetti C, Peters-Golden M. Prostaglandin E2 inhibits alveolar macrophage phagocytosis through an E-prostanoid 2 receptor-mediated increase in intracellular cyclic AMP. *J Immunol.* 2004;173(1):559-565.
71. Medeiros A, Peres-Buzalaf C, Fortino Verdán F, Serezani CH. Prostaglandin E2 and the suppression of phagocyte innate immune responses in different organs. *Mediators Inflamm.* 2012;2012:327568.
72. Li J, Zhang Y. Relationship between promoter sequence and its strength in gene expression. *Eur Phys J E Soft Matter.* 2014;37(9):44.
73. Gurard-Levin ZA, Almouzni G. Histone modifications and a choice of variant: a language that helps the genome express itself. *F1000Prime Rep.* 2014;6:76.
74. Cramer P, Wolberger C. Proteins: histones and chromatin. *Curr Opin Struct Biol.* 2011;21(6):695-697.
75. Peterson CL, Laniel MA. Histones and histone modifications. *Curr Biol.* 2004;14(14):R546-551.

76. Ansel KM, Lee DU, Rao A. An epigenetic view of helper T cell differentiation. *Nat Immunol.* 2003;4(7):616-623.
77. Zhang X, Edwards JP, Mosser DM. Dynamic and transient remodeling of the macrophage IL-10 promoter during transcription. *J Immunol.* 2006;177(2):1282-1288.
78. Cao S, Zhang X, Edwards JP, Mosser DM. NF-kappaB1 (p50) homodimers differentially regulate pro- and anti-inflammatory cytokines in macrophages. *J Biol Chem.* 2006;281(36):26041-26050.
79. Watson A, Mazumder A, Stewart M, Balasubramanian S. Technology for microarray analysis of gene expression. *Curr Opin Biotechnol.* 1998;9(6):609-614.
80. Qian X, Ba Y, Zhuang Q, Zhong G. RNA-Seq technology and its application in fish transcriptomics. *OMICS.* 2014;18(2):98-110.
81. Freeman WM, Walker SJ, Vrana KE. Quantitative RT-PCR: pitfalls and potential. *Biotechniques.* 1999;26(1):112-122, 124-115.
82. Edwards JP, Zhang X, Mosser DM. The expression of heparin-binding epidermal growth factor-like growth factor by regulatory macrophages. *J Immunol.* 2009;182(4):1929-1939.
83. Domon B, Aebersold R. Mass spectrometry and protein analysis. *Science.* 2006;312(5771):212-217.
84. Sica A, Mantovani A. Macrophage plasticity and polarization: in vivo veritas. *J Clin Invest.* 2012;122(3):787-795.



85. Hussell T, Bell TJ. Alveolar macrophages: plasticity in a tissue-specific context. *Nat Rev Immunol*. 2014;14(2):81-93.
86. Mantovani A, Biswas SK, Galdiero MR, Sica A, Locati M. Macrophage plasticity and polarization in tissue repair and remodelling. *J Pathol*. 2013;229(2):176-185.
87. Murray PJ, Allen JE, Biswas SK, et al. Macrophage activation and polarization: nomenclature and experimental guidelines. *Immunity*. 2014;41(1):14-20.
88. Wynn TA, Chawla A, Pollard JW. Macrophage biology in development, homeostasis and disease. *Nature*. 2013;496(7446):445-455.
89. Mills CD, Kincaid K, Alt JM, Heilman MJ, Hill AM. M-1/M-2 macrophages and the Th1/Th2 paradigm. *J Immunol*. 2000;164(12):6166-6173.
90. Blanchard DK, Djeu JY, Klein TW, Friedman H, Stewart WE. Interferon-gamma induction by lipopolysaccharide: dependence on interleukin 2 and macrophages. *J Immunol*. 1986;136(3):963-970.
91. Foss DL, Zilliox MJ, Murtaugh MP. Differential regulation of macrophage interleukin-1 (IL-1), IL-12, and CD80-CD86 by two bacterial toxins. *Infect Immun*. 1999;67(10):5275-5281.
92. Mukhopadhyay S, Peiser L, Gordon S. Activation of murine macrophages by *Neisseria meningitidis* and IFN-gamma in vitro: distinct roles of class A scavenger and Toll-like pattern recognition receptors in selective modulation of surface phenotype. *J Leukoc Biol*. 2004;76(3):577-584.

93. Canton J. Phagosome maturation in polarized macrophages. *J Leukoc Biol.* 2014.
94. Raes G, De Baetselier P, Noël W, Beschin A, Brombacher F, Hassanzadeh Gh G. Differential expression of FIZZ1 and Ym1 in alternatively versus classically activated macrophages. *J Leukoc Biol.* 2002;71(4):597-602.
95. Murray PJ, Wynn TA. Protective and pathogenic functions of macrophage subsets. *Nat Rev Immunol.* 2011;11(11):723-737.
96. Fleming BD, Mosser DM. Regulatory macrophages: setting the threshold for therapy. *Eur J Immunol.* 2011;41(9):2498-2502.
97. Anderson CF, Mosser DM. Cutting edge: biasing immune responses by directing antigen to macrophage Fc gamma receptors. *J Immunol.* 2002;168(8):3697-3701.
98. Livak KJ, Schmittgen TD. Analysis of relative gene expression data using real-time quantitative PCR and the 2(-Delta Delta C(T)) Method. *Methods.* 2001;25(4):402-408.
99. Bolger AM, Lohse M, Usadel B. Trimmomatic: a flexible trimmer for Illumina sequence data. *Bioinformatics.* 2014;30(15):2114-2120.
100. Trapnell C, Pachter L, Salzberg SL. TopHat: discovering splice junctions with RNA-Seq. *Bioinformatics.* 2009;25(9):1105-1111.
101. Bolstad BM, Irizarry RA, Astrand M, Speed TP. A comparison of normalization methods for high density oligonucleotide array data based on variance and bias. *Bioinformatics.* 2003;19(2):185-193.

102. Smyth GK. Linear models and empirical bayes methods for assessing differential expression in microarray experiments. *Stat Appl Genet Mol Biol.* 2004;3:Article3.
103. Law CW, Chen Y, Shi W, Smyth GK. voom: precision weights unlock linear model analysis tools for RNA-seq read counts. *Genome Biol.* 2014;15(2):R29.
104. Leek JT, Scharpf RB, Bravo HC, et al. Tackling the widespread and critical impact of batch effects in high-throughput data. *Nat Rev Genet.* 2010;11(10):733-739.
105. Krämer A, Green J, Pollard J, Tugendreich S. Causal analysis approaches in Ingenuity Pathway Analysis. *Bioinformatics.* 2014;30(4):523-530.
106. Gao JJ, Diesl V, Wittmann T, et al. Regulation of gene expression in mouse macrophages stimulated with bacterial CpG-DNA and lipopolysaccharide. *J Leukoc Biol.* 2002;72(6):1234-1245.
107. Gao JJ, Diesl V, Wittmann T, et al. Bacterial LPS and CpG DNA differentially induce gene expression profiles in mouse macrophages. *J Endotoxin Res.* 2003;9(4):237-243.
108. Palaga T, Buranaruk C, Rengpipat S, et al. Notch signaling is activated by TLR stimulation and regulates macrophage functions. *Eur J Immunol.* 2008;38(1):174-183.

109. Rodríguez-Prados JC, Través PG, Cuenca J, et al. Substrate fate in activated macrophages: a comparison between innate, classic, and alternative activation. *J Immunol.* 2010;185(1):605-614.
110. Odegaard JI, Chawla A. Alternative macrophage activation and metabolism. *Annu Rev Pathol.* 2011;6:275-297.
111. Colegio OR, Chu NQ, Szabo AL, et al. Functional polarization of tumour-associated macrophages by tumour-derived lactic acid. *Nature.* 2014.
112. Gérard C, Bruyns C, Marchant A, et al. Interleukin 10 reduces the release of tumor necrosis factor and prevents lethality in experimental endotoxemia. *J Exp Med.* 1993;177(2):547-550.
113. Howard M, Muchamuel T, Andrade S, Menon S. Interleukin 10 protects mice from lethal endotoxemia. *J Exp Med.* 1993;177(4):1205-1208.
114. Gallo P, Gonçalves R, Mosser DM. The influence of IgG density and macrophage Fc (gamma) receptor cross-linking on phagocytosis and IL-10 production. *Immunol Lett.* 2010;133(2):70-77.
115. Haschemi A, Kosma P, Gille L, et al. The sedoheptulose kinase CARKL directs macrophage polarization through control of glucose metabolism. *Cell Metab.* 2012;15(6):813-826.
116. Biswas SK, Mantovani A. Orchestration of metabolism by macrophages. *Cell Metab.* 2012;15(4):432-437.

117. Marchant A, Bruyns C, Vandenabeele P, et al. Interleukin-10 controls interferon-gamma and tumor necrosis factor production during experimental endotoxemia. *Eur J Immunol*. 1994;24(5):1167-1171.
118. Standiford TJ, Strieter RM, Lukacs NW, Kunkel SL. Neutralization of IL-10 increases lethality in endotoxemia. Cooperative effects of macrophage inflammatory protein-2 and tumor necrosis factor. *J Immunol*. 1995;155(4):2222-2229.
119. Yao Y, Li W, Kaplan MH, Chang CH. Interleukin (IL)-4 inhibits IL-10 to promote IL-12 production by dendritic cells. *J Exp Med*. 2005;201(12):1899-1903.
120. Bullens DM, Kasran A, Thielemans K, Bakkus M, Ceuppens JL. CD40L-induced IL-12 production is further enhanced by the Th2 cytokines IL-4 and IL-13. *Scand J Immunol*. 2001;53(5):455-463.
121. Hultgren O, Kopf M, Tarkowski A. Outcome of Staphylococcus aureus-triggered sepsis and arthritis in IL-4-deficient mice depends on the genetic background of the host. *Eur J Immunol*. 1999;29(8):2400-2405.
122. Huber S, Hoffmann R, Muskens F, Voehringer D. Alternatively activated macrophages inhibit T-cell proliferation by Stat6-dependent expression of PD-L2. *Blood*. 2010;116(17):3311-3320.
123. Beyer M, Mallmann MR, Xue J, et al. High-resolution transcriptome of human macrophages. *PLoS One*. 2012;7(9):e45466.

124. Gundra UM, Girgis NM, Ruckerl D, et al. Alternatively activated macrophages derived from monocytes and tissue macrophages are phenotypically and functionally distinct. *Blood*. 2014;123(20):e110-122.
125. Hardman CS, Panova V, McKenzie AN. IL-33 citrine reporter mice reveal the temporal and spatial expression of IL-33 during allergic lung inflammation. *Eur J Immunol*. 2013;43(2):488-498.
126. Seki E, De Minicis S, Gwak GY, et al. CCR1 and CCR5 promote hepatic fibrosis in mice. *J Clin Invest*. 2009;119(7):1858-1870.
127. Furuichi K, Gao JL, Horuk R, Wada T, Kaneko S, Murphy PM. Chemokine receptor CCR1 regulates inflammatory cell infiltration after renal ischemia-reperfusion injury. *J Immunol*. 2008;181(12):8670-8676.